

Medizinische Fakultät
der Martin-Luther-Universität Halle-Wittenberg

Epigenetic changes in preimplantation embryos from a diabetic pregnancies

Dissertation

To obtain the academic degree of
Doktor rerum medicarum (Dr. rer. medic.)
for the subject area of
medical pathology

by **Katarzyna Joanna Grybel**

born 6th of December 1988 in Legnica (Poland)

Supervisor: **Prof. Dr. Dr. Bernd Fischer**

Reviewers: apl. Prof. A. Navarrete-Santos

Prof. H. Behre

Prof. T. Haaf, Würzburg

26.06.2018

24.02.2021

Abstract

Processes occurring in early pregnancy decide on pregnancy outcomes. Many complications have its origin in adverse nutritional and hormonal maternal signals in early pregnancy. A diabetic pregnancy often causes miscarriages or has consequences on the health of the offspring, giving predispositions to metabolic syndrome disorders, such as obesity or diabetes type 2. We have hypothesized that changes in the uterine environment due to diabetes may be related to the DNA methylation status at specific gene promoters in the early embryo. Therefore, we have investigated epigenetic changes in preimplantation blastocysts (day 6 p.c.) from diabetic rabbits.

At first we have addressed an observed delay in development to the formation of the first embryonic lineages: epiblast, hypoblast and trophoblast. The expression of lineage-specific markers is disturbed by diabetes. The epiblast lineage specifier Oct4, together with pluripotency genes Sox2 and Nanog, was upregulated in epiblasts from late gastrulating blastocysts from diabetic rabbits. Hypoblasts markers Cer1 and Dkk1 were downregulated in late gastrulation stages. Moreover, DNA methyltransferases (DNMTs) were upregulated in epiblasts from embryos from diabetic rabbits, suggesting an involvement of DNA methylation processes in the delay of development. An in vitro culture with insulin, IGF2 or branched chained amino acids (BCAAs) did not identify a factor responsible for the observed upregulation of DNMTs.

Next we have analyzed the DNA methylation pattern of the epiblast lineage specifier Oct4 (POU5F1) promoter at its conserved regions and functional elements using a bisulfite sequencing method. We found a hypomethylation of hypoblasts from late gastrulation blastocysts from diabetic rabbits. Minor changes were found in the epiblast and trophoblast. Furthermore, the analysis of the metabolites necessary for the DNA methylation, S-adenosyl methionine (SAM) and a side product of the reaction, S-adenosylhomocysteine (SAH), were qualified in rabbit maternal blood plasma at day 6 *post coitum*. The results of a modified liquid chromatography-tandem mass spectrometry showed no differences in the sample from diabetic rabbits. Possibly the global methylation process is not disturbed in embryos from diabetic pregnancies.

We conclude that the delay in development in rabbit preimplantation embryos from diabetic pregnancies is manifested as retention of pluripotency in the epiblast lineage and slower differentiation of the hypoblast cell population. Moreover, upregulation of DNMTs in epiblasts in embryos from diabetic rabbits is another sign of a delay in development, as the embryo remethylation occurs at specific times of embryogenesis. The hypomethylation at Oct4 promoter region indicates a delay in hypoblast differentiation. However, the change in Oct4 promoter methylation is less likely to be driven by changes in global methylation. Possibly a delay in differentiation of the hypoblast tissue has an impact on signaling between the hypoblast and epiblast.

Grybel, Katarzyna Joanna: Epigenetic changes in preimplantation embryos from a diabetic rabbits, Halle (Saale), Univ., Med. Fak., Diss., 82 pages, 2017

Referat

Vorgänge, die während der frühen Schwangerschaft geschehen, wirken sich auf den weiteren Verlauf der Schwangerschaft aus (DOHaD-Konzept). Typische Komplikationen in der Frühschwangerschaft sind unphysiologische Hormon- und Ernährungssignale der Mutter. Unsere Arbeitshypothese ist, dass die durch Diabetes induzierten Veränderungen im uterinen Milieu zu einer Verzögerung in der Embryonalentwicklung führen und dass die Entwicklungsverzögerung durch DNA-Methylierungsstörungen an spezifischen (Gen-) Promotoren bedingt sein können. Wir haben die epigenetischen Veränderungen in Präimplantationsembryonen (6 Tage alte Blastozysten) von diabetischen Kaninchen untersucht.

Zuerst haben wir die Bildung der ersten embryonalen Zelllinien, Epiblast, Hypoblast und Trophoblast, untersucht. Die Genexpression von Zelllinien-spezifischen Markern ist durch Diabetes gestört. Das Epiblast-spezifische Oct4, zusammen mit den Pluripotenzgenen Sox2 und Nanog, war im Epiblast von spät gastrulierenden Blastozysten von diabetischen Kaninchen erhöht. Im Unterschied hierzu waren die Hypoblastmarker Cer1 und Dkk1 herunterreguliert. Zudem waren DNA-Methyltransferasen (DNMTs) im Epiblast von Blastozysten diabetischer Kaninchen hochreguliert, so dass eine Beteiligung der DNA-Methylierung für die Entwicklungsverzögerung naheliegt. Eine *in vitro* Kultur mit Insulin, IGF2 oder verzweigtkettigen Aminosäuren konnte keinen Faktor identifizieren, der für die Hochregulation von DNMTs verantwortlich ist.

Als nächstes haben wir die Verteilung der DNA-Methylierung in den konservierten Regionen und funktionalen Elementen des Promotors für das Epiblast-spezifische Oct4 mittels Bisulfit-Sequenzierung analysiert. Wir konnten eine Hypomethylierung des Hypoblasts in den Blastozysten von diabetischen Kaninchen finden. Zusätzlich quantifizierten wir S-Adenosylmethionin (SAM) und S-Adenosylhomocystein (SAH), die für die DNA-Methylierung notwendig sind, im maternalen Plasma von Kaninchen am Tag 6 post coitum. Das Ergebnis der modifizierten Flüssigchromatographie gekoppelt mit einer Tandemmassenspektrometrie zeigte keine Unterschiede in den Proben von diabetischen und gesunden Kaninchen. Möglicherweise ist der globale Methylierungsprozess in Embryonen von diabetischen Kaninchen gestört.

Wir schlussfolgern, dass die beobachtete Entwicklungsverzögerung in Präimplantationsembryonen von diabetischen Kaninchen auf den Erhalt der Pluripotenz im Epiblast und verlangsamerter Differenzierung des Hypoblasten zurückzuführen sind. Zudem ist die Hochregulierung von DNMTs im Epiblast in Embryonen von diabetischen Kaninchen ein weiteres Anzeichen für die Entwicklungsverzögerung, da die Remethylierung zu spezifischen Zeitpunkten in der Embryogenese erfolgen muss. Dennoch ist es unwahrscheinlich, dass die Änderungen der Methylierung des Oct4-Promotors aufgrund von globalen Änderungen der Methylierung erfolgte. Möglicherweise hat die Differenzierungsverzögerung des Hypoblast einen Einfluss auf die Signalkaskade zwischen Hypoblast und Epiblast und damit auf dem normalen Fortgang der Gastrulation.

Table of contents

1.Introduction.....	1
1.1 Aim of the study	1
1.2 Early development events.....	2
1.2.1 Formation of first embryonic lineages	2
1.3 DNA methylation and enzymes involved in DNA methylation.....	3
1.4 Oct4 protein	6
1.4.1 Oct4 structure and function	6
1.4.2 Oct4 promoter organization.....	6
1.4.3 Oct4 expression in early development.....	8
1.4.4 Regulation and role of Oct4 in first embryonic lineages.....	9
1.5 Environmental influence on epigenetic modifications during early development.....	10
1.6 Animal diabetic pregnancies model	11
1.6.1 Rabbit diabetic pregnancy model.....	12
1.7 Diabetes mellitus in early development – heart malformations	13
2. Materials and methods	15
2.1 Materials: chemicals and prefabricated systems.....	15
2.2 Laboratory equipment.....	17
2.4 Animal model	17
2.4.1 Embryo recovery	18
2.4.2 Embryo dissections.....	18
2.4.3 Embryo in vitro culture.....	18
2.4.4 Induction of Diabetes mellitus Type 1.....	19
2.4.5 Recovery of maternal blood plasma	19
2.5 SAM and SAH levels measurements.....	19
2.6 mRNA isolation from embryonic tissues	19
2.7 cDNA synthesis for embryonic tissues	20
2.8 RNA isolation from rabbit tissues.....	21
2.8.1 DNase digestion.....	21
2.8.2 cDNA synthesis from RNA of rabbit tissue	22
2.9 Polymerase chain reactions (PCRs)	22
2.9.1 Reverse transcriptase-Polymerase chain reaction (RT-PCR)	22

2.10 Bisulfite sequencing.....	23
2.10.1 Genomic DNA isolation of rabbit tissue	24
2.10.2 Bisulfite conversion	25
2.10.3 Purification of bisulfate treated DNA	25
2.10.4 “Nested” PCR reaction with Conserved region-specific primers of POU5F1 (Oct4) gene promoter	26
2.11 Extraction of the DNA fragment from agarose gel.....	27
2.12 Cloning.....	28
2.12.1 Ligation	28
2.12.2 Transformation.....	28
2.12.3 Selection of positive clones	29
2.12.4 Plasmid isolation from E.coli bacteria	29
2.12.5 Restriction reaction	29
2.12.6 Sequencing	30
2.12.7 Purification of sequencing reaction	30
2.13 Bisulfite sequencing data analysis.....	30
2.14 Real Time PCR.....	31
2.14 Real Time PCR standards	31
2.15 Statistics.....	31
3. Results	32
3.1 Effect of maternal diabetes on the expression of pluripotency genes and differentiation-related gene markers in rabbit preimplantation embryos.....	32
3.1.1 Expression of pluripotency genes in gastrulating blastocysts.....	32
3.1.2 Expression of extraembryonic tissue-specific genes for hypoblasts and trophoblasts from blastocysts day 6 stages 0 and 2	33
3.1.3 Expression of heart developmental markers: Mef2C, Gata6, Gata4 and Nkx2-5 in rabbit fetal hearts at day 12 and 14.....	34
3.2 Oct4 (POU5F1) promoter region methylation analysis in rabbit adult heart tissue and gastrulating blastocysts day 6 stage 2.....	35
3.2.1 Oct4 (POU5F1) promoter region methylation analysis in rabbit adult heart tissue	35
3.3 Comparison of data for groups of epiblasts, hypoblasts and trophoblasts pools.....	37
3.4 Oct4 (POU5F1) conserved region 1 methylation analysis in embryonic tissues of gastrulating blastocysts day 6 stage 2.....	38
3.4.1 Oct4 (POU5F1) conserved region 1 methylation analysis in epiblasts from healthy and diabetic rabbits.....	38

3.4.2 Oct4 (POU5F1) conserved region 1 methylation analysis in hypoblasts from healthy and diabetic rabbits.....	39
3.4.3 Oct4 (POU5F1) conserved region 1 methylation analysis in trophoblasts from healthy and diabetic pregnancies	39
The elements of minimal promoter shared a parallel proportion of methylation between the fragment outside the conserved region, upstream to CR1 and the CR1 (61 % to 36 % of me-CpGs). HRE and beginning of exon was slightly higher methylated than in trophoblasts from healthy blastocysts (Figure 18A and 18B).	39
3.4.4 Oct4 (POU5F1) conserved region 1 methylation analysis in rabbit adult heart tissue and embryonic tissues from healthy and diabetic pregnancies.....	43
3.5 POU5F1 (Oct4) conserved region 4 methylation analysis in embryonic tissues of gastrulating blastocysts day 6 stage 2.....	44
3.5.1 Oct4 (POU5F1) conserved region 4 methylation analysis in epiblasts from healthy and diabetic rabbits.....	44
3.5.2 Oct4 (POU5F1) conserved region 4 methylation analysis in hypoblasts from healthy and diabetic rabbits.....	45
3.5.3 Oct4 (POU5F1) conserved region 4 methylation analysis in trophoblasts from healthy and diabetic rabbits.....	45
3.5.4 Oct4 (POU5F1) conserved region 4 methylation analysis in rabbit adult heart tissue and embryonic tissues from healthy and diabetic pregnancies.....	49
3.6 Influence of maternal diabetes on expression of enzymes involved in the DNA methylation process.	50
3.6.1 In vivo expression of DNA methyltransferases in 6 day old rabbit blastocysts	50
3.6.2 In vivo expression of DNA methyltransferases in fetal rabbit hearts at day 12 and 14 of pregnancy	51
3.7 Expression of DNA methyltransferases in vitro culture	51
3.7.1 Influence of in vitro culture with insulin, BCAAs, IGF2 and LIF on DNMT1 expression in embryonic tissues of rabbit blastocysts day 6 stage 1	52
3.7.2 Influence of in vitro culture with insulin, BCAAs, IGF2 or LIF on DNMT3A expression in embryonic tissues of rabbit blastocysts day 6 stage 1	52
3.7.3 Influence of in vitro culture with insulin, BCAAs, IGF2 or LIF on DNMT3B expression in embryonic tissues of rabbit blastocysts day 6 stage 1	53
3.8 Measurements of metabolites: S-adenosylmethionin and S-adenosylhomocystein in rabbit maternal blood plasma at day 6 of pregnancy.....	54
4. Discussion	55
4.1 Oct4 is a lineage specifier in early rabbit blastocyst	55
4.1.1 Pluripotency markers are upregulated in blastocysts of diabetic rabbits.....	55
4.1.2 Development in diabetic conditions impairs trophoblast lineage decisions.....	56

4.2 Effect of maternal diabetes on specific (Oct4) promoter methylation.....	56
4.2.1 Methylation rate of the Oct4 promoter is higher in differentiated cells.....	57
4.2.2 Limitations of bisulfite conversion in DNA methylation studies.....	57
4.3 General scheme of DNA methylation dynamics and Oct4 promoter regulation in early development.....	58
4.3.1 Diverse methylation patterns of Oct4 promoter in embryonic tissues.....	59
4.3.2 Diabetic pregnancy influences methylation of Oct4 promoter in epiblasts, hypoblasts and trophoblasts of rabbit blastocysts.....	61
4.3.3 Oct4 expression correlates with level of Oct4 promoter methylation in rabbit embryonic tissues at the blastocyst stage.....	62
4.3.4 Diabetes affects embryonic lineages by influence on Oct4 expression through changes in its promoter methylation.....	63
4.3.5 Delay in epiblast differentiation is associated with hypoblast underdevelopment in diabetic blastocysts.....	64
4.3.6 Changes in Oct4 promoter methylation are not depending on global DNA methylation processes.....	64
4.4 Delay in development due to maternal diabetes is manifested during organogenesis.....	65
4.5 DNA methyltransferases are highly expressed in embryonic tissues of 6 day old blastocysts and fetal rabbit heart.....	65
4.5.1 Maternal diabetes influences DNMTs expression in rabbit blastocysts.....	66
4.5.2 DNA methyltransferases expression in fetal rabbit heart differs from the embryonic levels and is not influenced by maternal diabetes.....	66
4.5.3 DNMT1 and DNMT3B showed a downregulation in diabetic epiblasts upon insulin and IGF2 in vitro culture.....	67
5. Summary.....	68
6. Literature.....	70
7. Supplement.....	81
7.1 List of figures.....	81
7.2 List of tables.....	82

List of abbreviations

BSM	basal synthetic medium
EDTA	Ethylenediaminetetraacetic acid
Hox	homeobox
IPTG	Isopropyl-Beta-D-Thiogalactoside
mRNA	Messenger Ribonucleic Acid
NaCi	Sodium Citrate
5`-UTR	5' Untranslated Region
aa	Amino acid
AGEs	Advanced Glzcation End products
BCAAs	Branched-chain amino acid
bp	bais pair
cDNA	complementary DNA
Cdx2	Caudal type homeobox 2
CpG	dinucleotide of Cytosine by a Guanine
CpHs	dinucleotide of Cytosine with Adenin, Cytosine or Thymin (CpA, CpC and CpT)
CR1	Conserved Region 1
CR4	Conserved Region 4
CT	Cycle Treshold
DE-1A	Distal Enhancer 1A
DEPC	Diethyl pyrocarbonate
DNA	Deoxyribonucleic acid
DNase	Deoxyribonuclease
DNMT	DNA methyltransferase
dNTP	Deoxynucleotide
DOHaD	Developmental Origins of Health and Diseas
EtOH	Ethanol
Gapdh	Glyceraldehyde 3-phosphate dehydrogenase
Gata4	GATA binding protein 4
Gata6	GATA binding protein 6
H3Kx	Histone 3 Lysine x
HCl	Hydrochloric acid
HDAC3	Histone deacetylase 3
Hex	Hematopoietically expressed homeobox
HRE	Hormone Response Element
ICM	Inner Cell Mass
ICSI	Intracytoplasmic Sperm Injection
IGF	Insulin Growth Factor
IVF	<i>In vitro</i> fertilisation
KAT2B	K(lysine) acetyltransferase 2B
KCl	Potassium chloride
LC-MS/MS	Liquid chromatography with tandem mass spectrometry
LIF	Leukemia inhibitory factor
me-CpG	methylation at CpG position
Mef2C	Myocyte-specific enhancer factor 2C
mESC	mouse Embryonic Stem Cells
MgCl2	Magnesium chloride
MgSO4	Magnesium sulfate
mTOR	mechanistic target of rapamycin
NaCl	Sodium chloride
NaOAc	Sodium acetate
Oct4	Octamer-binding transcription factor 4

p.c	post coitum
PCR	Polymerase chain reaction
PE-1A	Proximal Enhancer 1A
PE-1B	Proximal Enhancer 1B
pH	potential of Hydrogen
PMSG	Pregnant mare's serum gonadotropin
PTMs	Posttranslational modifications
rDNase	Recombinant DNase I
RNA	Ribonucleic acid
RNase	Ribonuclease
rpm	Revolutions per minute
RT	Room Temperature
RT-qPCR	Real-Time quantitative Polymerase Chain Reaction
SAH	S-adenosyl homocysteine
SAM	S-adenosyl methionine
SEM	Standard error of the mean
SetDB1	Histone-lysine N-methyltransferase
Sirt	NAD-dependent deacetylase sirtuin
Sox2	SRY (sex determining region Y)-box 2
Sp1/Sp3	Transcription factor Sp1/Sp3
STAT3	Signal transducer and activator of transcription 3
TAE buffer	Tris base, acetic acid and EDTA buffer
TGFβ	Transforming growth factor beta
Tm	Melting temperature
type-1 DM	Diabetes mellitus type 1
UV	Ultraviolet
V	Volt
VEGF-A	Vascular endothelial growth factor A
X-Gal	5-bromo-4-chloro-3-indolyl- β -D-galactopyranoside)

1. Introduction

1.1 Aim of the study

Extensive time observation of long-lasting effects of diabetic pregnancies on offspring led to the hypothesis by Prof. David J.P. Barker in middle 1980s called "Developmental Origins of Health and Disease (DOHaD)". Originally, it was based on undernutrition during gestation recognizing its correlation with cardiac and metabolic disorders later in adult life. Later on, the hypothesis was broadened up to include all adverse factors influencing the intrauterine environment early embryonic development.

Maternal intrauterine environment is a critical factor in early embryonic development. An adverse intrauterine milieu leading to miscarriages was observed in diabetic pregnancies. Furthermore, children born after a diabetic pregnancy often suffer from metabolic syndrome, type 2 diabetes mellitus and obesity in adult life, without clear genetic predispositions for those diseases. Therefore, the phenomenon of non-genetical transmission of metabolism-related diseases was assigned to epigenetics. Epigenetics is correlated with changes in DNA methylation and in histone posttranslational modifications.

Early embryogenesis is a time of an extensive remodeling at the epigenetic level. The epigenome is sensitive towards metabolic signals, what might result in the delay of the formation of cell- and tissue-specific epigenetic patterns or the creation of adverse epigenetic patterns, leading to changes in gene expression.

Maternal diabetes is a reason for a lower rate of blastocysts number and a delay in blastocyst gastrulation in diabetic rabbits. In current study focusing in embryonic tissues specific markers were investigated to better understand the underlying in molecular process for the delay in gastrulation. The epiblast lineage specifier Oct4 and the expression of pluripotency genes (Sox2 and Nanog) together with the trophoblast marker Cdx2 and the hypoblast marker Hex RNA levels were investigated at the beginning and in later stages of gastrulation in the embryonic tissue: embryoblast (epiblast and hypoblast) and trophoblast. The heart tissue-specific developmental markers (Mef2C, Gata6, Gata4 and Nkx2-5) were measured at day 12 and 14 of pregnancy to follow up, whether the disruption of embryonic tissue formation had an impact on fetal organogenesis. Furthermore, a specific gene promoter methylation was performed for Oct4 (POU5F1) to investigate whether and how diabetes impacts tissue-specific relevant genes and on the gene transcript level and DNA methylation level. Transcriptional and DNA methylation-related data about embryonic lineage specific genes can help better understand the mechanisms of embryonic tissues formation in diabetic pregnancies.

The DNA methylation process is executed by DNA methyltransferases (DNMTs) on a very tight schedule, so the expression of DNMTs was assessed in embryonic tissues of early and late gastrulation embryos and in fetal heart day at 12 and 14. To identify the factors regulating DNMTs

expression, an *in vitro* culture with insulin, IGF, branched chained amino acids (BCAAs) and LIF was applied.

The level of metabolites often limits reactions. The substrate for methylation reactions S-adenosylmethionine (SAM) can affect also the DNA methylation process. On the other side, the rate of methylation reaction can be controlled by measuring the side product of reaction S-adenosylhomocysteine (SAH). Both metabolites are present in large amounts during the demethylation and *de novo* DNA methylation during the preimplantation period of pregnancy, and they can be measured in maternal blood plasma. We have compared the SAM and SAH levels in maternal blood plasma from healthy and diabetic rabbits to verify if the methylation reaction rate is affected by a diabetic pregnancy.

1.2 Early development events

Blastocyst formation is a big milestone in mammalian embryogenesis (Daughtry and Chavez, 2016). Development from zygote to blastocyst requires extensive remodeling at the genetic and epigenetic level (Marcho et al., 2015; Canovas and Ross, 2016). In contrast to germline, adult mammalian cells maintain a constant epigenetic pattern. The purpose of epigenetic remodeling is to revert the totipotent state and to promote differentiation, in order to build a complex organism (Burton et al., 2014). Although the genetic information is preserved, the epigenome undergoes a constant processing at cell-type and context-dependent level (Canovas and Ross, 2016). All starts when maternal transcripts are erased and the activation of zygotic genome occurs.

Blastocyst formation cell-fate decisions are entailed together with main epigenetic mechanisms controlling gene expression, such as covalent alteration of DNA by methylation, histone posttranslational modifications and noncoding RNAs (Canova and Ross, 2016). All levels of epigenetic components are reprogrammed starting from DNA methylation, histone posttranslational modification, histone deposition and higher order of chromatin organization (Biechele et al., 2015).

1.2.1 Formation of first embryonic lineages

Although the blastocyst seems to present a simple structure, differs in modes of formation, morphology, longevity and developmental capacity to interact with uterine endometrium in mammals (Frankenberg et al., 2016). One of the most important events in blastocyst development is the derivation of first embryonic lineages: epiblast, hypoblast and trophoblast. Self-organizing properties of mammalian blastocyst were recently reviewed in the mouse (Chazaud and Yamanaka, 2016).

The first lineages formation proceeds differently in amniote groups (see more details in Figure 1; Sheng, 2015). Indeed, the establishment of the first three cell lineages is proposed to be driven by cell-cell interactions, gene expression and cells microenvironment. The role of the intrauterine

environment was considered important, but not crucial for the development of first lineages (Chazaud and Yamanaka, 2016).

Gene regulatory networks maintaining pluripotency are highly conserved in mammalian blastocyst lineages (Cañon et al., 2011). Studies of mouse embryonic development gave an insight in inner cell mass (ICM) and trophectoderm divisions with a reciprocal expression of Oct4 and Cdx2 (Kuijk et al., 2008). Mosaic expression of Gata6 and Nanog was reported in mouse ICM, what might cause further segregation of the primitive ectoderm from the primitive endoderm (Kuijk et al., 2008). It is likely that first embryonic lineages formation directs pluripotency pathways in different ways in epiblast, hypoblast and trophoblast cells.

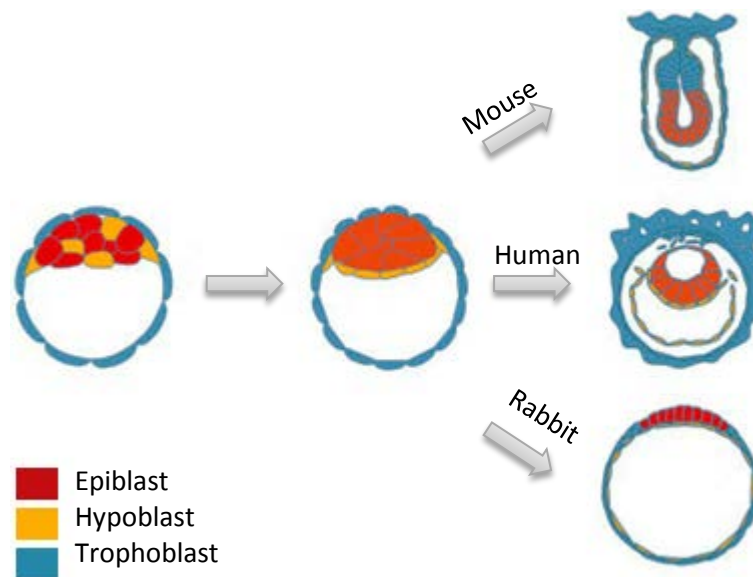


Figure 1. **Scheme of morphogenetic diversity in epiblast formation.** Representative features of morphogenetic events leading to the formation of the epiblast in several amniote groups. Red: epiblast; Yellow: hypoblast; Blue: trophoblast. (A) mouse; (B) human; (C) rabbit. (Modified after Sheng, 2015).

1.3 DNA methylation and enzymes involved in DNA methylation

Control of development-related gene expression is executed by epigenetic mechanisms, especially by DNA methylation (Lee et al., 2014). DNA methylation undergoes dynamic changes during embryonic development and has to stay under tight control of DNA demethylating and methylating enzymes (Weaver et al., 2009).

DNA methyltransferases (DNMTs) create a reversible trait on the DNA by adding the methyl group to cytosine in CpG contexts (see Figure 2). A possible outcome of epigenetic processes including DNA methylation is the creation of active/repressive chromatin states and changes in chromatin accessibility (Turek-Plewa and Jagodziński, 2005). Due to modifications in chromatin conformation, a change in genes expression is induced.

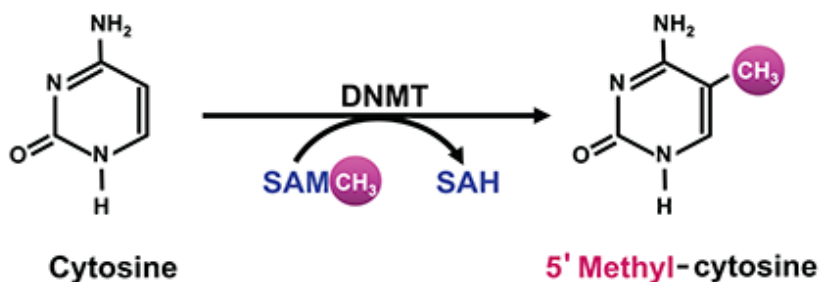


Figure 2. **Schematic representation of cytosine methylation reaction by DNA methyltransferases. DNMT converts cytosine to 5'methyl-cytosine.** DNA methylation typically occurs when cytosines are followed by a guanine (i.e., CpG motifs). SAM = S-adenosylmethionine; SAH = S-adenosylhomocysteine (modified after Zakhari, 2013).

In adult life, epigenetic patterns are permanent and define tissue-specific gene expression. During development, epigenetic marks are more dynamic and specific to embryo developmental time-points (Turek-Plewa and Jagodziński, 2005).

The dynamics of epigenetic reprogramming at the preimplantation stage is sex-specific (see details in Figure 3; Leseva et al., 2015). At first, the new zygotic genome needs to be demethylated. The result of global demethylation is a gain to a state close to pluripotency (Guibert et al., 2009). This process is accomplished by the TET family of DNA demethylases (Lee et al., 2014). The demethylation process is necessary to erase the gamete-specific methylation pattern and to start *de novo* DNA methylation patterns in later developmental stages (Sawai et al., 2010).

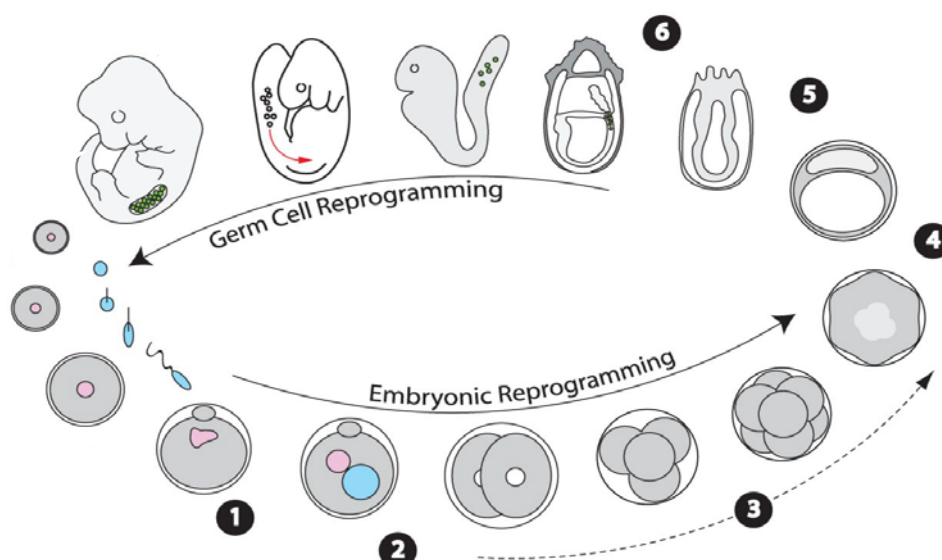


Figure 3. **Epigenetic reprogramming during the murine reproductive cycle.** (1) Epigenoms of male and female germs are specialized. (2) Postfertilization, the paternal genome (blue) is rapidly demethylated. (3) The maternal genome (pink) is passively demethylated. (4) In consequence the inner cell mass of the blastocyst is established. (5) Blastocyst cells begin to establish DNA methylation marks according to differentiation schedule. (6) Primordial Germ Cells (PGCs) in the epiblast are specified at the epigenetic level (modified after Leseva et al., 2015).

After demethylation, the DNA methylation pattern is reestablished by the activity of DNA methyltransferases DNMT3A and DNMT3B, in a process called *de novo* methylation (Uysal et al., 2015). Molecular mechanisms of DNA *de novo* methylation are not fully understood. Some studies indicate a possible role of histone modification in the induction of certain *de novo* DNA methylation patterns (Chandrasekhar and Raman, 1997). The DNMT3A methylates CpG and non-CpG islands. The importance of non-CpG methylation remains unknown.

At the beginning, DNMT3A transcripts are of maternal origin, but an embryonic expression of DNMT3A is kept during the preimplantation stage. DNMT3B is specific for CpG in repeated DNA sequences. DNMT3B expression in embryos at the preimplantation stage is higher in ICM than in TE cells. DNMT3L is a necessary protein for DNMT3, known to increase the activity of *de novo* DNMTs (Uysal et al., 2015).

DNMT1 is responsible for the maintenance of DNA methylation. After replication, DNMT1 methylates the new strand of DNA according to patterns of the old DNA strand. For this reason, DNMT1 possess a high affinity with hemi-methylated DNA (Weaver et al., 2009). The division of DNMTs and their function has recently been reviewed (Jeltsch and Jurkowska, 2014). Indeed, favoring *de novo* and maintenance of DNMTs are believed to be oversimplifications. The role of DNMT1 only as a DNMT responsible for the maintenance of DNA methylation was undermined. In a new concept, DNMT1 and DNMT3 are establishing together a *de novo* DNA methylation pattern in early embryo (Jeltsch and Jurkowska, 2014).

Mammalian genomes have a low density of CpG nucleotides, which are mainly grouped in short stretches of DNA (from 30-200 CpG per 1 kbp) being a target for DNMTs. Such structures are usually correlated with promoter regions and often this part of the gene is methylated (Guibert et al., 2009).

Regulation of DNMTs is not fully understood. They are regulated in an allosteric way by DNMTs interacting proteins and through non-coding RNAs (Jeltsch and Jurkowska, 2016). Interestingly, the expression of DNMTs seems to be also regulated by DNA methylation (Ko et al., 2005).

Current understanding of DNA methylation perceives this process as superior compared to other epigenetic marks (Jin et al., 2011). It has been proved that DNA methylation can be heritable and reversible (Kvaratskhelia et al., 2014). This process plays also an important role in gene imprinting, regulating genes in parent-of-origin specific manner (Weaver et al., 2009). DNA methylation is also recognized as protective against transposons, retrotransposons and viruses (Vassena et al., 2005). Additionally aging is usually associated with an increase in DNA methylation (Kim et al., 2009).

1.4 Oct4 protein

1.4.1 Oct4 structure and function

Oct4 belongs to the POU (Pit-Oct-Unc) family. Proteins of the POU family are transcription factors. The Oct4 protein consists of 3 domains: N-terminal domain, C-terminal domain and the high affinity sequence-specific POU domain, responsible for DNA binding. The binding to an octameric sequence motif of an ATGCAAAT consensus sequence activates the expression of its target genes (Wu and Schöler, 2014).

Since the role of Oct4 in pluripotency in 1998 was discovered, its transcriptional function was further identified as a gatekeeper of pluripotency and used to reprogram somatic cells (Stefanovic et al., 2010). Oct4 acts as a transcriptional factor as well as a chromatin remodeler by building complexes with other proteins (Pardo et al., 2010). Oct4 is associated with members of the repressor complexes NuRD and SWI/SNF, indicating that Oct4-interacting proteins are relevant to regulate its activity. Oct4 interacts also with nucleosome repositioning agents. In this way, it modulates the chromatin structure during early development events (Abboud et al., 2015).

1.4.2 Oct4 promoter organization

Oct4 is a product of the POU5F1 gene mapped in rabbit at chromosome 12q1.1. Open reading frame counts 1083 bp and encodes 360 aa protein. The gene itself contains 5 exons and four introns at approximately 6kb length (Shi et al., 2008). In humans the POU5F1 gene products have two isoforms: POU5F1_iA and POU5F1_iB (Cauffman et al., 2006). The property to promote pluripotency was assigned to POU5F1_iA, because of its nuclear location in blastocyst cells. POU5F1_iB is detectable in cytoplasm, what might explain the previously reported Oct4 expression in trophoblast cells (Cauffman et al., 2006).

Sequence analysis of Oct4 promoter showed a high similarity between the mammalian species. The rabbit Oct4 gene sequence and its expression patterns are highly conserved between the human and rabbit (Táncos et al., 2015). Rabbit Oct4 gene sequences share a great similarity in gene organization also with other orthologues from mouse and bovine (Shi et al., 2008). Multiple sequence comparisons of conserved regions and functional elements of the Oct4 promoter is shown in Table 1.

A great interest was given to the rabbit POU5F1 (Oct4) promoter region (Kobolak et al., 2009). In the 2.6 kb of the promoter sequence four conserved regions were identified. Remarkably, rabbit and human sequences of conserved regions share the highest homology among studied mammalian species.

Table 1. **Pairwise comparison method was used to compare the *POU5F1* regulatory regions of the rabbit and four mammalian species.** The largest homologies of the regions are bolded; (-) no data (adapted after Kobolak et al., 2009).

The homology (%) between the nucleotide sequences of conserved regions and the complete upstream region				
Conserved region of <i>Oryctolagus cuniculus</i>	<i>Mus musculus</i>	<i>Homo sapiens</i>	<i>Bos taurus</i>	<i>Canis familiaris</i>
CR1	82.3	88.4	86.8	84.8
CR2	92.0	93.9	90.7	-
CR3	79.6	80.9	73.8	68.2
CR4	67.6	83.6	78.0	67.1
PE 1A	76.5	73.2	77.8	83.3
PE 1B	96.0	96.4	96.4	-
DE 2A	87.5	95.0	90.0	85.7
MP	74.2	76.8	79.1	79.3
5' region	52.5	57.7	57.0	51.9

Additionally three regulation elements were recognized: a proximal enhancer 1A and 1B (PE-1A, PE-1B), and distal enhancer (DE-1A) (Kobolak et al., 2009).

Functional analysis of conserved regions inside of the *POU5F1* (Oct4) promoter revealed that the Sox2/Oct4 binding site is placed in the distal enhancer in the conserved region 4 (CR4). The hormone response element (HRE) and Sp1/Sp3 binding site are located within the conserved region 1 (CR1) together with the C/G rich region (Kobolak et al., 2009). The conserved region 1 is a part of minimal promoter, a core region required for initiation of transcription. Transcriptional factors activating (green frame) and blocking (red frame) are listed in Figure 4 (binding sites indicated with arrows).

Oct4 mRNA levels are controlled in a switch-like fashion during the differentiation due to its promoter methylation (Pardo et al., 2010). If the promoter is methylated, the transcriptional factors cannot bind to the enhancers or response elements, switching off Oct4 transcription. High methylation of Oct4 promoter correlates with low expression and inversely, low Oct4 promoter methylation correlates with high expression (Pardo et al., 2010).

Oct4 promoter methylation links with infertility and the outcome of assisted reproductive technologies (Al-Khtib et al., 2012). Oct4 promoter methylation status was used in recent studies to correlate it with embryo survival capacity and normal development.

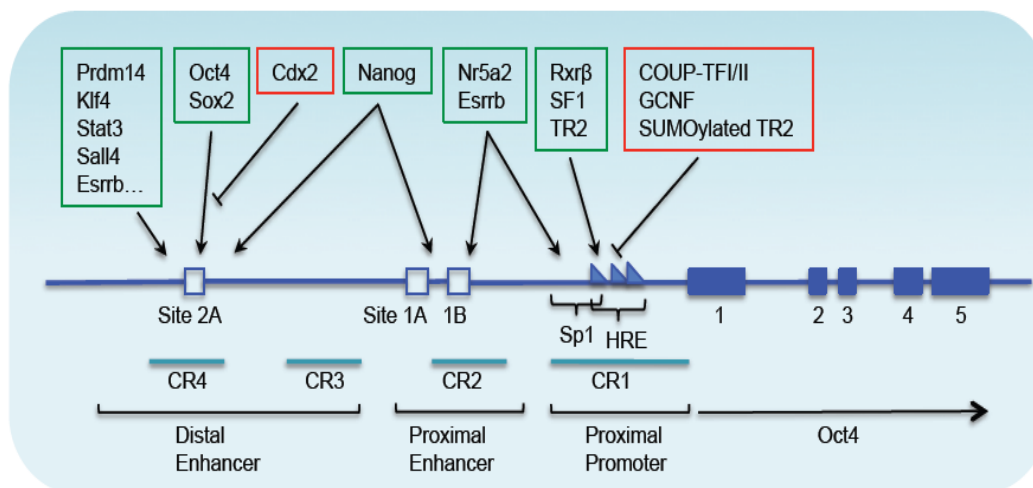


Figure 4. **POU5F1 gene structure with indication of transcriptional factors and transcriptional factors binding sites relevant for Oct4 regulation.** The transcription factors bind to these regions, and are shown above within colored boxes; they either activate (green box) or repress (red box) transcription. HRE = hormone responsive element; Sp1 = GC-rich site recognized by the Sp1/Sp3 family of transcription factors. CR1, CR2, CR3, and CR4 are conserved regions (CRs) at the 5' upstream region of the *Oct4* gene (adapted after Wu et al., 2014).

1.4.3 Oct4 expression in early development

Initiation of Oct4 embryonic expression starts at the 8 cell stage and is detected in all cells at 16-32 cell stages (Nichols et al., 1998). During the first lineage decisions Oct4 expression is excluded in the trophectoderm and restricted to the ICM and then to the epiblast. In blastocyst cells Oct4 distribution differs between species (Kurosaka et al., 2004; Nichols et al., 1998). In mouse blastocyst Oct4 is restricted only to ICM, while in bovine blastocysts Oct4 protein can be detected in trophoblast cells as well. This indicates that at the blastocyst stage Oct4 might not be the most important regulator of pluripotency in the bovine. Despite of that, Oct4 transcriptional downregulation is conserved in mammals (Kurosaka et al., 2004).

It was reported that Oct4 levels during embryogenesis are crucial for proper development (Rizzino and Wuebben, 2016). Oct4 expression is lost progressively with differentiation during embryo development and is only preserved in primordial germ cells (Cañon et al., 2011). A decrease in Oct4 levels by 50% induces differentiation toward the trophectoderm lineage, whereas a 50% increase causes differentiation into mesoderm and endoderm (Niwa et al., 2000 and Shimozaki et al., 2003).

Most studies focused on Oct4 mRNA transcript levels. The Oct4 protein cellular localization seems to indicate Oct4 activity. It was shown that Oct4 is localized only in cytoplasm in human oocytes, single blastomers, morulae and blastocysts (Cauffman et al., 2005). Nuclear localization of Oct4 is detected at the stage of compaction, what suggests that it is a time point for the Oct4 biological activity.

1.4.4 Regulation and role of Oct4 in first embryonic lineages

Oct4 is not only a key player in keeping the pluripotency, but it is also a lineage specifier. The model of Oct4 collaboration with lineage-determining transcription factors was proposed by Simandi et al., (2016). Oct4 is required to form epiblast tissue, but also for the formation of the primitive endoderm (PE), where it interacts with others pathways than in epiblast cells (Frum et al., 2013). Oct4-deficient mammalian embryos can progress up to the blastocyst stage, but promoting only extraembryonic lineages, what emphasizes the importance of Oct4 in embryoblast formation (Nichols et al., 1998).

Expression of Oct4 is regulated differently in epiblasts and in other pluripotent lineages. Activation of the Oct4 expression at the proximal enhancer of Oct4 promoter secures the epiblast derivation, while in the other pluripotent lineages Oct4 expression is driven by its distal enhancer (Gu et al., 2005). Oct4 was also used to assess the epiblast morphology, while growing evidences indicate that the epiblast lineage has a mixed homogeneity (Han et al., 2010).

It has been demonstrated that the mouse epiblast stem cells (EpiSC) are divided in subpopulations. While one population expresses Oct4, the other does not. It suggests, that epiblast cells subpopulation have distinct pluripotential capacities and therefore diverse roles in development (Han et al., 2010). Oct4 seems to gain more importance between the pluripotency pathway genes, since a Sox2 gene deficiency was recently described as a factor leading to a lower amount of Nanog, but not influencing Oct4 expression. In bovine embryos Sox2 is a marker of the ICM and is necessary to generate ICM/trophoblast lineage (Goissis et al., 2014).

Several pathways regulating Oct4 expression and function depend on the DNA methylation-mediated switch-like way (see details at Figure 5). STAT3 plays an important role in activation of Oct4 during embryonic development (Do et al., 2013). In a model of (Lif)-null embryos, where lack of LIF blocks translocation of STAT3 to the nucleus, STAT3 cannot bind to the Oct4 enhancer and does not promote its expression. Therefore STAT3 through activation of Oct4 takes part in maintenance of ICM (Do et al., 2013).

It was also demonstrated that Oct4 is recruiting the retinoic acid receptor dimer and β -catenin to gene promoters and promotes cell type-specific differential gene expression in mESC (Simandi et al., 2016). Beside of Oct4 role in the β -catenin-mediated transcription, it was shown that a balance between Oct4 and β -catenin promotes a pluripotent state and that Oct4 is involved in control of β -catenin stability (Li et al 2012; Abu-Remaileh et al., 2010).

A novel model of Oct4 regulation in ICM/trophoblast differentiation was proposed by Bou et al., in porcine embryos. It was reported that Oct4 repression by Cdx2 works in a dose dependent manner. High Cdx2 concentrations in the nucleus correlate with Oct4 translocation to cytoplasm and higher rate of its proteasome degradation. In this way Cdx2 is able to take the Oct4 chromatin binding sites and to control cell differentiation towards the trophoblast lineage (Bou et al., 2016).

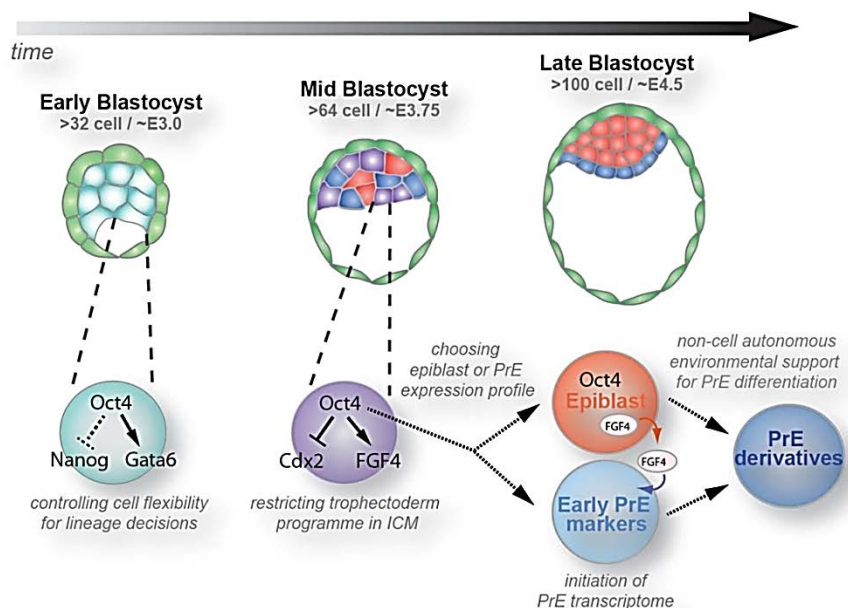


Figure 5. **Model of Oct4 functions during first lineages development in mammalian embryogenesis** (modified after Le Bin et al., 2014). PrE - primitive endoderm

It is known that together with epigenetic cofactors, Oct4 transcriptionally regulates the expression of the trophoblast lineage marker Cdx2 (Yeap et al., 2009). Oct4 binds a domain of histone methyltransferase (ESET). In consequence the histones at the Cdx2 promoter region are getting a lysine 9 trimethylation (H3K9me3) tag, which is a signal of a repressive chromatin state. This mechanism is a possible way in which the blastocyst initiates the ICM/trophoblast lineage (Yeap et al., 2009).

1.5 Environmental influence on epigenetic modifications during early development

Adaptive metabolic development is a consequence of embryo sensitivity to nutrients and hormonal signals as well as its availability in the uterine environment (Kaneko, 2016). A capacity to deal with imbalances requires a change in gene expression. Pathological conditions impacts through epigenetic factors on gene promoters, promoting more dynamic gene expression than it was anticipated (Rountree et al., 2001, Wu et al., 2012).

During the differentiation process cells start to collect a unique set of epigenetic markers (Guibert et al., 2009). Although the mammalian embryo developmental progress is controlled primary by the genetic events, the metabolic adaptation seems to be important. Nevertheless, maternal intrauterine environment impacts not only on the developmental potential or pregnancy outcome, but sets up long-lasting effects to the offspring through epigenetic modifications (Kaneko, 2016).

The maternal organism communicates with the embryo through the uterine microenvironment, where nutrients balance plays a crucial role (Velazquez, 2015). Adult diseases have their source as early as during the preimplantation phase of pregnancy through epigenetic changes (Fleming et al., 2015). In both cases: malnutrition and overnutrition generate adaptive metabolism in the

embryo (Velazquez, 2015). An often metabolic complication is the metabolic syndrome, a chronic disease and complex disorder manifested by adiposity, hyperlipidemia and hypertension (Smith et al., 2015). When a mother is affected by adiposity, has shortage of vitamin D or small period of breast-feeding, the developmental plasticity leads to childhood obesity (Godfrey et al., 2016).

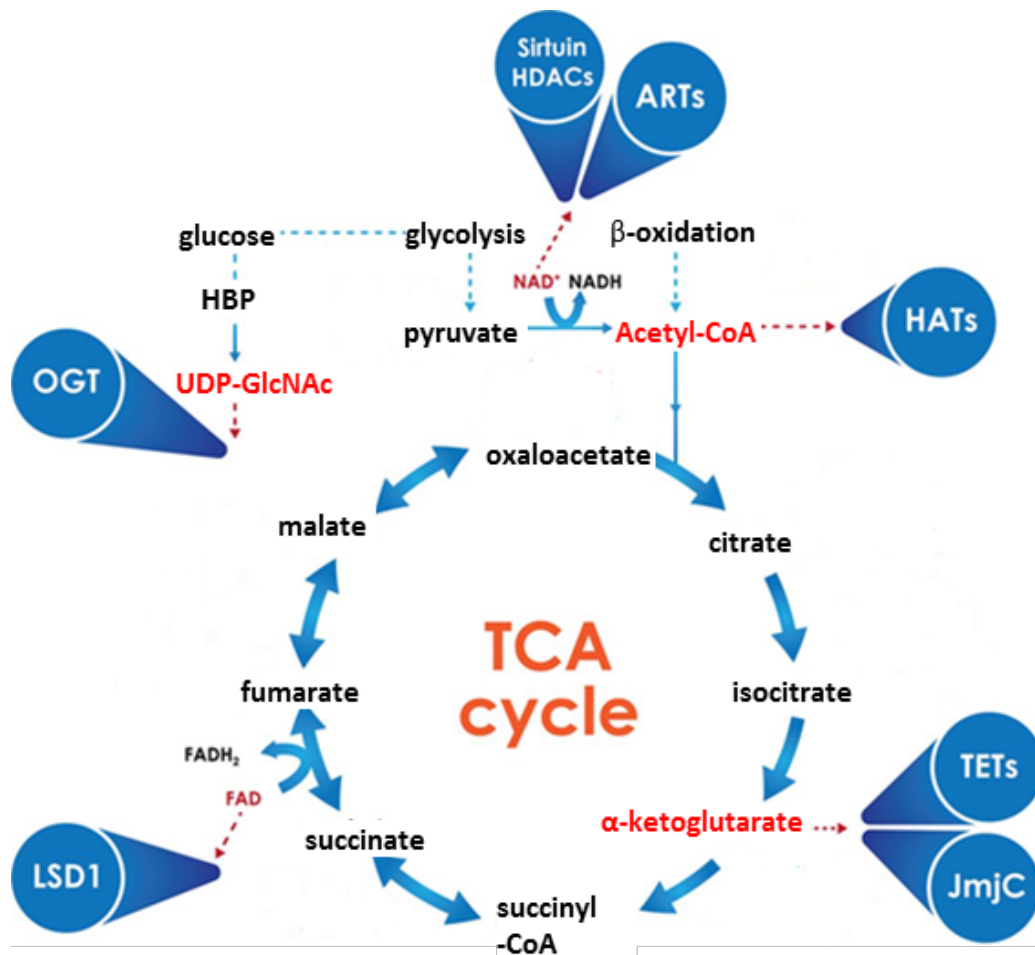


Figure 6. **Relation between the metabolism and epigenetic processes** (modified after Keating and El-Osta, 2015). OGT - N-acetylglucosaminyltransferase; LSD1 - Lysine-specific histone demethylase 1A; HATs - Histone acetyltransferases; HDACs - Histone deacetylases; JmJc – Histone demethylase.

A great deal is given to identify environmental factors influencing metabolism and changes in metabolism by epigenetic changes. There is growing evidence, that metabolism is directly changing the epigenetic potential by changes in supply of acetyl- or methyl-donor groups or by dropping down the production of co-factors for histone-modifying enzymes (see details at Figure 6; Keating and El-Osta, 2015). A new field of studies relating epigenetic to nutrition and metabolism was named nutri epigenomics (Paparo et al., 2014).

1.6 Animal diabetic pregnancies model

Diabetes is a worldwide threatening disease. Equally alarming is the fact, that an increasing number of woman is affected by diabetes during pregnancy (Silva et al., 2017). Offspring of diabetic pregnancies are suffering from multiple complications at the early stages of life as well in adulthood (El Hajj et al., 2014). Ethical reasons allows to study the mechanisms in early embryonic

development only in animal models. Induction of diabetes can be planned before conception and the most frequently used and practical animal models of diabetic pregnancy can be divided into:

- surgical, like partial pancreatectomy, giving a mild diabetes; used to induce diabetes in rats and sheep,
- genetic, like non-obese diabetic (NOD) mice, where diabetes develops spontaneously as a polygenic type with mild/severe diabetes, or due to introduction of mutation (Akita mouse has a mutation at *ins2* gene),
- chemical-induced diabetes through administration of a compound damaging pancreatic beta-cells: streptozocin, what causes usually severe type of diabetes, or alloxan, where different doses can induce either a mild or severe type of diabetes (Kiss et al., 2009; Jawerbaum et al., 2010).

1.6.1 Rabbit diabetic pregnancy model

The rabbit (*Oryctolagus cuniculus*) is often used as laboratory animal, especially in studies of physiology and pathology of development and reproduction. There are many similarities between the pregnancy in human and rabbit, embryogenesis and placentation (Fischer et al., 2012).

Rabbit blastocysts are the biggest spherical mammalian blastocysts. Large size serves not only as an opportunity to collect a lot of material for analysis, but, most importantly, also to observe morphological changes between the stages of blastocyst development during the gastrulation (see details at Figure 7).

In our model of rabbit diabetic pregnancy, diabetes is induced to female rabbits chemically by administration of alloxan. Alloxan promotes the specific destruction of pancreatic beta-cells. Two days later the rabbits present a diabetic phenotype with hyperglycemia and hypoinsulinaemia, and from this moment rabbits need to be supplemented with insulin to survive. Diabetic female rabbits are mated approximately two weeks after introduction of diabetes. Blastocysts are collected just before implantation, at day 6 *p.c.*

Embryo development under diabetic pregnancy serves a 40 % lower number of blastocysts (Ramin et al., 2010). A delay in gastrulation was observed in blastocysts from diabetic rabbits too and was expressed by downregulation of insulin-stimulated metabolic genes. One hypothesis is that due to the decrease in insulin and IGF receptors, the blastocyst cannot react properly to insulin and IGF signals, what delays gastrulation (Ramin et al., 2010). Moreover *in vitro* studies with insulin supplementation show, that insulin is necessary to promote expression of Brachyury and therefore to proceed with mesoderm formation (Thieme et al., 2012). Increased production of IGF by the endometrium might be a way to compensate insufficient amounts of insulin to secure blastocyst developmental progress (Thieme et al., 2012).

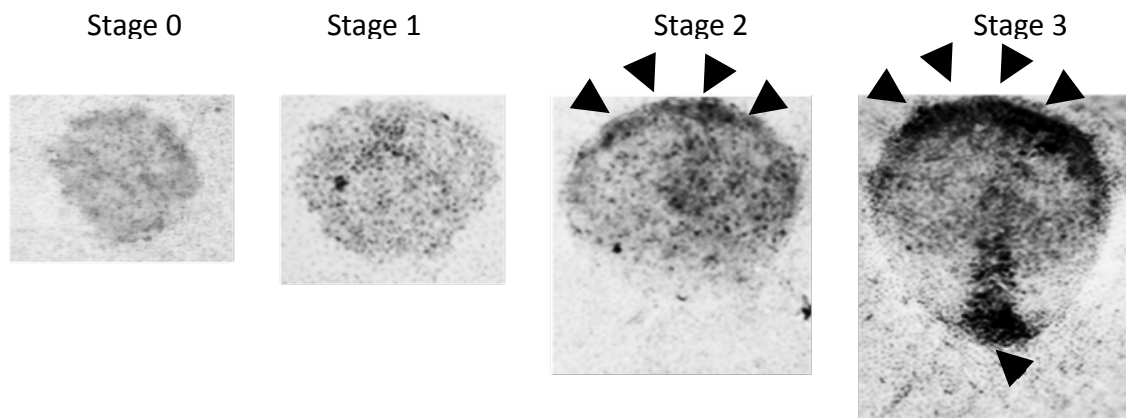


Figure 7. **Rabbit blastocyst day 6 p.c. and its gastrulation stages.** Stage 0 is characterized by an irregular shape of the embryonic disc, while at stage 1, the embryonic disc is having a defined border line. Stage 2 blastocyst undergoes gastrulation, with visible increase in density at the anterior part of embryonic disc (indicated by arrows). Elongation at the posterior pole appears at stage 3 (indicated by arrows) (modified after Viebahn et al., 1995).

1.7 Diabetes mellitus in early development – heart malformations

Danish cohort studies of offspring from diabetic pregnancies have revealed that 3.18% of live births were affected by congenital heart diseases (Øyen et al., 2016). The number is even higher, when the mother was having a previous acute diabetes complication. Moreover, the data from a Canadian cohort show a decrease in all congenital malformations general numbers, but an alarming increase in malformations caused by maternal diabetes from 0.8% in 2002/2003 up to 1.4% in 2012/2013 (Liu et al., 2015). Considering this, it is necessary to improve the preconception care and study further the molecular mechanisms underlying the origin of congenital malformations, especially in the case of diabetic pregnancies (Pauliks, 2015).

The process of heart malformation development was investigated using a mouse model. Apoptosis caused by oxidative stress was recognized as the main reason for heart malformations due to development in a diabetic pregnancy (Wu et al., 2016). Other molecular reasons tangling common malformations, like ventricular separation and outflow track development, may be connected with cell cycle inhibition (Wang et al., 2015). Moreover an oxidative stress and ER stress conditions were identified as a reason for slower proliferation of the endocardial cushions (Vijaya et al., 2013; Zhao, 2014). A downregulation of the TGF β and Wnt signaling pathways led to cardiac outflow tract defects (Wang et al., 2015; Zhao, 2014; Zhao, 2010). In animal models possible treatments were considering TGF β recombinant proteins (Activin A) and agonist as well as antioxidants like N-acetyl-L-cysteine (NAC) (Vijaya et al., 2013; Wang et al., 2015).

Studies of expression profiles related to maternal diabetes revealed upregulation of hypoxia and HIF-1 α at the protein level, as well as vascular endothelial growth factor A (VEGF-A), which can directly cause developmental malformations (Bohuslavova et al., 2015). The effect of pregestational diabetes on fetal hearts was investigated in mice (Moazzen et al., 2015). Contrary to Bohuslavova et al., downregulation of proteins and regulators of the hypoxia pathway was

reported. Additionally a disrupted epicardial epithelial-to-mesenchymal transition was reported (EMT), with glucose being identified as the main factor impairing this process (Moazzen et al., 2015).

Recently a new theory of genesis of diabetic embryopathies was proposed, where yolk sack vasculopathies are the ones, who promote further malformations of the fetus, including heart malformations. The main factors involved in the origin of yolk sack embryopathies were proteins in the hypoxia and apoptosis pathways (Dong et al., 2016).

Process of cardiogenesis is strongly depending on GATA proteins (Charron F. and Nemer M.; 1999). The importance of GATA-4 in activation of Nkx 2.5 was shown in the mouse model, where overexpression of GATA-4 caused upregulation of Nkx 2.5 (Brewer, 2005; Molkentin et al., 2000). Interestingly, clinical data about patients with non-syndromic congenital heart defects mutations were observed in genes which are relevant for early fetal heart development, like NKX2.5, GATA4, GATA6, and MEF2C (Kodo et al., 2012). Clinical data show that mutations carrying loss-of-function and dysregulation at transcriptional level of GATA6 gene are also associated with minor heart defect in human offspring of diabetic pregnancies (Chao et al., 2015). It is probable that an insight in expression profiles of the mentioned genes will help to understand the pathogenesis of heart malformations caused by maternal diabetes.

2. Materials and methods

2.1 Materials: chemicals and prefabricated systems

10x Buffer B with BSA	Fermentas GmbH, St. Leon-Rot, Germany
10x Crimson Taq Buffer	New England Biolabs Inc., Ipswich, Massachusetts, USA
10x DNase I Buffer	Promega Corporation, Madison, Wisconsin, USA
2x <i>Rapid Ligation Buffer</i>	Promega GmbH, Mannheim, Germany
5x PCR Buffer	New England Biolabs GmbH, Frankfurt am Main, Germany
5x Reaction Buffer	Thermo Fisher Scientific Inc., Ipswich, Massachusetts, USA
Acetate	Carl Roth GmbH & Co. KG, Karlsruhe, Germany
Acetic acid	Carl-Roth GmbH & Co.KG, Karlsruhe, Germany
Agar agar Carl	Roth GmbH & Co. KG, Karlsruhe, Germany
Agarose	Biozym Scientific GmbH, Hessisch Oldendorf, Germany
Alloxan	Sigma-Aldrich, Taufkirchen, Germany
Ampicillin	Carl Roth GmbH & Co. KG, Karlsruhe, Germany
Apa I (10 U/μl)	Thermo Fisher Scientific Inc., Ipswich, Massachusetts, USA
BigDye® Terminator v1.1 Cycle Sequencing Kit	Applied Biosystems, Darmstadt, Germany
Bovines Serum Albumin (BSA)	Serva Electrophoresis GmbH, Heidelberg, Germany
Bromphenol Blue sodium salt	Sigma-Aldrich Co., Steinheim, Germany
BSM II	Biochrom AG, Berlin, Germany
Chloral hydrate	Fuka Chemie AG, Steinheim, Germany
Chloroform	Carl Roth GmbH & Co. KG, Karlsruhe, Germany
Citric acid	Merck, Darmstadt, Germany
Crimson <i>Taq</i> ™ DNA-Polymerase (5 U/ml)	New England Biolabs GmbH, Frankfurt am Main, Germany
Diethylpyrocarbonat (DEPC)	Sigma-Aldrich, Taufkirchen, Germany
Dithiothreitol (DTT)	Carl-Roth GmbH & Co.KG, Karlsruhe
DNA Ladder 100bp <i>Gene Ruler</i>	Thermo Fisher Scientific Inc., Ipswich, Massachusetts, USA
DNA-free™ (<i>DNase-Treatment & Removal</i>)	Ambion INC, Austin
DNase Inactivation Reagent	Promega Corporation, Madison, Wisconsin, USA
dNTP-mixture	Fermentas GmbH, St. Leon-Rot, Germany
Domitor®	SPC Janssen Animal Health, Neuss
Dynabeads® mRNA Direct™ Kit	Invitrogen, Karlsruhe, Germany
EpiTect® Plus DNA Bisulfite Kit	Qiagen GmbH, Hilden, Germany
EpiTect® Plus LyseAll Lysis Kit	Qiagen GmbH, Hilden, Germany
Ethanol absolute	Sigma-Aldrich Co., Steinheim, Germany
Ethidium bromide	Carl Roth GmbH & Co. KG, Karlsruhe, Germany
Ethylendiamintetraazetat (EDTA)	Sigma-Aldrich, Taufkirchen, Germany
Glucose	Sigma-Aldrich Chemie GmbH, Steinheim
Glycerin	Serva Electrophoresis GmbH, Heidelberg
Glycerol	Carl Roth GmbH & Co. KG, Karlsruhe, Germany
HOT BIOAmp 10x Buffer B2 (Mg ²⁺ free)	Biofidal, Vaulx en Velin, France
HOT BIOAmp® DNA Polymerase (5 U/μl)	Biofidal, Vaulx en Velin, France

Humanes Choriongonadotropin (hCG)	Intervet, Unterschleißheim, Germany
Hydrochloric acid (36%)	Carl-Roth GmbH & Co.KG, Karlsruhe, Germany
Hydrogen peroxide	Merck KGaA, Darmstadt, Germany
IGF2	Life Technologies, Darmstadt, Germany
Insulin (bovin)	Sigma-Aldrich Chemie GmbH, München
Insulin	Life Technologies, Darmstadt, Germany
Isopropanol	Carl Roth GmbH & Co. KG, Karlsruhe, Germany
Isopropyl- β -D-thiogalaktopyranosid (IPTG)	Carl-Roth GmbH & Co.KG, Karlsruhe, Germany
Potassium aluminum sulfate	Merck, Darmstadt, Germany
Ketanest®	Pfizer, Karlsruhe, Germany
Leucine, Isoloucine, Valin, Methionine	AppliChem GmbH, Darmstadt, Germany
Magnesium chloride	Serva Electrophoresis GmbH, Heidelberg, Germany
Magnesium sulfate	Serva Electrophoresis GmbH, Heidelberg, Germany
MESA Blue qPCR® Mastermix Plus for SYBR®	
Methanol	Carl-Roth GmbH & Co.KG, Karlsruhe, Germany
Monarch® Plasmid DNA Miniprep Kit	New England Biolabs Inc., Ipswich, Massachusetts, USA
NaCl (isotonic)	Fresenius Kabi Deutschland GmbH, Bad Homburg, Germany
NaCl	Carl-Roth GmbH & Co.KG, Karlsruhe, Germany
Neb 5-alpha Competent <i>E.coli</i> cells	New England Biolabs Inc., Ipswich, Massachusetts, USA
Oligonukleotide	Sigma-Aldrich, Taufkirchen, Germany
Penicillin/ Streptomycin	PAA GmbH, Cölbe, Germany
Pentobarbital	Sigma-Aldrich, Taufkirchen, Germany
Pepton	Carl Roth GmbH & Co. KG, Karlsruhe, Germany
peqGold TriFast™	Peqlab Biotechnologie GmbH, Erlangen, Germany
pGEM®-T Vector System I	Promega Corporation, Madison, Wisconsin, USA
Phosphate buffer solution (PBS)	Dulbecco Biochrom AG, Berlin, Germany
Plasmid Miniprep Kit I, peqGOLD	Peqlab Biotechnologie GmbH, Erlangen, Germany
Potassium chloride	Carl Roth GmbH & Co. KG, Karlsruhe, Germany
Precellys beads	Peqlab Biotechnologie GmbH, Erlangen, Germany
Pregnant Mare Serum Gonadotropin (PMSG)	Intervet, Unterschleißheim, Germany
QIAGEN Plasmid Mini Kit	Qiagen, Hilden, Germany
QIAquick® Gel Extraction Kit	Qiagen, Hilden, Germany
Random Primer	Thermo Fisher Scientific Inc., Ipswich, Massachusetts, USA
rDNase I	Promega Corporation, Madison, Wisconsin, USA
Reika feed	Reinsdorf Kraftfutterwerk, Reinsdorf, Germany
Reverse Transcriptase (200 U/ μ l)	Thermo Fisher Scientific Inc., Ipswich, Massachusetts, USA
rRNasin® RNase-Inhibitor	Promega Corporation, Madison, Wisconsin, USA
Sac I (10 U/ μ l)	Thermo Fisher Scientific Inc., Ipswich, Massachusetts, USA
Sodium acetate	Serva Electrophoresis GmbH, Heidelberg, Germany

Sodium chloride	Carl Roth GmbH & Co. KG, Karlsruhe, Germany
Sodium hydroxide	Merck KGaA, Darmstadt, Germany
Sodiumdodecylsulfate (SDS)	Serva Electrophoresis GmbH, Heidelberg, Germany
T4 DNA-Ligase (3 U/μl)	Promega GmbH, Mannheim, Germany
TRI Reagent®	Sigma-Aldrich Co., Steinheim, Germany
TRIS	Carl Roth GmbH & Co. KG, Karlsruhe, Germany
Triton X100	Sigma-Aldrich, St. Louis, US
Tween® 20	Sigma-Aldrich, Taufkirchen, Germany
X-Gal	Carl Roth GmbH & Co. KG, Karlsruhe, Germany
Yeast extract	Carl Roth GmbH & Co. KG, Karlsruhe, Germany
α-D-Glucose	Serva Electrophoresis GmbH, Heidelberg, Germany
ε-Aminocarpoic acid	Sigma-Aldrich, Taufkirchen, Germany

2.2 Laboratory equipment

Incubator	Heraeus, Hanau
Incubator	HERACell 150i (Stimulation) Thermo Fisher Scientific GmbH, Bonn
Electrophoresis Power Supply EV 202	Consort, Turnhout, Belgium
Gel Documentation System	LTF Labortechnik
Gel electrophoresis chamber	Agagel Mini und Maxi Biometra, Göttingen
LaminAir® HP72 (semi-sterile work bench)	Heraeus, Hanau
Cooling centrifuge, Biofuge fresco 17	Heraeus, Hanau
Magnetic stirrer with heating MR 2002	Heidolph, Schwabach
Microwave	AEG
Mikroskop Olympus IX-70	Olympus, Hamburg
Novex Electrophoresis chamber	Invitrogen, Karlsruhe
Precision® Xceed™ (Blood glucose meter)	Abott, Wiesbaden
Precellys24 lysis & homogenization (Homogenisator)	peqLab Biotechnologie GmbH, Erlangen
Rotary vacuum concentrator RVC 2-18	Christ, Osterode
Shaker GFL 3006	GFL, Burgwedel
Spektrophotometer Nano Vue™ GE	Healthcare, München
StepOnePlus™ Real-Time PCR Systems	Applied Biosystems, Darmstadt
Thermocycler T3000	Biometra, Göttingen
Vortex-Genie 2 (G560E)	Scientific Industries, Inc., New York
Weihl BP 210 S & BP 3100 S	Sartorius, Göttingen
Waterbath	GFL, Burgwedel
Centrifuge Biofuge 13	Heraeus, Hanau

2.4 Animal model

An animal model used for experiments was the Rabbits of New Zealand ZiKa hybrid obtained from R. Krieg breeding farm (Niederwuensch, Germany).

Sexually mature female rabbits with a body weight between 3.5 to 4.5 kg were kept in single cages in room with defined day and night rhythm 12:12 hours and the temperature of 18°C. Rabbits were fed *ad libitum* with dry fodder (REIKA Kraftfutter) and water. The animals chosen for experiments were resting at least two weeks before the time of experiment started.

2.4.1 Embryo recovery

Female rabbits were injected subcutaneously with 150 U of pregnant mare's serum gonadotropin (PMSG) three days before mating with fertile male rabbits. To support the ovulation, 75 U of human choriongonadotropin (hCG) was injected in the *Vena auricularis* after mating. The embryos were harvested 6, 12 and 14 days after coitus (*post coitum, p.c.*). At first the rabbits were sacrificed with injection of high dose of pentobarbital. Then uteri and ovaries with oviducts were cut out. Embryos were wash out of the uteri with the wash media (basal synthetic medium (BSM II)) under the semi-sterile bench. The wash was repeated two times in order to remove the remaining uterus tissue and its secretion.

BSM II

Basal Synthetic Medium (BSM)	7.64	g/l
NaHCO ₃	2.1	g/l
Glucose	1.8	g/l
Penicillin	0.061	g/l
Streptomycin	0.15	g/l

The embryos recovered out of three to four rabbits were pooled together to randomize the embryos, staged according to morphology described in Fischer et al., (2012) and prepared for dissections or *in vitro* culture. Heart dissections at embryos day 12 and 14 was done mechanically with usage of micro scissors and forceps. Fetal hearts day 12 and day 14 were store in -80⁰C.

2.4.2 Embryo dissections

Embryo was dissected in cold PBS. Stage 0 blastocysts were dissected into two embryonic tissues: embryoblast and trophoblast, while stage 2 embryos were dissected already in three embryonic tissues: epiblast, hypoblast and trophoblast. All samples were frozen down in – 80⁰C till the moment of analysis.

PBS (phosphate buffered saline (pH 7,4))

Sodium chloride (NaCl)	8.00	g
Potassium chloride (KCl)	0.20	g
Disodium hydrogen phosphate	1.44	g
Potassium dihydrogenphosphate	0.24	g
<i>Aqua dest.</i>	Ad 1L	

2.4.3 Embryo *in vitro* culture

Stage 1 embryos were shortly washed in adapting media (BSM II with 1.5 % BSA), then divided in groups of 4-5 embryos and transferred to culture dish with 1 ml of culture media.

To study the influence of branched chained amino acids (BCAAs) on embryo, the stimulation with of leucine (99.85 μM), isoleucine (19.8 μM), valine (29.87 μM) and methionine (30.17 μM) was employed (according to Gürke et al., 2016).

<u>Media with normal concentration of BCAAs:</u>			<u>Media with diabetic concentration of BCAAs:</u>		
Leucine	7.5	μl	Leucine	24.86	μl
Isoleucine	5.6	μl	Isoleucine	17.66	μl
Valine	17.8	μl	Valine	39.06	μl
Methionine	2.0	μl	Methionine	2.0	μl
Medium BSM	<i>ad 10 ml</i>		Medium BSM	<i>ad 10 ml</i>	

The influence of insulin and IGF2 was studied by 2h preculture and 4h culture with addition of 17 nM insulin or 13 nM IGF2. All *in vitro* culture procedures were carried in incubator under 5 % O₂, 5 % CO₂ and 90 % of N₂ in 37⁰C. After *in vitro* culture embryos were dissected into epiblast, hypoblast and trophoblasts. The embryonic tissues of 4-5 embryos from each group were pooled together. LIF stimulated embryo sample were previously generated by the group as a whole embryo sample.

2.4.4 Induction of Diabetes mellitus Type 1

In order to introduce diabetes to female rabbits an Alloxan (Sigma-Aldrich) injection was performed in ear vein regarding to body weight (120 mg/kg). Alloxan recognizes and destructs pancreatic β-cells, what leads to diabetes. Anesthesia was carried by intramuscular injection of Ketanest (15 mg/kg body weight; Pfizer, Berlin, Germany) and Dorbene (Domitor, 0.25 mg/kg body weight; Zoetis, Berlin, Germany). Rabbits established diabetes in 48 h post treatment exhibiting hyperglycemia and hyperinsulinemia and after this time an insulin supplementation was initiated (0.5 – 3 I. E., 3 times per day). Rabbits were kept diabetic at least for two weeks prior mating.

2.4.5 Recovery of maternal blood plasma

Blood probes were collected from female pregnant rabbits at day 6 of pregnancy from the lateral ear vein (Vena auricularis lateralis) to EDTA-Monovette. Then blood was centrifuged for 15 min in 2000 rpm (300 x g) in 4⁰C. The upper part (plasma) was transferred to new tubes and frozen down in -80⁰C until sending for the metabolite: SAM (S-adenosyl methionine) and SAH (S-adenosyl homocysteine) measurements (UPLC-MS/MS) to University Clinic of Saarland and Medical Faculty of the University of Saarland.

2.5 SAM and SAH levels measurements

Quantification of SAM (methyl group donor in methylation reactions) and SAH (side product of methylation reactions) was done by ultra performance liquid chromatography tandem mass spectrometry (UPLC-MS/MS) by Prof. Rima Obeid group according to method described by Kirsch et al., (2009).

2.6 mRNA isolation from embryonic tissues

Isolation of mRNA of the embryonic tissues was performed using a Dynabeads^R mRNA DirectTM Purification Kit (Invitrogen, Karlsruhe, Germany). This isolation protocol relies on base paring between the poly A residues at the 3' end of the most mRNA, and the oligo (dT)₂₅ residues covalently coupled to the surface of the Dynabeads[®]. At first sample was prepared for isolation by

removal of remaining PBS by a centrifugation 10 (6) min, 13000 rpm. Next step was lysis by addition of 150 μ l lysis buffer/per sample and incubate with continuous mixing for 10 min at room temperature (600 rpm IKAMS3 digital). The Dynabeads[®] were suspended and prepared for further steps, then transferred 13 μ l of beads (for whole embryo) or 10 μ l of beads (in case of embryoblast/trophoblast or epiblast/hypoblast/trophoblast separation) from the stock tube to an RNase-free 1,5 ml tube. Tubes with Dynabeads[®] were placed on a Magnetic Particle Concentrator (Dyna MPC[®]) for 1-2 min, then the supernatant was removed with the pipette while the tube remains on the magnet. 10 μ l Binding Buffer (BB) was add to sample to suspend the beads and placed back on the magnet for 1-2 min. This step was repeated twice (removal of the supernatant done only while the tube remained on the magnet). Prepared beads were suspended in 10 μ l Binding Buffer. Finally isolation of mRNA was done by addition of 10 μ l of beads to each sample, then incubation with continuous mixing for 10 min at room temperature. Next vials were placed on the magnet for 1 min and remove the supernatant. The Dynabeads[®]/mRNA complex was washed two times with 100 μ l of Washing Buffer A and three times with 100 μ l of Washing Buffer B with usage of magnet to for separation of the beads from solution. Finally 11 μ l of PCR-H₂O to the beads/mRNA complex out of magnet and incubate at 65 °C for 3 min to release mRNA. Supernatants with mRNA were immediately transferred to new RNase-free tube and kept on ice till cDNA synthesis.

Binding buffer:

20 mM Tris-HCl, pH 7.5
1.0 M LiCl
2 mM EDTA

Washing buffer A:

10 mM Tris-HCl, pH 7.5
0.15 M LiCl
1 mM EDTA
0.1% LiDS

Lysis/Binding buffer:

100 mM Tris-HCl, pH 7.5
500 mM LiCl
10 mM EDTA, pH 7
1% LiDS
5 mM dithiothreitol (DTT)

Washing buffer B:

10 mM Tris-HCl, pH 7.5
0.15 mM LiCl
1 mM EDTA

2.7 cDNA synthesis for embryonic tissues

cDNA synthesis is a reaction catalyzed by Reverse Transcriptase. In this step a whole isolated mRNA isolated from embryonic tissues was reverted to complementary DNA (cDNA).

Reaction setup for embryonic tissues (per one sample):

10 x Buffer		2 μ l
MgCl ₂	50 mM	2 μ l
dNTP	10 mM	2 μ l
Random primer	50 pM	1 μ l
Reverse Transcriptase	200 U/ μ l	0.5 μ l
RNase-Inhibitor	40U/ μ g RNA	0.2 μ l
H ₂ O		1.3 μ l

9 μ l of mastermix was distributed to each tube.

cDNA synthesis requires the thermocycler conditions: 25 °C for 10 min; 45 °C for 60 min; 99 °C for 5 min.

After the reaction, probes were filled with water depending on the type of tissue: epiblast - 20 µl, hypoblast - 20 µl, trophoblast - 60 µl and in case of whole embryo with 80 µl.

2.8 RNA isolation from rabbit tissues

Isolation of the RNA from rabbit fetal hearts as well as the adult rabbit tissues was performed using a protocol TRIzol® method. Frozen tissue was transferred to vials. 1 ml of TRIzol® Reagent was added. In order to homogenize the tissue ceramic beads Precellys (Precellys24) were used, till a homogenous suspension was observed. Next 0.2 ml of chloroform per 1 ml of TRIzol® was added and shook vigorously for 15 sec. After incubation for 10 min samples were centrifuged at 13000 rpm for 15 min at 4 °C. Centrifugation separates the mixture into 3 phases: a red organic phase containing the protein, an interphase, usually white, containing the DNA and proteins, and a colorless upper aqueous phase (containing RNA). The colorless upper aqueous phase was transferred to a new clean tube, avoiding the interphase (containing the DNA). Up to 700 µl of a colorless phase were transferred to the new tube (the interphase and organic phase was stored at 4 °C for subsequent isolation of the DNA). Isopropanol was added in the same per ml of used TRIzol® reagent to precipitate RNA, then mixed gently by inverting the sample five times. After 10 min at room temperature incubation, samples were centrifuged at 13000 rpm for 15 min at 4 °C. Supernatant was removed in order to wash the RNA pellet by adding 1 ml of 70 % ethanol per 1 ml of TRIzol® used in sample preparation, centrifuged for 15min at 13000 rpm. Supernatant was removed and the wash was repeated two times more. RNA pellet dehydrated using SpeedVacc (10 min). Dry RNA pellet was resuspended in DEPC-treated water.

The quantity of RNA was measured with *NanoVue* spectrophotometer and the quality of RNA was assessed by agarose gel electrophoresis with 0.5 µg of RNA from each sample.

2.8.1 DNase digestion

To eliminate any genomic DNA out of the RNA sample, a 30 min of DNase digestion according to RNA-free™Kit DNase Treatment and Removal Reagents Catalog Number AM1906 was applied. At first 0.1 volume of 10X DNase I Buffer and 1 µL rDNase I was added to the RNA, mixed gently and incubated at 37°C for 30 min. Next a DNase Inactivation Reagent (0.1 volume) was added, mixed and incubated 2 min at room temperature, with occasional mixing. Then RNA sample was centrifuged at 13000 rpm for 1.5 min and supernatant was transferred to a fresh tube.

Standard DNase reaction was set up for 6 µg of RNA with following master mix:

DNase Buffer	2.5 µl
rDNase (2U/up to 10 µg RNA)	2 µl
<u>RNase inhibitor (40 U/µg RNA)</u>	<u>0.5 µl</u>
DEPC water	ad 25 µl
DNase Inactivation Reagent	2.5 µl

To confirm that the digestion reaction was successful, a PCR with GAPDH primers on RNA was performed. Products of PCR reactions were developed by electrophoresis in agarose gel and no signal was interpreted as a DNA-free RNA sample. Quantity of RNA was measured again with *NanoVue* spectrophotometer. DNA-free RNA samples were used to generate cDNA libraries.

2.8.2 cDNA synthesis from RNA of rabbit tissue

2µg of RNA was used to prepare a cDNA from RNA of rabbit tissue. Standard reaction was done with following procedure. At first volume of 2 µg of RNA was adjusted up to 11,5 µl with DEPC water. Addition of 1 µl of *random* primer (50 pmol) requires 10 min incubation in 70 °C. Next master mix is distributed and reaction proceeds under following conditions: 10 min in 22 °C, 50 min in 42 °C and 15 min in 70 °C.

Reverse transcription master mix

5xRT-Buffer		4 µl
RNase-inhibitor	(40 U/µg RNA)	0.5 µl
dNTP	(10 mM)	2 µl
Superscript II (RT)	(200 U/µl)	1 µl

To define, if the cDNA synthesis reaction was proper, a PCR reaction with GAPDH primers was performed. Products of the PCR reaction were developed by electrophoresis in agarose gel. cDNA libraries were used to assess transcription level of specific genes using real time quantitative PCR reactions.

2.9 Polymerase chain reactions (PCRs)

2.9.1 Reverse transcriptase-Polymerase chain reaction (RT-PCR)

If cDNA library is prepared properly, the target genes can be amplified. To check if the cDNA synthesis reaction was successful, a PCR with GAPDH primers was performed. Primers used in PCR reaction are listed in Table 2.

<u>Following mastermix was used per one standard reaction:</u>			<u>Reaction was carried in thermocycler under following conditions:</u>		
Buffer Taq	5	µl	Denaturation (initiation)	95 °C	4 min
Primer <i>forward</i>	0.5	µl	Denaturation	95 °C	1 min
Primer <i>reverse</i>	0.5	µl	Primer annealing	60 °C	1 min
dNTP	0.5	µl	Elongation	72 °C	1 min
Taq DNA-Polymerase	0.125	µl	Final elongation	72 °C	10 min
<i>Aqua dest.</i>	17.875	µl	Final hold	4 °C	∞

Denaturation, primer annealing and elongation were repeated 40 times. Primer annealing temperature was always adjusted to specific primer set (details in Table 2). Products of PCR reaction were developed using electrophoresis in an agarose gel.

Table 2. **Primer list of oligonucleotides used in PCR reactions with the length of PCR reaction product.**

Name		Number of base pairs	Primer sequence 5' -> 3'	Fragment length (bp)
hum_DNMT3A	<i>forward</i>	21	GTGGGGGACTGTGTCTTCTGT	204
	<i>reverse</i>	20	TGAAAGCTGCATGCCTCAC	
rab_Cdx2	<i>forward</i>	15	GACCCGAAAGGCCTA	158
	<i>reverse</i>	15	ACCAGGCGAAAATAC	
rab_DNMT1	<i>forward</i>	20	CGCAACAAAGTCCAGGTGAA	211
	<i>reverse</i>	20	TGAAGCAGGTGAGTTTGTGC	
rab_DNMT3B	<i>forward</i>	20	GAGACAGAGATGCGGATGGA	240
	<i>reverse</i>	20	TGAAGTGTGGCTGAACAAC	
rab_GAPDH	<i>forward</i>	19	GCCGCTTCTTCTCGTGCAG	144
	<i>reverse</i>	24	ATGGATCATTGATGGCGACAACAT	
rab_GATA4	<i>forward</i>	20	AAACCAGAAAACGGAAGCCC	179
	<i>reverse</i>	20	ATAGTGAGATGACAGCCCGG	
rab_GATA6	<i>forward</i>	20	TGTGCAATGCTTGTGGACTC	223
	<i>reverse</i>	20	GCTGTGGGTTGTGTTGTAGG	
rab_Hex	<i>forward</i>	20	TCCAACGACCAGACCATTGA	180
	<i>reverse</i>	20	TTTGCCGCTTTGAGGGTTTT	
rab_KAT2B	<i>forward</i>	20	CCATCTCAACGAAGACTGCG	195
	<i>reverse</i>	20	TGCTTGTCCAGCAGTTGTC	
rab_Mef2C	<i>forward</i>	20	ACCAGGACAAGGAATGGGAG	203
	<i>reverse</i>	20	TAGTGCAAGCTCCCAACTGA	
rab_Nanog	<i>forward</i>	20	CCAGGTGCCTCTTACAGACA	209
	<i>reverse</i>	20	TGTCATTGAGCACACACAGC	
rab_Nkx2-5	<i>forward</i>	20	ACAACCTCGTGAACCTCGGC	216
	<i>reverse</i>	20	CGGAGAGACGGAGGATGATG	
rab_Oct4	<i>forward</i>	20	CGGAAGAGAAAGCGAACGAG	214
	<i>reverse</i>	20	TGGCCTCAAATCCTCTCGT	
rab_SetDB1	<i>forward</i>	20	GAAGCTCCGTGAAGCTATGG	223
	<i>reverse</i>	20	CGTCTTGGTCTCTTCTTGC	
rab_Sox2	<i>forward</i>	18	AGCATGATGCAGGAGCAG	229
	<i>reverse</i>	17	GGAGTGGGAGGAAGAGG	

2.10 Bisulfite sequencing

Bisulfite sequencing method was used to determine DNA methylation patterns of specific gene POU5F1 promoter. The basis of the method is ability to convert of the cytosine to uracil in the DNA sequence. Only unmethylated cytosine is prone to bisulfite conversion, so all methylated cytosine remained cytosine. A subsequent step is PCR reaction, where during amplification DNA with uracil (unmethylated cytosine) are rewrite as thymine and cytosine remain cytosine.

Products of PCR reactions are cloned into plasmids, what creates a possibility for sequencing. Principal of bisulfite sequencing are shown at Figure 8.

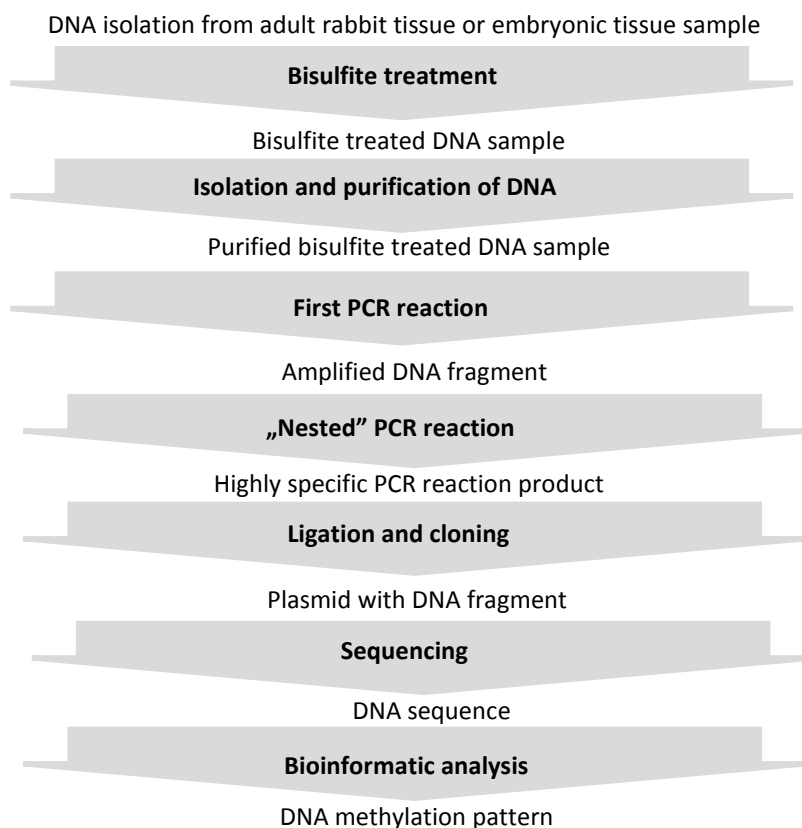


Figure 8. **Flow chart of the bisulfite sequencing method.**

2.10.1 Genomic DNA isolation of rabbit tissue

EpiTeck Plus LyseAll Lysis Kit (QIAGEN) is adjusted to samples with small amount of DNA. For this reason genomic DNA of rabbit tissue (heart) was isolated using following protocol. RNA extraction with TRIzol® offers an opportunity to use phase separation to obtain RNA and DNA layers. After removing the aqueous layer which contains RNA, DNA can be further extracted and purified. In order to do that, back extraction buffer was added to the intermediate and lower phase (0.5 ml of per ml of used TRIzol®). Samples were shook vigorously for 15 seconds and kept it for 10-15 min at room temperature, centrifuged down and the aqueous layer which contains the DNA was transferred to a separate tube. DNA was precipitated with 0.5 ml of isopropanol per ml of used TRIzol® used, mixed by inversion and incubated for 5 min in room temperature. Then samples were centrifuged with 13000 rpm for 5 min and supernatant was removed. DNA was washed additionally two times with 1 ml of 70% ethanol, centrifuged (13000 rpm, 5 min). Supernatant was removed and pellet was left for 20 min to dry. DNA sample were diluted in RNase and DNase-free water. Concentration was measured using *NanoVue*.

Back extraction buffer (for 250 ml):

Guanidine Thiocyanate 4 M
 Sodium Citrate NaCl 50 mM
 Tris (free base)Tris 1 M
 pH adjusted to 8.5-9 by addition of HCl
Aqua dest.

2.10.2 Bisulfite conversion

Bisulfite conversion was performed with EpiTeck Plus LyseAll Lysis Kit (QIAGEN). Pools of 3 epiblasts, hypoblasts and trophoblasts were thawed, centrifuged and the PBS was removed. To each pool of embryonic tissues and to 2 µg of DNA of rabbit adult heart tissue a volume of 10 µl of H₂O (RNase, DNase free), 10 µl of PBS (filtrated), 15 µl of the Lysis Buffer FTB and 5 µl proteinase K (x U/µl) was added. Samples were vortexed and briefly centrifuged, then incubated per 30min at 56°C in a thermoblock. After lysis samples were set up for bisulfite reaction. At first Bisulfite Mix powder was dissolved with the 800µl H₂O, with of the mixture the heating to 60°C. 85µl of bisulfite and 15µl of DNA protect buffer was added to all tubes. The reaction was carried under following thermocycler conditions:

Denaturation	5 min	95 °C
Conversion	25 min	60 °C
Denaturation	5 min	95 °C
Conversion	25 min	60 °C
Denaturation	5 min	95 °C
Conversion	2h 55 min	60 °C
Final hold		20 °C

2.10.3 Purification of bisulfate treated DNA

Embryonic tissues sample post lysis were directly treated with bisulfite to minimize loss of DNA used for conversion. In order to prepare converted DNA for further PCR reactions it need to be purified. Clean-up of the sample was accomplished with EpiTeck Kit (QIAGEN). First steps of the purification up till the wash should were performed for one sample at once in order to recover the highest amount of the DNA. Before starting with the purification BL Buffer was supplemented by dissolving carrier RNA to enhance DNA recovery. Samples were briefly centrifuged after bisulfite conversion and the content was transferred to the new 1.5 ml tube. 310 µl of BL Buffer was added subsequently, vortex and centrifuged briefly. Next 250 µl of ethanol (96 %) was added, mixed by pulse vortexing for 15 sec and briefly centrifuged. Then entire content was moved to the MinElute DNA spin column. Once the sample was applied on the column, the next one could be handed and prepared with the same manner. Spin columns were centrifuged at 13000 rpm for 1 min, and the flow-through was discarded together with collecting tube. Next 500µl of Buffer BW was applied to each spin column, columns were centrifuged at 13000 rpm for 1min, and again the flow-through was discarded together with collecting tube. Then 500µl of Buffer BD was added to each spin column, spin column lids was closed for proper incubation for 15 min at room

temperature (to minimize the exposure of BD Buffer to air and light and prevent acidification). Subsequently columns were centrifuged at 13000 rpm for 1min, trash the flow-through with the collecting tube. Next 500µl of Buffer BW was applied, columns were centrifuge the tube at 13000 rpm for 1min and flow-through discarded with the collecting tube (this wash was repeated twice). Lastly columns were washed with 250 µl of ethanol (96 %) and centrifuged at 13000 rpm for 1min, flow-through discarded with the collecting tube. Membranes were left to dry over 5 min with an open lid. Elution of converted DNA bounded to the column was performed with 20 µl of Elution Buffer. After 2 min of incubation, sample was collected by centrifugation for 1 min at 13000 rpm.

2.10.4 “Nested” PCR reaction with Conserved region-specific primers of POU5F1 (Oct4) gene promoter

PCR reaction was set up for chosen to be performed for two conserved regions (CRs) at POU5F1 (Oct4) promoter region: CR1 and CR4. Because of a small amount of cells, bisulfite treated and recovered DNA levels are to low and need to be amplified. In order to multiply the specific genomic DNA fragments and keep the specificity high, a “nested” PCR was applied. Primers used in this reaction were provided by Blachère T. and Godet M. from Stem-cell and Brain Research Institute (INSERM, University of Lyon, Lyon, France). Matrix in PCR1 reaction was 20 µl of bisulfite converted DNA.

Oct4 CR1-PCR1

Oct4_CR1_PCR1 forward	5' AAAACCTTAAAACTCAACCAAATCC 3'	Tm=61 °C
Oct4_CR1_PCR1 reverse	5' GTTTTTTTAGGGAGGGGGTAGAG 3'	Tm=60.5 °C
CR1 PCR1 PRODUCT SIZE: 467 bp		

Oct4 CR4-PCR1

Oct4_CR4_PCR1 forward	5'TAACCTATCAAACCTTCTAAAAAACT 3'	Tm=55.6 °C
Oct4_CR4_PCR1 reverse	5'GTTGGTTGGGTAGGAGTTTAT 3'	Tm=54.8 °C
CR4 PCR1 PRODUCT SIZE: 472 bp		

PCR reaction set up for PCR1:

HOT BIOAmp 10x Buffer B2	(Mg ²⁺ free)	5 µl
MgCl ₂	(25 mM)	3 µl
dNTP	(10 Mm)	1 µl
primer <i>forward</i>	(10 pM)	1 µl
primer <i>reverse</i>	(10 pM)	1 µl
Taq Hot Start	(5U/µl)	0.6 µl
<i>Aqua dest.</i>		Ad 30 µl

PCR1 reaction was carried under following thermocycler conditions:

Denaturation (initiation)	95 °C	13 min	} 35 cycles
Denaturation	95 °C	1 min	
Primer annealing	56 °C for CR1m and 51 °C for CR4	1 min	
Elongation	72 °C	1 min	
Final elongation	72 °C	10 min	
Final hold	8 °C	∞	

PCR2 (“nested” PCR) was performed with 5 µl of PCR1 product as a matrix and specific primers.

Oct4 CR1-PCR2

Oct4_CR1_PCR2 *forward* 5' AAAATCCACCCAACCTAACTCC 3' Tm=60,4 °C
 Oct4_CR1_PCR2 *reverse* 5' ATGGGGTGGAAGGGAttttAG 3' Tm=61,2 °C

CR1 PCR1 PRODUCT SIZE: 403 bp

Oct4CR4-PCR2

Oct4_CR4_PCR2 *forward* 5'ATAAGTTAAAGAGTTTTGTTTTGG 3' Tm=54,7 °C
 Oct4_CR4_PCR2 *reverse* 5'AACTTCTAAAAAACTAAATAACCTAACTCT 3' Tm=55,5 °C

CR4 PCR1 PRODUCT SIZE: 434 bp

PCR reaction set up for PCR2:

HOT BIOAmp 10x Buffer B2 (Mg ²⁺ free)		3 µl
MgCl ₂	(25 mM)	1.8 µl
dNTP	(10 Mm)	0.6 µl
primer <i>forward</i>	(10 pM)	0.6 µl
primer <i>reverse</i>	(10 pM)	0.6 µl
Taq Hot Start	(5U/µl)	0.36 µl
<i>Aqua dest.</i>		Ad 25 µl

PCR2 reaction was carried under following thermocycler conditions:

Denaturation (initiation)	95 °C	13 min	} 35 cycles
Denaturation	95 °C	1 min	
Primer annealing	60 °C for CR1 and 54 °C for CR4	1 min	
Elongation	72 °C	1 min	
Final elongation	72 °C	10 min	
Final hold	8 °C	∞	

Products of PCR2 were developed using electrophoresis in 1,8 % agarose gel with 70 V, 30 min running conditions.

1,8 % of agarose gel

Agarose	1.8 g
10x concentrated TAE buffer	10 ml
<i>Aqua dest.</i>	90 ml
Etidiumbromide	3 µl

PCR products were identified in agarose gel by size under exposition to UV light. Excise the DNA fragments from agarose gel was done using a clean, sharp scalpel, and placed in 2ml tube. Glass shallow under the gel was applied to minimize damage of product due to UV exposure. Gel fragments were stored in -20°C till product isolation.

2.11 Extraction of the DNA fragment from agarose gel

Recovery of the product amplified in PCR reaction from agarose gel was performed using QIAquick® Gel Extraction Kit (Qiagen). At first 1 ml of QG Buffer was added to tube with gel fragment and incubated for 10 min in 50°C (water bath) with vortexing every 2 min. Next 1ml of isopropanol was added and mixed. Sample was applied to the QIAquick column (800 µl), centrifuged 13000 rpm for 1 min, flow-through was discarded. Then 500 µl of QG Buffer was added and incubated for 2 min, centrifuged and flow-through discarded. Subsequently 750 µl of

PE Buffer was added, incubated 2 min, centrifuged and flow-through discarded. An additional centrifugation was done to ensure that membrane is free of ethanol remaining. To elute product out of the QIAquick column 50 μ l of Elution Buffer was applied, incubated 4 min and centrifuged 13000 rpm for 1 min. The flow-through was collected and stored in -20°C till ligation.

2.12 Cloning

The products of “nested” PCRs with bisulfite treated DNA carry the information about the methylation patterns from population of cells. To assess, how is a single methylation pattern from one cell, the product need to be cloned to a plasmid vector and then amplified in bacteria culture to produce sufficient material for sequencing reaction.

2.12.1 Ligation

An advantage of pGEM-T Vector System (Promega, Mannheim) is multiple cloning site with 3'-T-overhang. Products of PCRs with Taq-DNA Polymerase have a complementary 3'-A-overhang to 3'-T-overhang of pGEM-T Vector what helps to insert the product with high efficiency.

In order to ligate PCR product with pGEM-T Vector following reaction was prepared:

2xBuffer	10 μ l
T4 DNA Ligase (1U)	1 μ l
pGEM-T Vector	1 μ l

8 μ l of PCR product extracted from gel (insert) was added.

Ligation reaction was proceeding for at least 12h in 15°C .

2.12.2 Transformation

NEB 5-alpha Competent E. coli cells (C2987H, New England Biolabs., Ipswich, MA) were transformed with High Efficiency Transformation Protocol (C2987H/C2987I). At first tube with bacteria was thawed on ice for 10 min. After that time 5 μ l of ligation reaction was added and mixed carefully by flicking. Tube was incubated on ice for 30 minutes. Next bacteria were heat shocked at exactly 42°C for 30 sec and placed on ice for 5 min subsequently. 482.5 μ l of room temperature SOC media was added to transformation reaction and placed at 37°C for 60 min with vigorous rotation. Selection plates were preprepared and warmed-up at 37°C . After 60 min transformation reaction 200 μ l and 50 μ l were spreaded onto a selection plates and incubated overnight at 37°C .

SOC medium: SOB (super optimal broth) medium + glucose (so called SOC medium, for liquid colonies and for agar plates preparation)

Yeast extract	0.5 %	5 g
Peptone	2 %	20 g
NaCl	10 mM	0.584 g
KCl	2.5 mM	0.186 g
MgSO ₄	20 mM	2.4 g
Glucose	20 mM	3.603 g
(pH adjusted to orange from 6.8 - 7)		
<i>Aqua dest.</i>		<i>ad 1 l</i>

To prepare selection plates 50 mg/ml of ampicillin, 20 mg/ml of X-Gal (in dimethyl formamide) and 200 mg/ml of IPTG (in *Aqua dest.*) was added to 400 ml of SOC media.

2.12.3 Selection of positive clones

Selection plates give a possibility to growth only to transformed bacteria having a pGEM-T Vector with ampicillin resistance. To distinguish between the bacteria clones with pGEM-T Vector with integrated insert (positive clones) and clones with pGEM-T Vector without insert a discrimination regarding to clone color was done. Clones without insert have ligated multiple cloning site of pGEM-T plasmid, what results in with an integrated lacZ-gene and a transcription of a β -galactosidase enzyme. β -galactosidase can digest X-Gal and give as a blue side product of reaction (5-Bromo-4-Chloro-3-Indol). Bacteria having a pGEM-T plasmid with insert do not have a working lacZ-gene, because of integration of insert, so they are not able to digest X-Gal and remain white (colorless). IPTG (Isopropyl β -D-1-thiogalactopyranoside) is an inductor of β -galactosidase and enhances the gene transcription.

2.12.4 Plasmid isolation from E.coli bacteria

Positive bacteria clones were picked up with sterile pipette tip and placed in 4 ml of SOC Media with ampicillin and incubated overnight in 37°C by 250 rpm shaking. Next day liquid bacteria culture was used in plasmid isolation. Plasmid isolation was done using several plasmid isolation kits according to instructions (Monarch® Plasmid Miniprep Kit, New England Biolabs, Ipswich, MA; QIAGEN Plasmid Mini Kit, QIAGEN, US; Plasmid Miniprep Kit I, peqGOLD, VWR International GmbH, Darmstadt, Germany). Principals of the plasmid isolation method were described first time by Birnboim and Doly in 1979 (Nucleic Acids Res. 7, 1513-1523).

2.12.5 Restriction reaction

To reassure if the isolated plasmid is having ligated insert of interest an restriction reaction with endonucleases Apal and SacI was done with following setups:

Apal (5U)	1 μ l
SacI (5U)	1 μ l
Buffer B+	5 μ l
Isolated plasmid	3 μ l

Apal and SacI are digesting the plasmid at defined multiple cloning sites of the pGEM-T Vector. The products of restriction reaction were visualized by separation in agarose gel. Expected product size was estimated by adding the 80bp of multiple cloning side and the length of each insert. If the plasmid was carrying the right size of insert, the plasmid was dedicated for sequencing to ensure if the insert sequence is adequate.

2.12.6 Sequencing

Sequencing reaction of plasmids dedicated to prepare a real time PCR standards was prepared using a BigDye® Terminator v 1.1 Cycle Sequencing Kit (Applied Biosystems, Foster City, USA) using following setup:

T7.2 Primer (5 pmol/μl)	0.5 μl
Big Dye Terminator v1.1 Cycle Sequencing RR24	2 μl
Big Dye Terminator v1.1.3.1 5xSeq. Puffer	1.5 μl
H ₂ O	4 μl
Plasmid	2 μl

Thermocycler settings:

Denaturation (initiation)	95 °C	1 min	} 25 cycles
Denaturation	95 °C	1 min	
Primer annealing	55 °C	1 min	
Elongation	60 °C	1 min	
Final elongation	60 °C	10 min	
Final hold	4 °C	∞	

2.12.7 Purification of sequencing reaction

Product of sequencing reaction was purified. At first pH was adjusted by addition of 1 μl 3 M NaOAc (pH 5.2) and 40 μl 96% EtOH (4 °C) was added facilitate precipitation. Products were centrifuged for 30 min at 13000 rpm in 4 °C, the supernatant was gently discarded. Next steps were two washes in 200 μl of 70% EtOH (4 °C) followed by 20 min centrifugation in 13000 rpm in 4 °C. Supernatant was always carefully taken off. Pellets were left to dry in vacuum for 5 min (SpeedVac). Plasmids prepared in such way were sent to Nucleotide Sequencing and Fragment Analysis Service at Center for Basic Medical Research (ZMG) of the Medical Faculty (MLU Halle-Wittenberg) or to sequencing service Microsynth AG (Lindau, Germany). The outcomes of sequencing were analyzing by alignment of obtained sequence with its mRNA sequence using Nucleotide Basic Local Alignment Search Program (BLASTn). Once the identity of insert sequence was recognized, the plasmid was used as a standard for *real time* PCR.

2.13 Bisulfite sequencing data analysis

II plasmid sequences carrying the insert with DNA methylation pattern were submitted to QUMA: quantification tool for methylation analysis (Kumaki et al., 2008) and compared with the genomic unconverted sequence between PCR primer pair.

Following parameters were used after data submission.

- **Upper limit of unconverted CpGs** – represents a number of unconverted CpGs (CpA, CpC and CpT) and is used to exclude incomplete bisulfite conversion. Upper limit of unconverted CpGs was set on 20.

- **Lower limit of percent converted CpGs** – is a percent of "number of converted CpGs" to "number of CpGs" and this parameter is used to exclude incomplete bisulfite conversion. Lower limit of percent converted CpGs was set on 90 %.
- **Upper limit of alignment mismatches** – is a number of alignment mismatches and gaps between genomic and bisulfite sequences, this parameter allows to exclude low quality sequence read. Upper limit of alignment mismatches was set on 10.
- **Lower limit of percent identity** – is a percent of alignment identity between genomic and bisulfite sequences, this parameter excludes raw quality sequence read. Lower limit of percent identity was set on 80 %.

Experimental sequencing results were analyzed as methylated or unmethylated with rules presented at Figure 9.

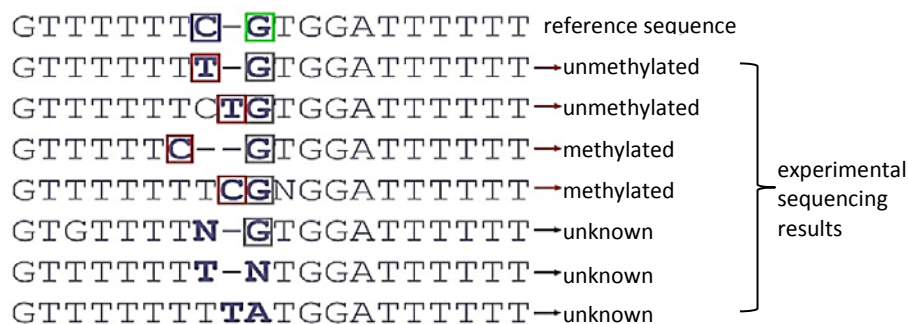


Figure 9. **CpG methylation assessment out experimental sequencing data (modified after Rohde et al., 2010).**

2.14 Real Time PCR

Real time PCR was performed and analyzed for all genes listed in Table 2 according to the settings previously described by Gürke et al., 2016.

2.14 Real Time PCR standards

All sequenced plasmids concentrations were measured with *NanoVue*. Next the plasmid was diluted to reach a 10^8 , 10^7 , 10^6 , 10^5 , 10^4 , 10^3 of plasmid molecules in 3 μ l.

2.15 Statistics

Statistical significance was estimated using student's t-test for data with normal distribution. Statistical comparison of groups with multiple factors was done by factorial variance analysis (ANOVA) adjusted according to Bonferroni (statistical software: Sigma Plot v. 11.0). p-value was used for each statistical model to summarize statistical significance as follows: *- $p < 0.05$, **- $p < 0.01$ and ***- $p < 0.001$. All experiments were carried out at least three times.

3. Results

3.1 Effect of maternal diabetes on the expression of pluripotency genes and differentiation-related gene markers in rabbit preimplantation embryos

3.1.1 Expression of pluripotency genes in gastrulating blastocysts

RNA amounts of Oct4, Nanog and Sox2, genes essential for pluripotency maintenance, were measured using RT-qPCR in blastocysts at day 6 p.c. stage 0, when the beginning of gastrulation occurs, and at stage 2, when gastrulation is proceeding.

At stage 0 Oct4 was highly transcribed in embryoblasts, while the expression was significantly lower in trophoblasts (see Figure 10). At stage 2 Oct4 RNA amounts was measured in all embryonic tissues. The epiblasts showed the highest expression of all embryonic tissues. The Oct4 RNA amount was higher in hypoblast than in trophoblast tissue.

Oct4 RNA amount transcription was compared in blastocyst day 6 p.c. stage 0 and stage 2 from healthy and diabetic pregnancies (see details at Figure 10A and 10B). At stage 0 epiblasts did not differ in Oct4 RNA amounts, while a significant upregulation of Oct4 mRNA was observed in epiblasts from diabetic pregnancies at stage 2 (Figure 10A). At stage 2 hypoblasts shared a similar Oct4 expression. Trophoblasts from blastocysts at stage 0 developed in an diabetic pregnancies had higher Oct4 transcripts amounts than trophoblasts from healthy rabbits (Figure 10B). In stage 2 trophoblasts Oct4 expression was lower than at stage 0 and did not differ between the diabetic and healthy rabbits.

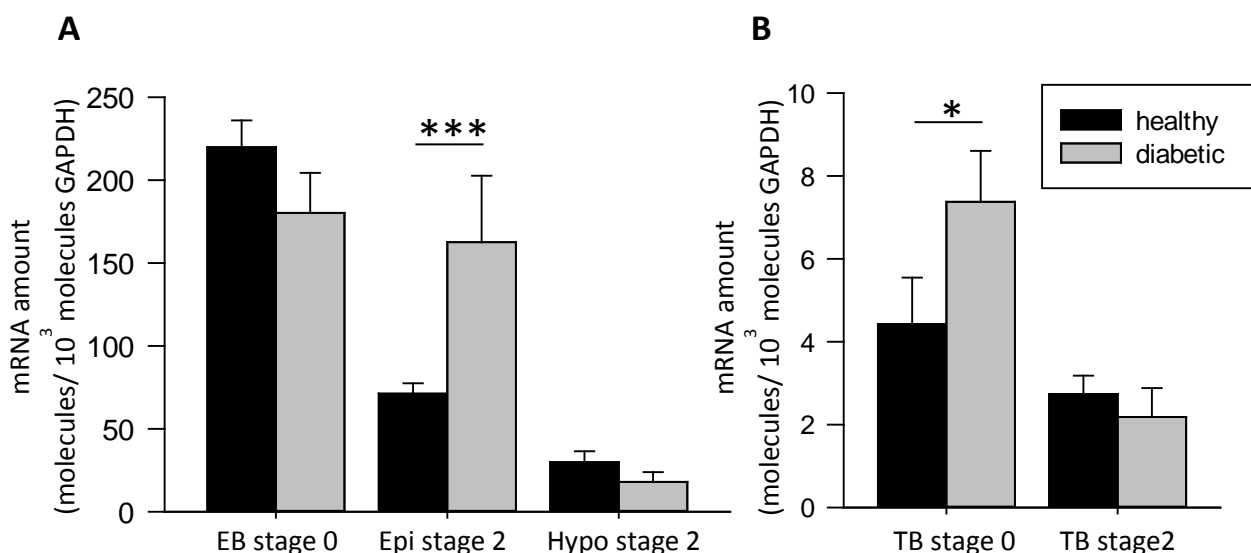


Figure 10. **Oct4 mRNA amount in epiblasts, hypoblasts and trophoblasts from blastocyst at stage 0 and 2 from diabetic and healthy rabbits.** Tissues were sampled from 6 day old staged rabbit blastocysts and analyzed by RT-qPCR for Oct4 transcription.

(EB – embryoblast; Epi – epiblast; Hypo – hypoblast, TB – trophoblast; mean \pm SEM, N=3, n=6 (n=pool of 3 embryonic tissues from different embryos); * $p \leq 0.05$; ** $p \leq 0.001$; *** $p \leq 0.0001$;))

Expression of Nanog and Sox2 was detected in epiblasts at blastocyst day 6 stages 2. The level of Nanog and Sox2 transcripts is higher in epiblasts of diabetic embryos (Figure 11).

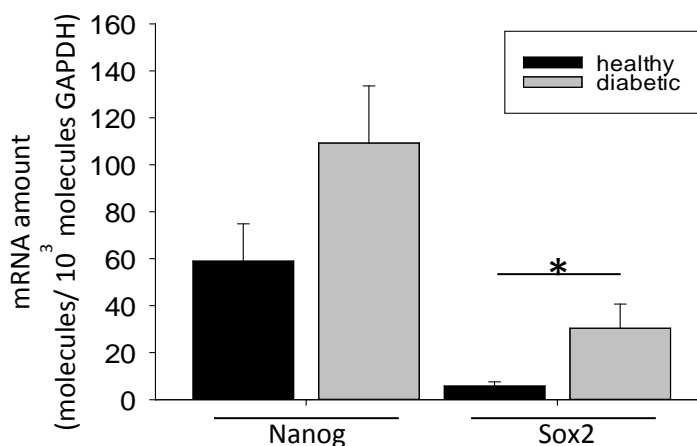


Figure 11. **Nanog and Sox2 mRNA amounts in epiblast tissue of blastocyst (stage 2) from diabetic and healthy rabbits.** (mean ± SEM; N=3, n=6 (n=pool of 3 embryonic tissues from different embryos); * $p \leq 0.05$; ** $p \leq 0.001$; *** $p \leq 0.0001$)

In epiblasts of blastocysts at day 6 *p.c.* Oct4 transcript amount was on the highest level among the investigated pluripotency genes. In case of both, Oct4 and Sox2 mRNA transcript levels were higher for the epiblasts of diabetic pregnancies, where Nanog expression patterns show a similar tendency without a statistical significance.

3.1.2 Expression of extraembryonic tissue-specific genes for hypoblasts and trophoblasts from blastocysts day 6 stages 0 and 2

Expression of genes involved in formation of extraembryonic tissues was investigated by RT-qPCR. The Cdx2, gene involved in trophoblast cell differentiation and segregation, was identified in

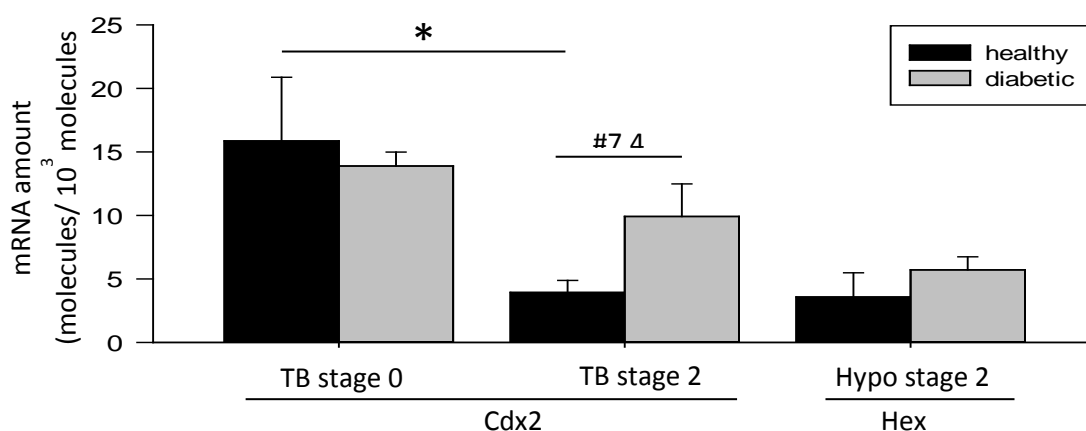


Figure 12. **Cdx2 and Hex mRNA amount in trophoblasts and hypoblasts of blastocyst (stages 0 and 2) from healthy and diabetic rabbits.** (TB – trophoblast, Hypo - hypoblasts; mean ± SEM, N=3, n=6 (n=pool of 3 embryonic tissues from different embryos); * $p \leq 0.05$)

trophoblasts stage 0 and 2 from blastocysts day 6 *p.c.* (Figure 12). In trophoblasts of healthy embryos the Cdx2 RNA amount was decreasing from stage 0 to stage 2, while the Cdx2 transcript levels in trophoblasts of diabetic embryos between stage 0 and 2 remained similar. The hypoblast differentiation marker Hex was quantified in hypoblasts of stage 2 blastocysts. Hex levels were not differing between hypoblasts from healthy and diabetic pregnancies.

3.1.3 Expression of heart developmental markers: Mef2C, Gata6, Gata4 and Nkx2-5 in rabbit fetal hearts at day 12 and 14

The expression of gene markers of heart fetal development - Mef2C, Gata6, Gata4 and Nkx2-5 - was measured in rabbit fetal hearts day 12 and 14 developed in healthy and diabetic mothers. Transcription levels for Mef2C and Gata4 genes were similar at day 12 and 14 and did not differ between healthy and diabetic rabbits (Figure 13A). RNA amounts of Gata6 were higher in healthy fetal hearts day at 14 than in hearts harvested at day 12. In opposite, Mef2C expression in diabetic fetal hearts did not vary between hearts at day 12 and 14. In hearts from healthy and diabetic pregnancies the expression of Gata6 was similar at day 12, while at day 14 of development the Gata6 transcript level was lower in the diabetic group (Figure 13A). The Nkx2-5 mRNA amount was at a similar level in fetal hearts at day 12 and 14 from healthy pregnancies. The fetal hearts from diabetic pregnancies showed a lower Nkx2-5 expression at day 14 than at day 12 of development (Figure 13B). Among the investigated heart development markers the relative transcript level was the highest for Gata6 and Gata4 gene.

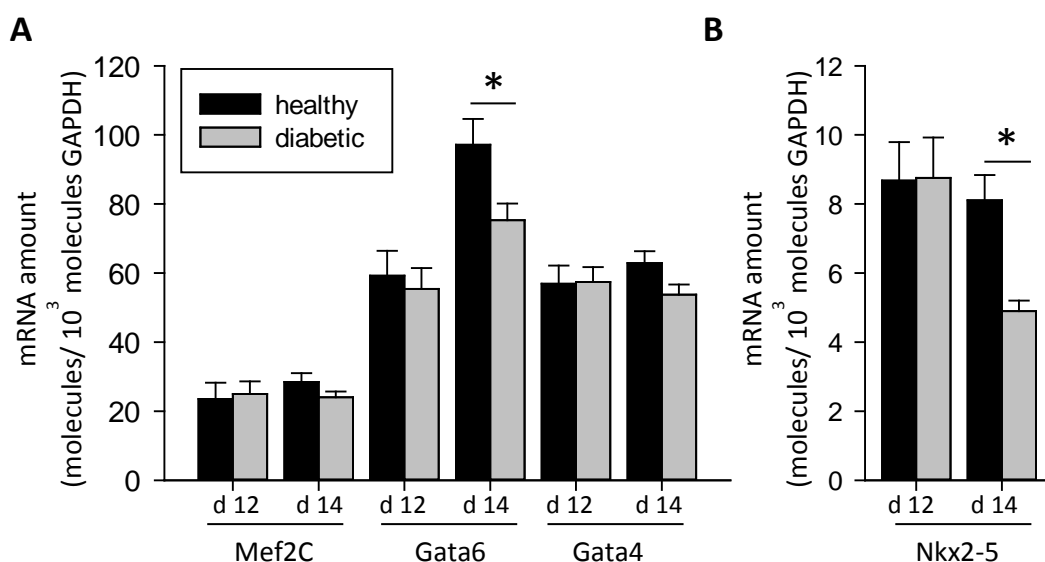


Figure 13. **Transcript amounts of genes involved in heart development investigated in rabbit fetal hearts at day (d) 12 and 14 from healthy and diabetic pregnancies.**

A - mRNA amounts of Mef2C, Gata6 and Gata4 gene; B - mRNA amounts of Nkx2-5 gene; * - 9+ mean \pm SEM (N=3, n=8; * $p \leq 0.05$)

3.2 Oct4 (POU5F1) promoter region methylation analysis in rabbit adult heart tissue and gastrulating blastocysts day 6 stage 2

Analysis of Oct4 (POU5F1) promoter region methylation was performed using the bisulfite sequencing method. Sequencing data were compared to the template (-2600 bp downstream to POU5F1 gene sequence, GenBank: AC235550.2) by the QUantification tool for Methylation Analysis Software (QUMA) developed in the Center for Developmental Biology RIKEN (Japan) by Kumaki et al., 2008. All sequences were characterized by the following parameters: identity to template higher than 80 % and cytosine bisulfite conversion rate higher than 90 %. The sequences fulfilling the parameters were included in the evaluation of the Oct4 (POU5F1) promoter methylation state. Additionally, identical clones possessing the same percentage of identity and conversion rates were identified by QUMA multiple alignment tool and excluded because of a high risk of amplification of the DNA material from the same cell (Kumaki et al., 2008).

3.2.1 Oct4 (POU5F1) promoter region methylation analysis in rabbit adult heart tissue

Methylation patterns at the Oct4 (POU5F1) promoter region were conducted in adult rabbit heart tissue for the conserved regions 4 (CR4-) and 1 (CR1-) overlapping fragments. CR1 is placed close to the transcription start side and CR4 is localized about 1900 bp downstream (Figure 14A).

The total percentage of CpGs methylation at CR4-overlapping fragment was 66 %. The methylation of 17 CpGs was investigated (Figure 14B). The analyzed fragment covers 7 CpGs from CR4 and 10 CpGs outside the conserved region (placed upstream to CR4). Both areas were methylated at the same level (66 %). Methylation of CpG at the distal enhancer 1A (DE-1A) was roughly 24 %, what was much lower than for the rest of the analyzed CpGs inside the CR4-overlapping fragment. CpGs surrounding the Oct4/Sox2 binding site were slightly higher methylated than the total percentage of CpGs methylation.

The CR1-overlapping fragment was methylated in 52 % (data for 24 CpGs, 9 sequences, see details at Figure 14C). The CR1-overlapping fragment was covering minimal promoter (me-CpGs 53 %) with CR1 and the beginning of the first exon. The highest methylation in the minimal promoter was at the fragment outside the conserved region (67 %) and the lowest methylation was at the hormone response element (44 %). CR1 has 46 % of methylation, what is lower than the total methylation for CR1-overlapping fragment. Beginning of the first exon had 50 % of methylated CpGs, what was similar to the total methylation observed for analyzed fragment.

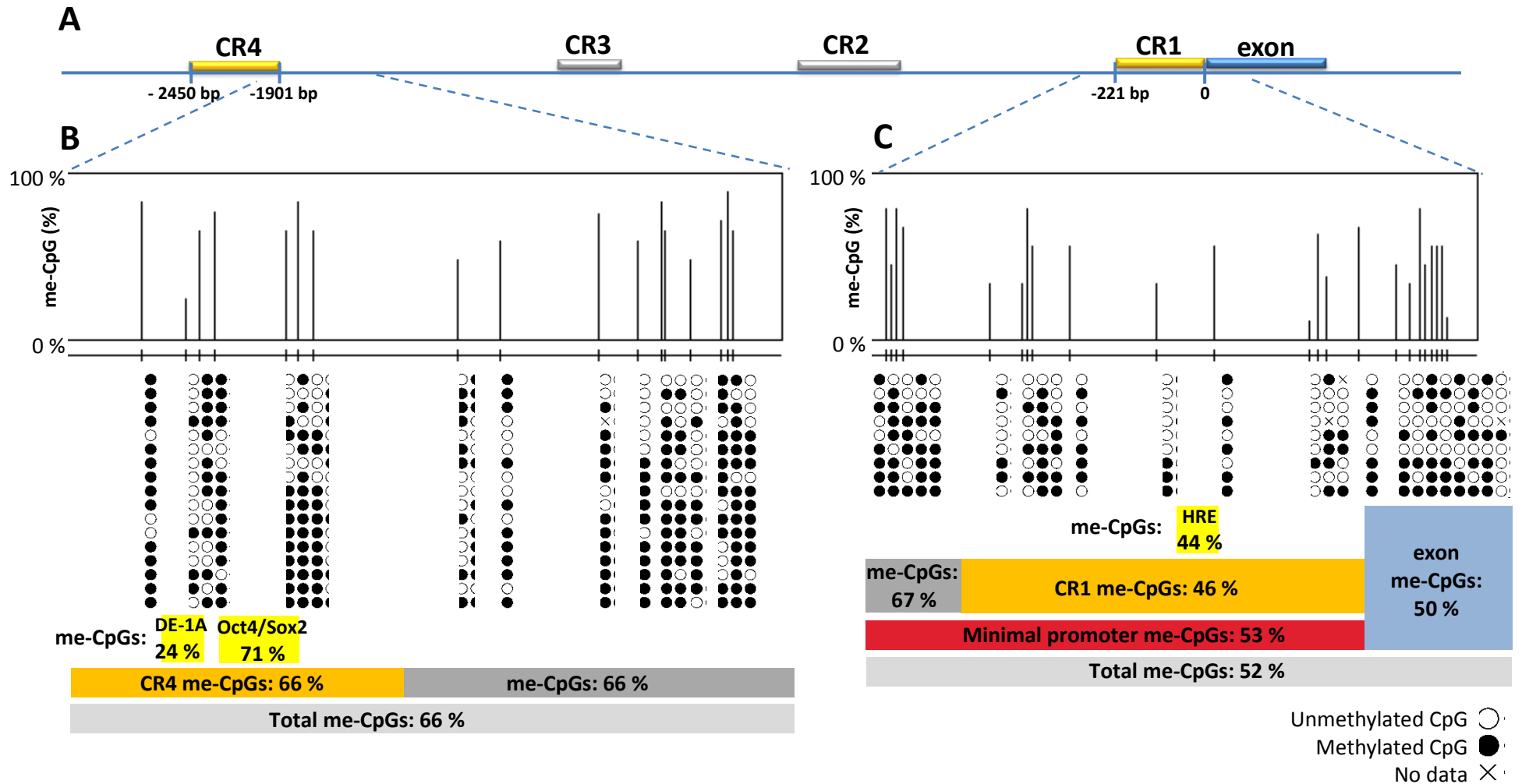


Figure 14. Bisulfite sequencing DNA methylation data for the Oct4 (POU5F1) promoter region in rabbit adult heart tissue

A: Organization of Oct4 promoter region with indicated positions of conserved regions 1 and 4; B: Data for CR4-overlapping fragment (comparison for 17 sequences); C: Data for CR1-overlapping fragment (comparison for 9 sequences). Column graphs show the percentage of methylation at single CpG positions in analyzed promoter fragments. Lollypop-style graphs demonstrate methylation patterns from different alleles (each row represents data for one sequence); CR1/2/3/4 – conserved region 1/2/3/4; Me-CpG – methylation at single CpG position; me-CpGs – methylation at indicated number of CpGs; DE-1A – distal enhancer 1A; Oct4/Sox2 – Oct4 and Sox2 binding site; HRE – hormone response element.

The CR4-overlapping fragment has a higher methylation than the CR1-overlapping fragment in rabbit adult heart tissue. Comparison of methylation of conserved regions showed a higher percentage for CR4 (7 CpGs analyzed for CR4, 10 CpG for CR1). Me-CpGs was decreasing in the surrounding and at the functional elements inside of both fragments. Methylation percentage outside the conserved regions was at a similar level in case of the CR1- and CR4-overlapping fragment.

3.3 Comparison of data for groups of epiblasts, hypoblasts and trophoblasts pools

Methylation data were collected for two groups of epiblasts, hypoblasts and trophoblasts pools sampled from blastocysts day 6 at stage 2. Each pool of epiblasts, hypoblasts and trophoblasts was obtained from three blastocysts developed in healthy or diabetic rabbits. The total methylation percentage was calculated for each pool to see if results were repetitive (see Figure 15). The total methylation for each of group was calculated as a percentage of methylated CpGs against all CpGs in analyzed CR1 or CR4 overlapping fragment.

The total methylation was at low levels for pools of epiblasts in CR1- and CR4-overlapping fragments (Figure 15). Epiblasts from diabetic blastocysts had a higher difference between total CpGs methylation of group 1 and 2 in CR1-overlapping fragments. This was not seen in case of diabetic epiblasts pools for CR4-overlapping fragment. The rest of epiblasts pools for group 1 and 2 were at similar methylation levels.

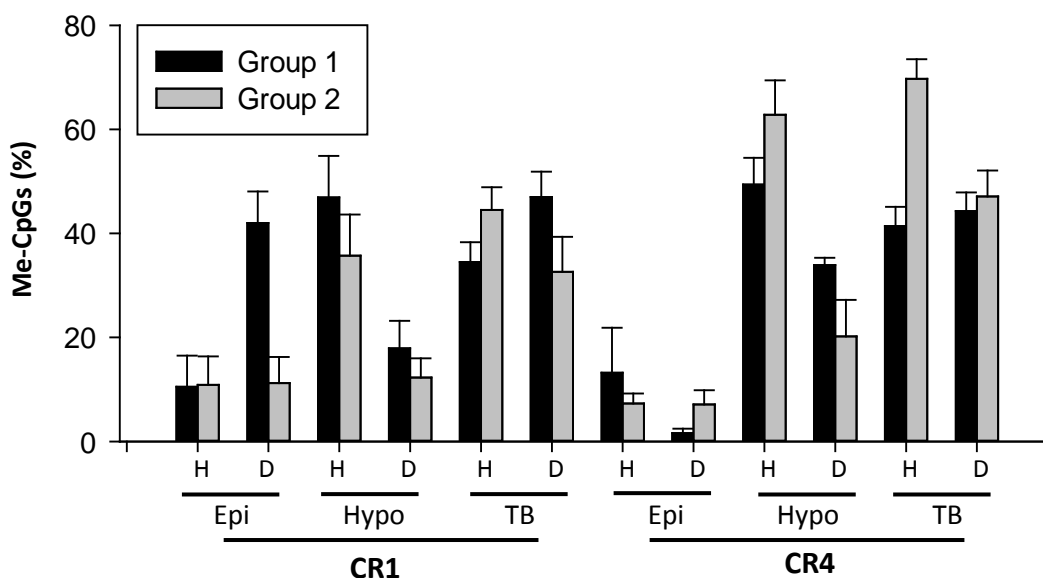


Figure 15. Total CpGs methylation at CR1- and CR4-overlapping fragment. Group 1 and 2 of epiblasts, hypoblasts and trophoblasts was sampled from blastocysts from healthy and diabetic rabbits. (H – healthy pregnancy, D – diabetic pregnancy, Epi – epiblast, Hypo – hypoblast, TB – trophoblast; Me-CpGs – methylation at CpGs; mean of total CpG methylation \pm SEM (error bars represent SEM between the total CpGs methylation of sequences); N=2; n \geq 8)

Pools of hypoblasts of healthy blastocysts showed no change between groups and were higher methylated at CR1- and CR4-overlapping fragments than in the diabetic ones. Trophoblasts pools were equally methylated at the CR1-overlapping fragment. Group 2 of trophoblasts from healthy blastocysts was higher methylated than group 1.

Methylation of epiblasts was lower than in hypoblasts and trophoblasts for CR1- and CR4-overlapping fragments. The differences between methylation of CR1- and CR4-overlapping fragments in pools from group 1 and 2 have been seen in some cases, what was a consequence of natural variation. The methylation data for all sequences (of different alleles) obtained for group 1 and group 2 were combined in further analysis for each epiblasts, hypoblasts and trophoblasts to present the dynamic states of embryonic tissues methylation at Oct4 (POU5F1) promoter region and better see the influence of the three major lineages.

3.4 Oct4 (POU5F1) conserved region 1 methylation analysis in embryonic tissues of gastrulating blastocysts day 6 stage 2

CpGs methylation at conserved region 1 (CR1) was investigated using sequencing data for group 1 and 2 of epiblast, hypoblast and trophoblast pools. Methylation of embryonic tissues of healthy rabbit blastocysts was compared to diabetic ones, using single CpG methylation analysis (column and lolly-pop graphs at Figure 16, 17, 18) and by clustering CpGs in structural and functional groups (see tables at Figure 16, 17 and 18).

3.4.1 Oct4 (POU5F1) conserved region 1 methylation analysis in epiblasts from healthy and diabetic rabbits

Epiblasts from healthy blastocysts were methylated in 11 % for 24 CpGs analyzed at CR1-overlapping fragment (see Figure 16A). Methylation was equally distributed in the fragment. Exon and minimal promoter had me-CpGs of 11 %, CR1 was methylated in 9 % (all 10 CpGs of conserved region 1 were covered). The fragment upstream to the CR1, but within minimal promoter was slightly higher methylated with me-CpGs of 14 %. The smallest methylation (5 %) shared two CpGs in close proximity to the hormone response element (HRE). The data was obtained from 21 different alleles, sequences were homogenously methylated at single CpGs (see lollypop-style graph at Figure 16A).

Epiblasts from diabetic blastocysts at the CR1-overlapping fragment had 25 % of methylated CpGs, what was higher than in case of epiblasts of healthy blastocysts (see details at Figure 16B). CR1, exon and HRE CpGs methylation was oscillating from 18 to 20 % (result is twice higher than for similar regions in epiblasts of healthy blastocysts). The fragment upstream to the CR1 was methylated in 46 %, what was lifting minimal promoter me-CpGs up to 29 %. Calculations were done based on 20 sequences representing different alleles. Sequences differ between low or no

methylation to methylated in nearly 40 %. This variety was not seen in case of epiblasts from healthy blastocysts.

3.4.2 Oct4 (POU5F1) conserved region 1 methylation analysis in hypoblasts from healthy and diabetic rabbits

Total CpGs methylation for hypoblasts from healthy blastocysts for whole analyzed fragment was 42 % (see Figure 17A). The part of minimal promoter upstream to CR1 was highly methylated (me-CpGs 56%), while CR1 and exon were methylated in 38 %. CpGs in close proximity to HRE were methylated in 48 %. Considering the single CpG methylation the three CpGs of CR1 close to transcription start side were lower methylated in most sequences (total 18 sequences were used for analyzes).

Hypoblasts of blastocysts from diabetic pregnancies were lower methylated at CR1-overlapping fragment than the healthy ones (see details Figure 17B). Total me-CpGs was 15 %, while minimal promoter was methylated in 16 %. Areas inside the minimal promoter differed in methylation: CR1 was methylated in 14 %, while CpGs of the fragment outside CR1 placed upstream to conserved region were methylated in 21 %. The lowest methylation inside of CR1-overlapping fragment was at CpGs close to the HRE (me-CpGs=11 %) and at the beginning of exon (13 %). All functional elements inside the CR1-overlapping fragment of hypoblasts from diabetic blastocysts were at least in 25 % lower methylated than the same regions in hypoblasts of healthy blastocysts (Figure 17A and 17B). Sequences of hypoblasts of diabetic blastocysts were homogenous.

3.4.3 Oct4 (POU5F1) conserved region 1 methylation analysis in trophoblasts from healthy and diabetic pregnancies

Trophoblasts from healthy blastocysts had a total me-CpGs of 39 % (see Figure 18A). Exon (me-CpGs=24 %) was lower methylated than the minimal promoter (48 %). Inside of minimal promoter the fragment outside conserved region and placed upstream to CR1 was in 76 % methylated, while CpGs inside of CR1 were methylated in 34 %. CpGs close to HRE were the part of minimal promoter with the lowest methylation – 21 %. Total CpGs methylation at CR1-overlapping fragment for trophoblasts of diabetic blastocysts was similar to healthy ones (me-CpGs=40 %, Figure 18B).

The elements of minimal promoter shared a parallel proportion of methylation between the fragment outside the conserved region, upstream to CR1 and the CR1 (61 % to 36 % of me-CpGs). HRE and beginning of exon was slightly higher methylated than in trophoblasts from healthy blastocysts (Figure 18A and 18B).

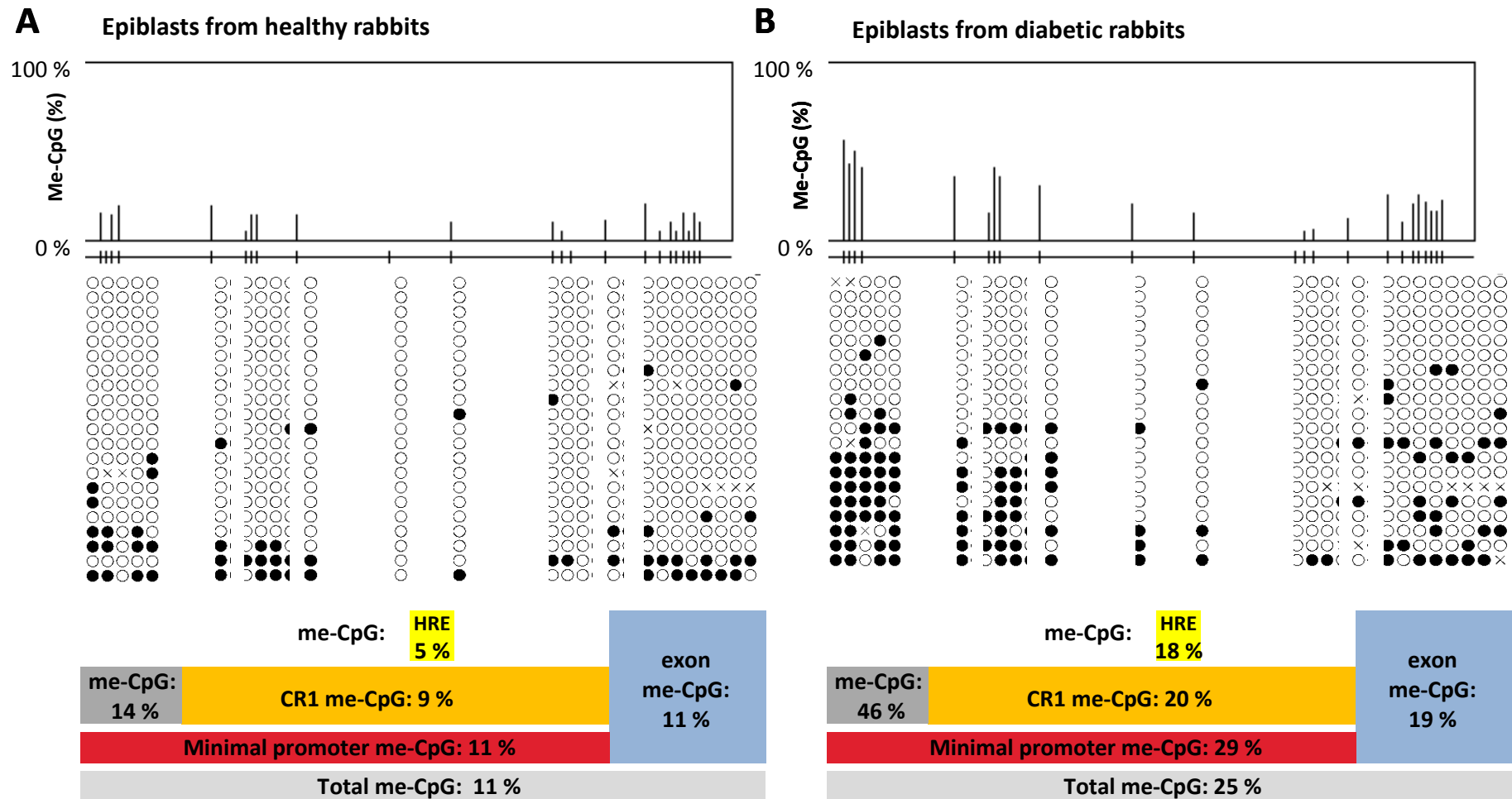


Figure 16. Bisulfite sequencing DNA methylation data for CR1-overlapping fragment of Oct4 (POU5F1) promoter region in epiblasts of rabbit blastocysts from healthy (A) and diabetic (B) rabbits.

Column graphs display the percentage of methylation at single CpG position in analyzed promoter fragments. Lollypop-style graphs demonstrate methylation patterns from different alleles (each row represent data for one sequence); CR1 – conserved region 1; Me-CpG – methylation at single CpG position; HRE – hormone response element.

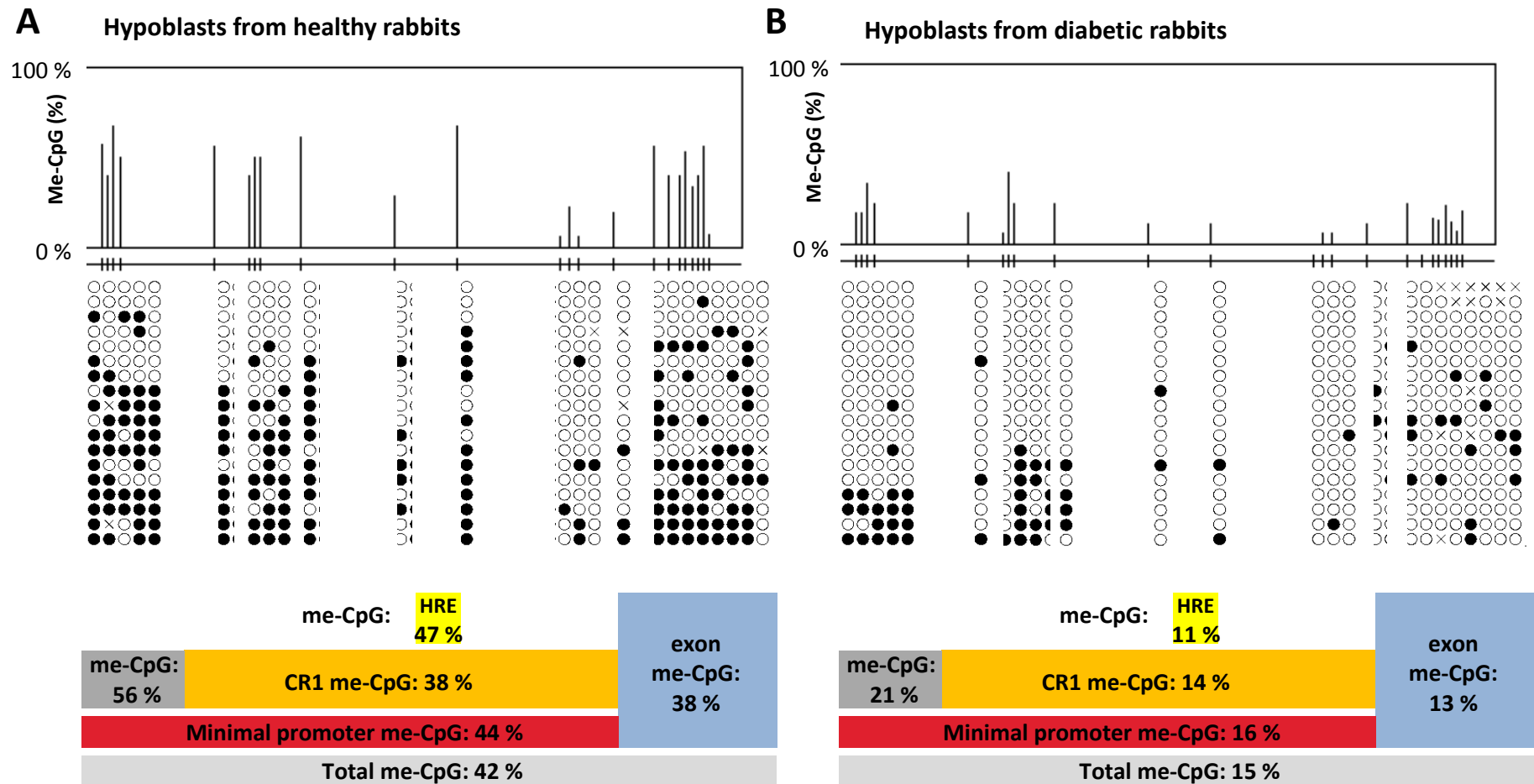


Figure 17. Bisulfite sequencing DNA methylation data for CR1-overlapping fragment of Oct4 (POU5F1) promoter region in hypoblasts of rabbit blastocysts from healthy (A) and diabetic (B) rabbits.

Column graphs display the percentage of methylation at single CpG position in analyzed promoter fragments. Lollypop-style graphs demonstrate methylation patterns from different alleles (each row represent data for one sequence); CR1 – conserved region 1; Me-CpG – methylation at single CpG position; HRE – hormone response element.

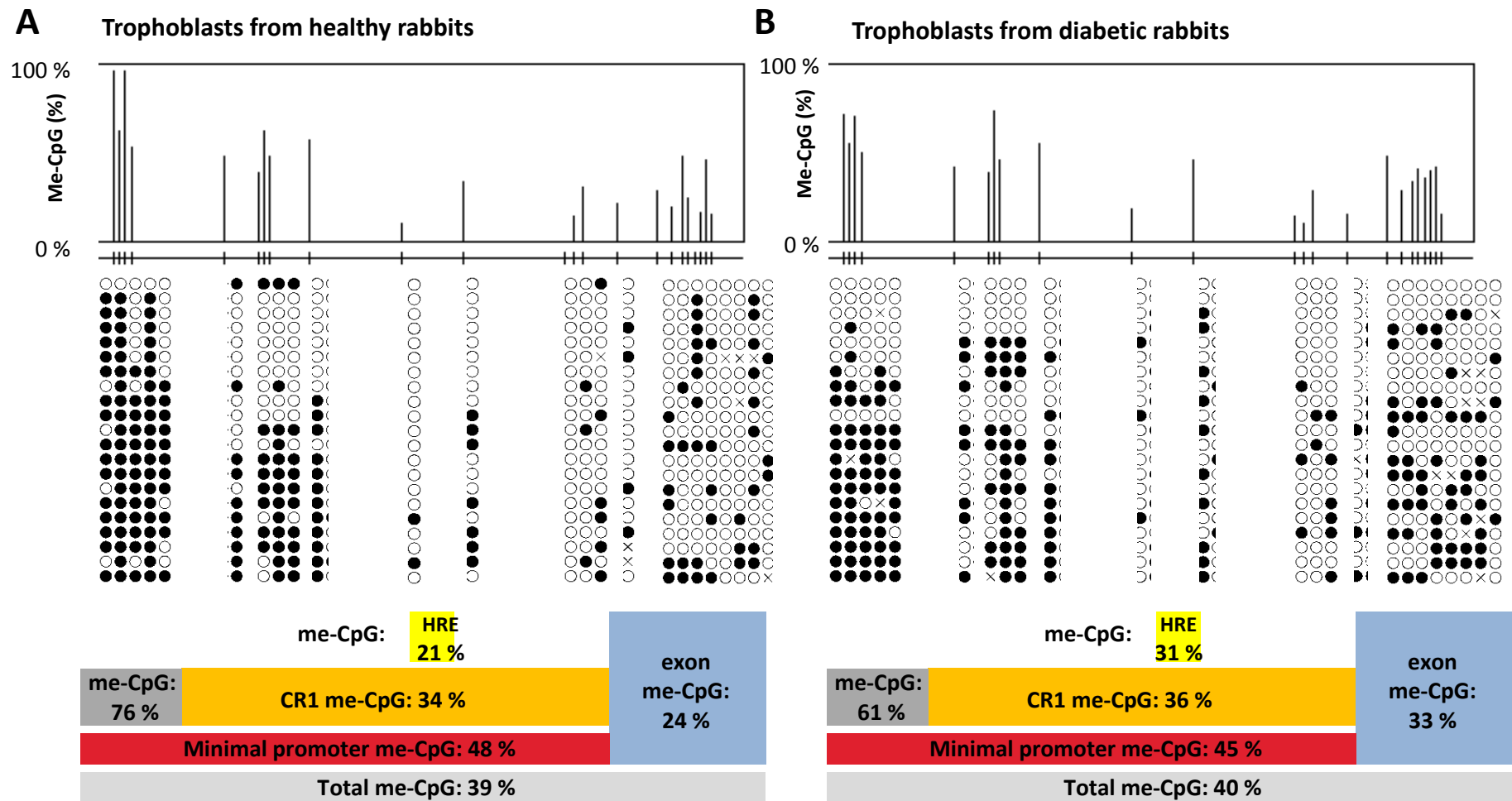


Figure 18. Bisulfite sequencing DNA methylation data for CR1-overlapping fragment of Oct4 (POU5F1) promoter region in trophoblasts of rabbit blastocysts from healthy (A) and diabetic (B) rabbits.

Column graphs display the percentage of methylation at single CpG position in analyzed promoter fragments. Lollipop-style graphs demonstrate methylation patterns from different alleles (each row represent data for one sequence); CR1 – conserved region 1; Me-CpG – methylation at single CpG position; HRE – hormone response element.

3.4.4 Oct4 (POU5F1) conserved region 1 methylation analysis in rabbit adult heart tissue and embryonic tissues from healthy and diabetic pregnancies

The methylation at the CR1-overlapping fragment of the POU5F1 promoter region and its functional elements was calculated as a percentage of methylation at CpGs included in a given area and shown at column graphs to better visualize the results in rabbit heart tissue as well as in embryonic tissues of blastocysts from healthy and diabetic females (see Figure 19). The error bar was expressed as the standard error from the average methylation of single CpGs included for each region and showed whether the single CpGs methylation is equally distributed inside of an analyzed area.

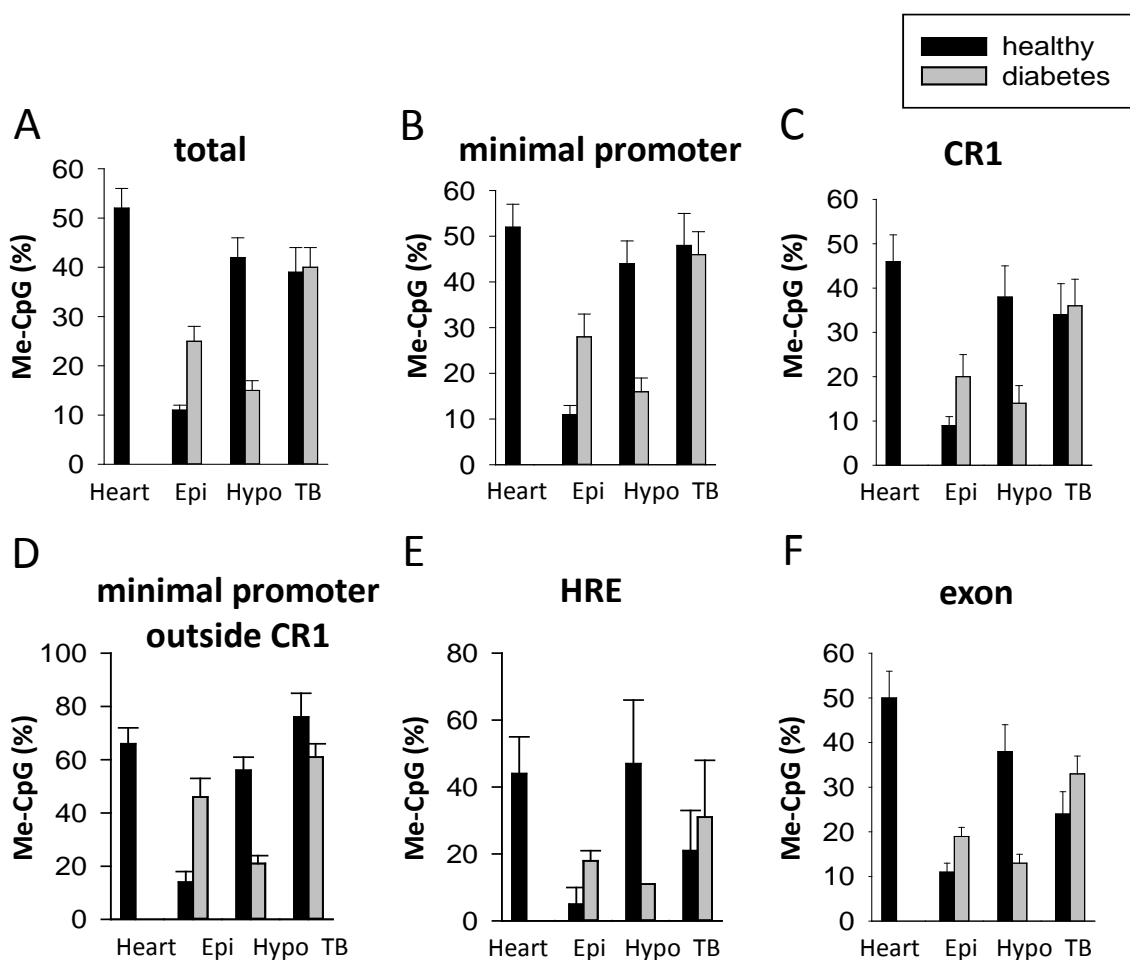


Figure 19. Bisulfite sequencing DNA methylation data for CR4-overlapping fragment of Oct4 (POU5F1) promoter region in rabbit adult heart tissues and embryonic tissues of blastocysts from healthy and diabetic rabbits. Column graphs show the average percentage of methylation at CpGs of the analyzed area in the promoter fragment, error bars show the standard error between average single CpG methylation inside of the analyzed fragment; A – methylation of total CpGs in the CR1-overlapping fragment; B – methylation of CpGs at the minimal promoter; C – methylation of CR1; D – methylation at the fragment of the minimal promoter outside the conserved region, upstream to CR1; E – methylation of CpGs at the hormone response element; F – methylation of the beginning of exon; CR1 – conserved region 1; Me-CpGs – methylation at indicated CpGs; HRE – hormone response element

The total methylation at the CR1-overlapping fragment was the highest in rabbit heart tissue with 24 CpGs being analyzed (Figure 19A). Trophoblasts from healthy and diabetic rabbits and hypoblasts from healthy blastocysts were reaching similar CpGs methylation values. Hypoblasts from diabetic blastocysts were lower methylated than the healthy hypoblasts, trophoblasts and rabbit adult heart tissue. At this region the lowest methylation was in epiblasts from healthy blastocysts. This pattern was multiplied for each area inside of the CR1-overlapping fragment (Figure 19A-F). The data for the minimal promoter were obtained from 15 CpGs, for CR1 from 10 CpGs, the fragment outside CR1, but in the minimal promoter it was including 5 CpGs and the beginning of exon - 9 CpGs. The fragment outside the conserved region, placed upstream to the CR1 was the highest methylated area in all CR1-overlapping fragments in all investigated tissues (Figure 19D). Epiblasts of healthy and diabetic blastocysts showed a smaller difference in methylation of CpGs in close proximity to the hormone response element (HRE). Beside that the methylation of healthy hypoblasts was higher than trophoblasts and had the same value like in rabbit adult heart tissue. This region had a high error bar, what means that the distribution of methylation in sequence varied.

3.5 POU5F1 (Oct4) conserved region 4 methylation analysis in embryonic tissues of gastrulating blastocysts day 6 stage 2

Methylation for the CR4-overlapping fragment at the POU5F1 (Oct4) promoter region was obtained by joining the sequencing data from group 1 and 2 for each epiblast, hypoblast and trophoblast pool. Data were presented like in case of the CR1-overlapping fragment, the results are shown as a single CpG methylation plot (lollypop-style graphs and column graphs) as well as in clusters of CpGs representing the methylation status of each functional area in the CR4-overlapping fragment.

3.5.1 Oct4 (POU5F1) conserved region 4 methylation analysis in epiblasts from healthy and diabetic rabbits

The methylation of epiblasts from healthy blastocysts was at a low level (me-CpGs=10%). The covered part of CR4 was even lower methylated – 5 % (Figure 20A). The fragment outside the CR4, placed downstream to CR4, was methylated in 13 %. Distal enhancer located inside of the CR4 was a 1A (DE-1A), covering one CpG with average methylation of 9.5 %.

Additionally two CpGs surrounding the Oct4/Sox2 binding sites were investigated. Me-CpGs at this region was the lowest in the whole area reaching 5 %.

Epiblasts of diabetic blastocysts were lower methylated than the epiblasts of healthy blastocysts at the CR4-overlapping fragment (Figure 20B). The total me-CpGs was 4 %, while the CR4 was 3 % and the fragment outside CR4, placed downstream, was methylated in 5 %. DE-1A methylation

was the same like in epiblasts from healthy blastocysts. There was no methylation in the surrounding of Oct4/Sox2 binding sides.

3.5.2 Oct4 (POU5F1) conserved region 4 methylation analysis in hypoblasts from healthy and diabetic rabbits

Hypoblasts from healthy blastocysts were highly methylated reaching 57 % total me-CpGs (Figure 21A). CR4 was lower methylated than the part of the fragment not covering CR4, placed upstream to CR4. The CpGs, in the distal enhancer 1A were methylated in 56 %, while the CpGs close to Oct4/Sox2 binding side were methylated in 46 %.

Total CpGs methylation at CR4-overlapping fragment in hypoblasts from diabetic blastocysts was twice lower than in hypoblasts from healthy blastocysts (Figure 21B). The methylation inside of analyzed fragments was not equally distributed between the CR4 and the fragment outside CR4, placed downstream to CR4. Conserved region 4 was methylated in 14 %, while the CpGs of the fragment outside and downstream to conserved region was methylated in 38 %. Methylation of CpG in distal enhancer 1A was also lower methylated (me-CpG=12,5 %) as well as for the Oct4/Sox2 binding side - 4 % of CpGs were methylated.

3.5.3 Oct4 (POU5F1) conserved region 4 methylation analysis in trophoblasts from healthy and diabetic rabbits

The CR4-overlapping fragment in trophoblast tissue sampled from healthy blastocysts is methylated in 59 % (Figure 22A). The CpGs inside CR4 were methylated in 38 %, what is lower than the CpG methylation of the fragment outside the CR4, placed downstream to CR4 (me-CpGs=73 %). Single CpGs from distal enhancer A1 had methylation at level of 50 %, what is higher than the average CpG methylation at CR4. CpGs close to the Oct4/Sox2 binding side were methylated in 37 %, what is similar to CR4 methylation. Trophoblasts of diabetic blastocysts showed lower total CpG methylation than the hypoblasts sampled from healthy blastocysts (me-CpGs=45 %, Figure 22B). The covered part of CR4 was methylated in 21 %, while the methylation of the fragment outside placed upstream to the conserved region was higher (62 %). CpGs in the distal enhancer 1A were methylated in 4,5 %, what is 45 % less than in trophoblasts of healthy blastocysts. The CpGs in close proximity to Oct4/Sox2 binding side were not methylated.

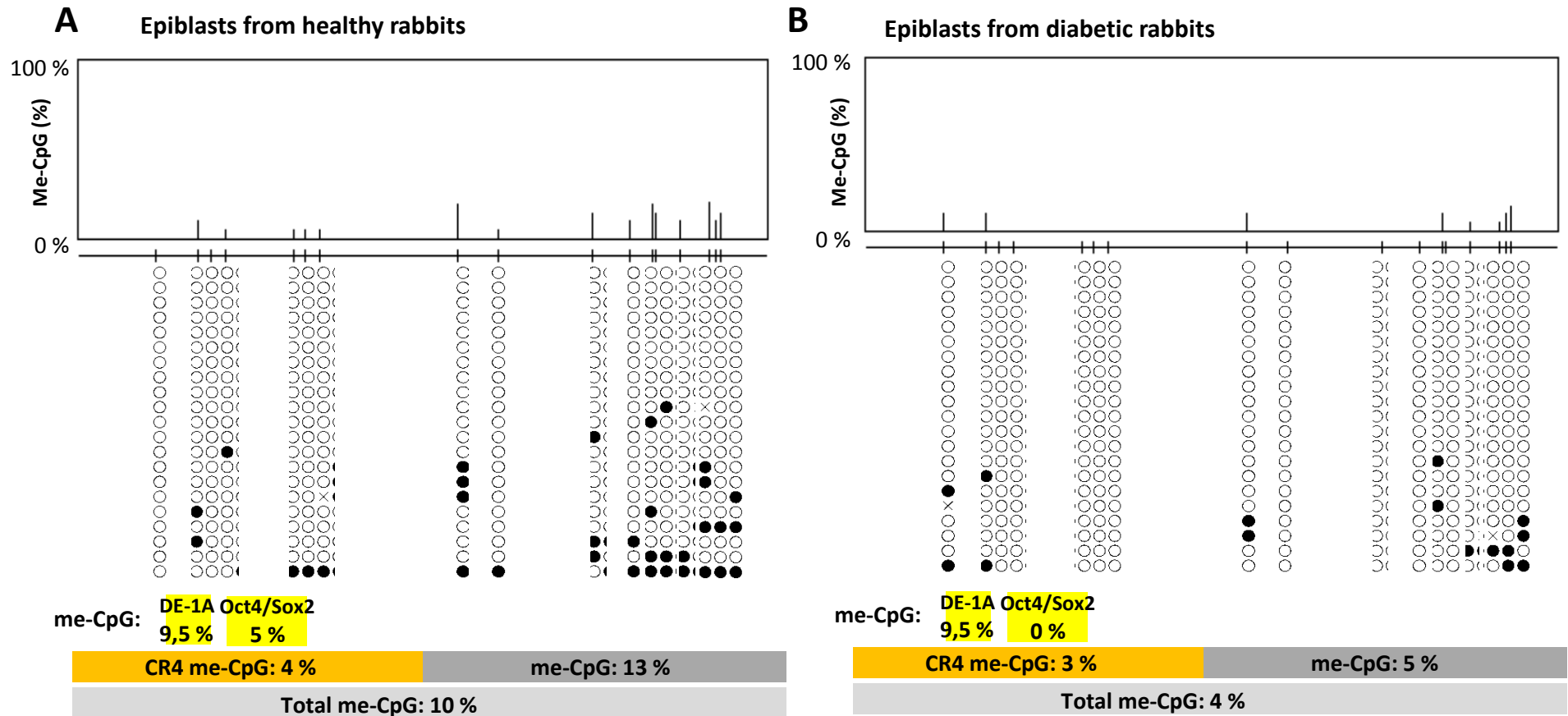


Figure 20. Bisulfite sequencing DNA methylation data for CR4-overlapping fragment of Oct4 (POU5F1) promoter region in epiblasts of rabbit blastocysts from healthy (A) and diabetic (B) rabbits

Column graphs display the percentage of methylation at single CpG position in analyzed promoter fragments. Lollypop-style graphs demonstrate methylation patterns from different alleles (each row represent data for one sequence); CR4 – conserved region 4; Me-CpG – methylation at single CpG position; DE-1A – distal enhancer 1A; Oct4/Sox2 – Oct4 and Sox2 binding site;

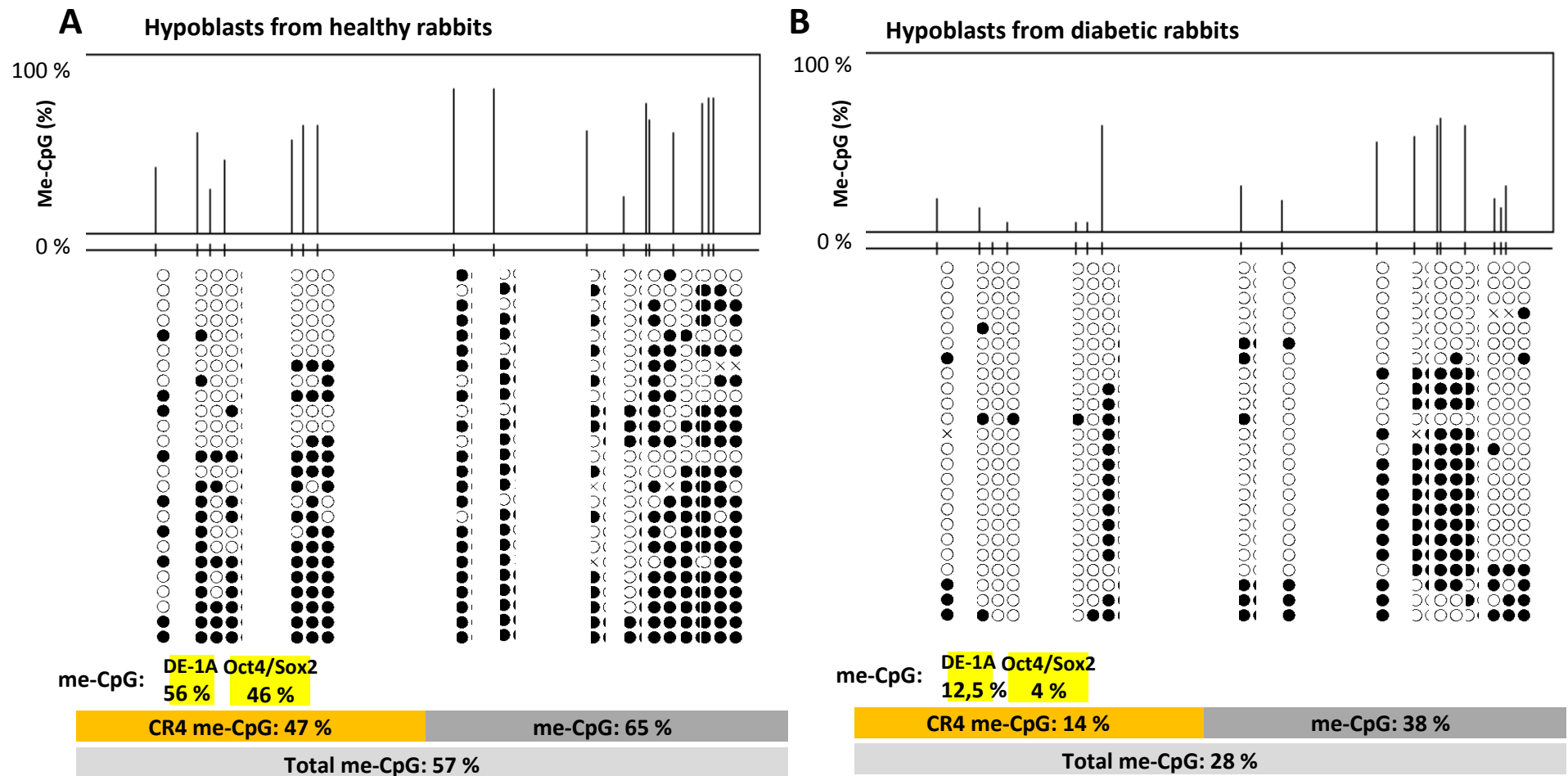


Figure 21. Bisulfite sequencing DNA methylation data for CR4-overlapping fragment of Oct4 (POU5F1) promoter region in hypoblasts of rabbit blastocysts from healthy (A) and diabetic (B) rabbits

Column graphs display the percentage of methylation at single CpG position in analyzed promoter fragments. Lollipop-style graphs demonstrate methylation patterns from different alleles (each row represent data for one sequence); CR4 – conserved region 4; Me-CpG – methylation at single CpG position; DE-1A – distal enhancer 1A; Oct4/Sox2 – Oct4 and Sox2 binding site;

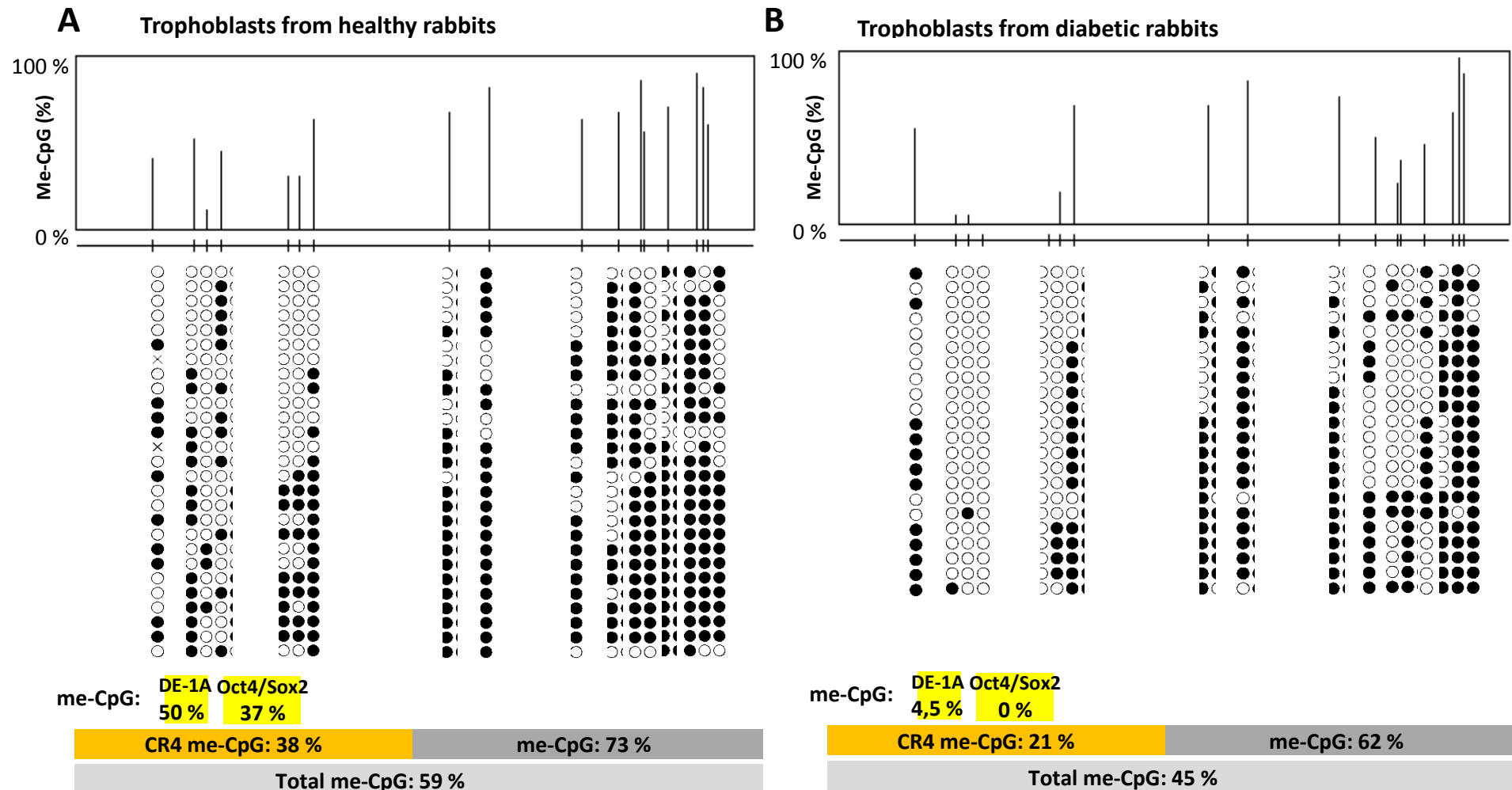


Figure 22. Bisulfite sequencing DNA methylation data for CR4-overlapping fragment of Oct4 (POU5F1) promoter region in trophoblasts of rabbit blastocysts from healthy (A) and diabetic (B) rabbits

Column graphs display the percentage of methylation at single CpG position in analyzed promoter fragments. Lollypop-style graphs demonstrate methylation patterns from different alleles (each row represent data for one sequence); CR4 – conserved region 4; Me-CpG – methylation at single CpG position; DE-1A – distal enhancer 1A; Oct4/Sox2 – Oct4 and Sox2 binding site;

3.5.4 Oct4 (POU5F1) conserved region 4 methylation analysis in rabbit adult heart tissue and embryonic tissues from healthy and diabetic pregnancies

Total CpGs methylation was the highest for adult rabbit heart tissue, but methylation of trophoblasts of healthy and diabetic blastocysts as well as the hypoblasts of diabetic blastocysts

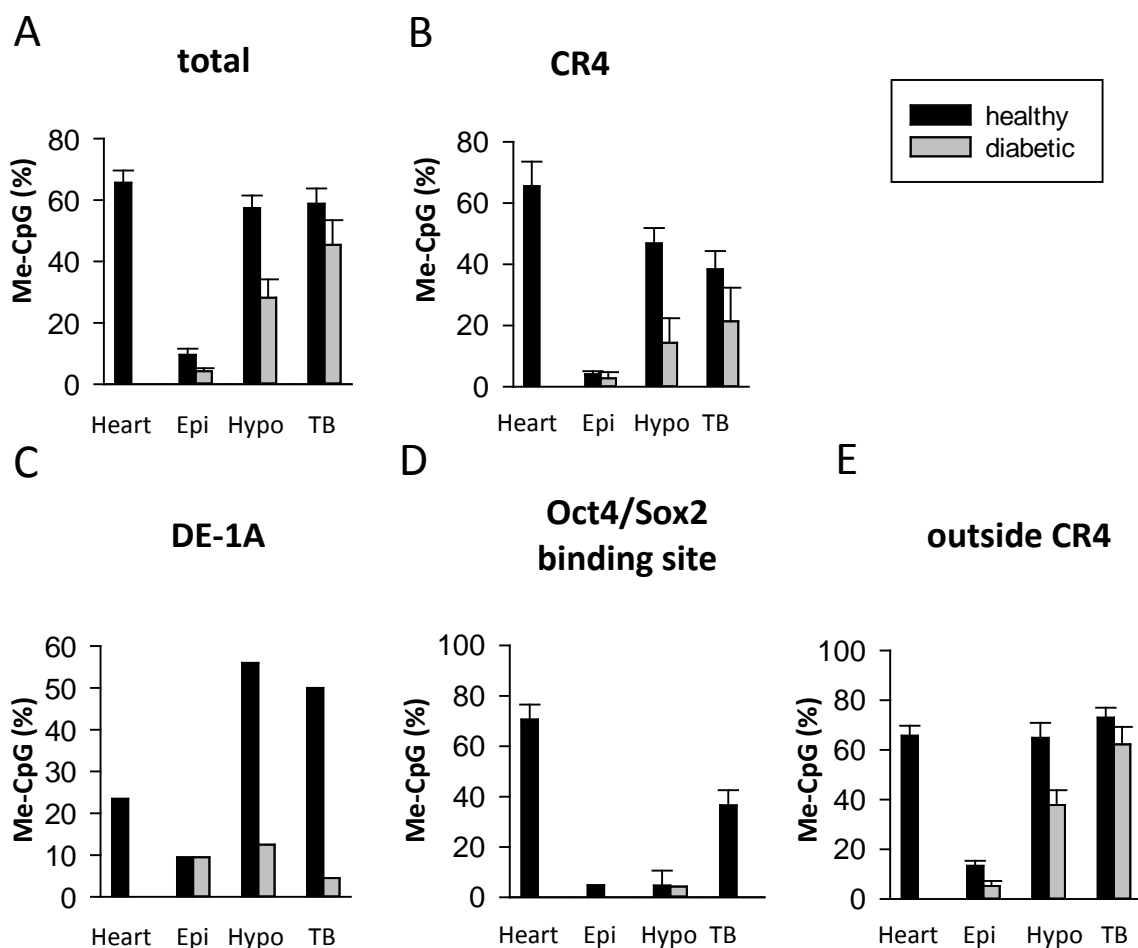


Figure 23. Bisulfite sequencing DNA methylation data for CR4-overlapping fragment of Oct4 (POU5F1) promoter region in rabbit adult heart tissues and embryonic tissues of blastocysts from healthy and diabetic pregnancies.

Column graphs show the average percentage of methylation at CpGs of the analyzed area in the promoter fragment, error bars show standard errors between average single CpG methylation inside of the analyzed fragments; A – methylation of total CpGs in CR4-overlapping fragment: B – methylation of CpGs at CR4; C – methylation of distal enhancer 1A (DE-1A); D – methylation of CpGs close to Oct4/Sox2 binding side; E – methylation at the fragment of outside the conserved region, downstream to CR4;

was also at high level. Methylation of diabetic hypoblasts was twice lower than for adult rabbit heart tissue. Epiblasts from healthy and diabetic blastocysts were methylated at the lowest level. In trophoblasts and hypoblasts methylation at the conserved region 4 was lower than in adult heart tissue, as well as in epiblasts with a methylation less than 5 % (Figure 23B). Hypoblasts and

trophoblasts of healthy blastocysts had a higher methylation of CpGs inside of the distal enhancer 1A than in the adult rabbit heart tissue (Figure 23C). Hypoblasts and trophoblasts of diabetic blastocysts had a lower methylation than healthy tissues. Epiblasts of healthy and diabetic blastocysts had a similar level of DE-1A CpGs methylation. CpGs close to the Oct4/Sox2 binding side were highly methylated in heart tissue, while the methylation in epiblast and hypoblasts from healthy and diabetic blastocysts was at a low level (Figure 23D). Trophoblasts of diabetic blastocysts showed no methylation in contrary to healthy ones, methylation in this area was 40 %. The fragment outside the conserved region, placed upstream to CR4, was methylated at a similar level in rabbit heart tissue and in hypoblasts and trophoblasts from healthy blastocysts (Figure 23E). Hypoblasts of diabetic blastocysts were lower methylated at this area than the hypoblasts of healthy blastocysts. The lowest methylation in this fragment was in epiblast tissues, showing no difference between the epiblasts of healthy and diabetic blastocysts.

3.6 Influence of maternal diabetes on expression of enzymes involved in the DNA methylation process.

3.6.1 *In vivo* expression of DNA methyltransferases in 6 day old rabbit blastocysts

The RNA amounts of the DNA methyltransferases DNMT1, DNMT3A and DNMT3B were analyzed in embryonic tissues of blastocysts from healthy and diabetic females harvested at day 6 *p.c.* and staged (Figure 7).

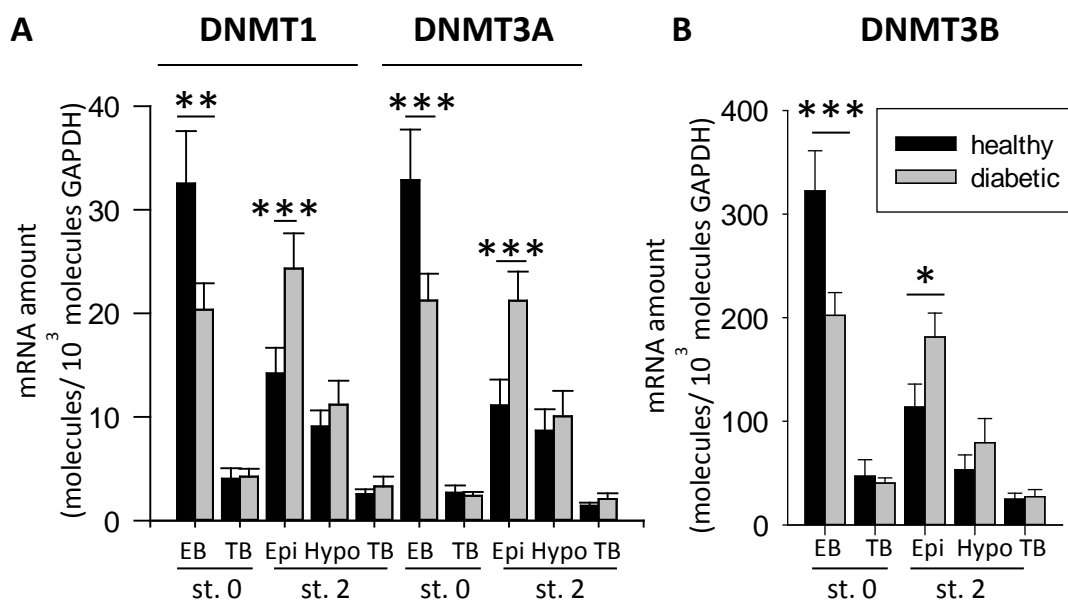


Figure 24. DNMTs mRNA amounts in embryonic tissues of 6 day old blastocysts (at stage 0 and 2) from healthy and diabetic rabbits (quantified by RT-qPCR). A – mRNA amounts of DNMT1 and DNMT3A; B – mRNA amounts of DNMT3B; mean \pm SEM ($N=3$, $n=6$ (n =pool of 3 embryonic tissues from different embryos); * $p \leq 0.05$; ** $p \leq 0.001$; *** $p \leq 0.0001$); EB –embryoblast, TB – trophoblast, Epi – epiblast, Hypo – hypoblast.

All DNMTs were expressed and demonstrated a comparable pattern of expression. For stage 0 embryoblasts from diabetic pregnancies the level of DNMTs amounts was significantly increased, while no difference was detectable for the trophoblast. Also stage 2 diabetic epiblasts showed an upregulation in DNMTs expression compared to embryos from healthy pregnancies. Among the extraembryonic tissues at stage 2 RNA amounts of DNMTs was higher for hypoblasts than for trophoblasts, while no difference was observed between the tissues from healthy and diabetic pregnancies. While the expression of DNMT1 and DNMT3A oscillate in similar ranges (Figure 24A), the DNMT3B RNA amounts were approximately ten times higher in each of the embryonic tissues (Figure 24B).

3.6.2 *In vivo* expression of DNA methyltransferases in fetal rabbit hearts at day 12 and 14 of pregnancy

Expression of DNMTs was investigated in rabbit fetal hearts collected at day 12 and 14 *p.c.* of healthy and diabetic pregnancies (Figure 25). Transcripts of all DNMTs were detectable and DNMT1 has shown the strongest expression. Between day 12 and 14 of development no differences were observed. Furthermore there was no difference between groups derived from healthy and diabetic pregnancies. Expression of the DNMT3A presented a tendency for downregulation in case of diabetic pregnancies, with $p=5,27\%$, while the DNMT1 was unchanged. RNA amounts of DNMT3A were twice smaller than DNMT1, while DNMT3B expression was on a basal level.

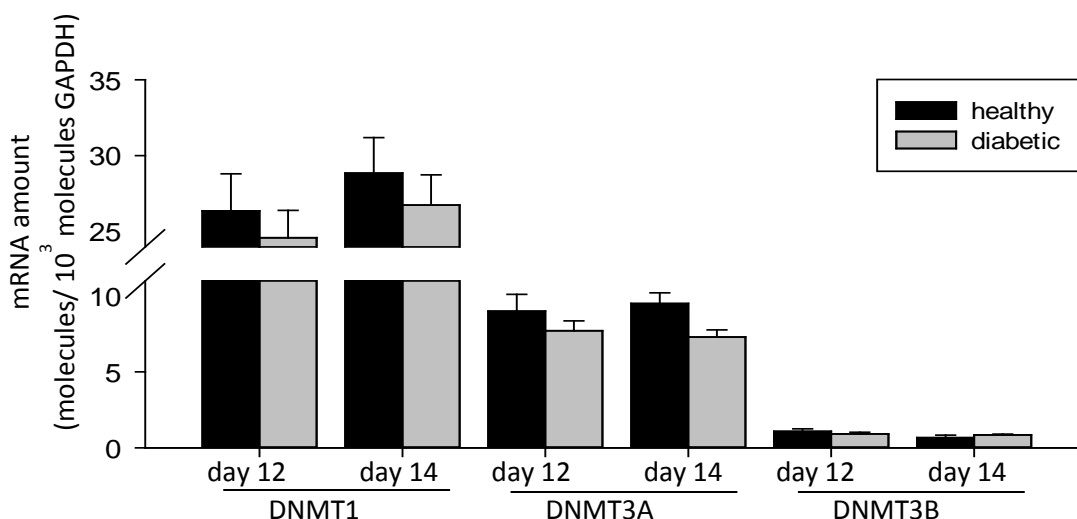


Figure 25. DNMT1, -3A and 3B RNA amount in fetal rabbit hearts day 12 and 14 from healthy and diabetic pregnancies quantified by RT-qPCR. Mean \pm SEM (N=3, n=8).

3.7 Expression of DNA methyltransferases *in vitro* culture

To identify the influence of hormone and nutritional factors on DNMT expression in preimplantation embryos, 6 day old rabbit blastocysts were cultured *in vitro* with:

- Insulin: 2 h of preculture and 4 h culture with 17 nM insulin and no insulin,
- Branched chain amino acids (BCAAs): 6 h culture with normal and diabetic concentrations of BCAAs,
- Insulin growth factor 2 (IGF2): 2 h of preculture and 4h culture with 13 nM IGF2 and no IGF2,
- Leukemia inhibitory factor (LIF): 6 h culture with 10ng/ml LIF and no LIF.

Relative amounts of DNMTs were measured by RT-qPCR (Figure 26, 27 and 28).

3.7.1 Influence of *in vitro* culture with insulin, BCAAs, IGF2 and LIF on DNMT1 expression in embryonic tissues of rabbit blastocysts day 6 stage 1

Upon culture with BCAAs, IGF2 or LIF DNMT1 transcript levels in embryonic tissues of cultured day 6 blastocysts were not changed. Levels of DNMT1 were higher in epiblasts after *in vitro* culture with insulin than in the epiblasts cultured without insulin stimulation (Figure 26).

RNA amounts of DNMT1 in blastocysts cultured with IGF2 were lower in epiblasts and hypoblasts than in epiblast and hypoblasts of embryos culture with BCAAs and insulin *in vitro*. The difference might be due to lower quality of sample.

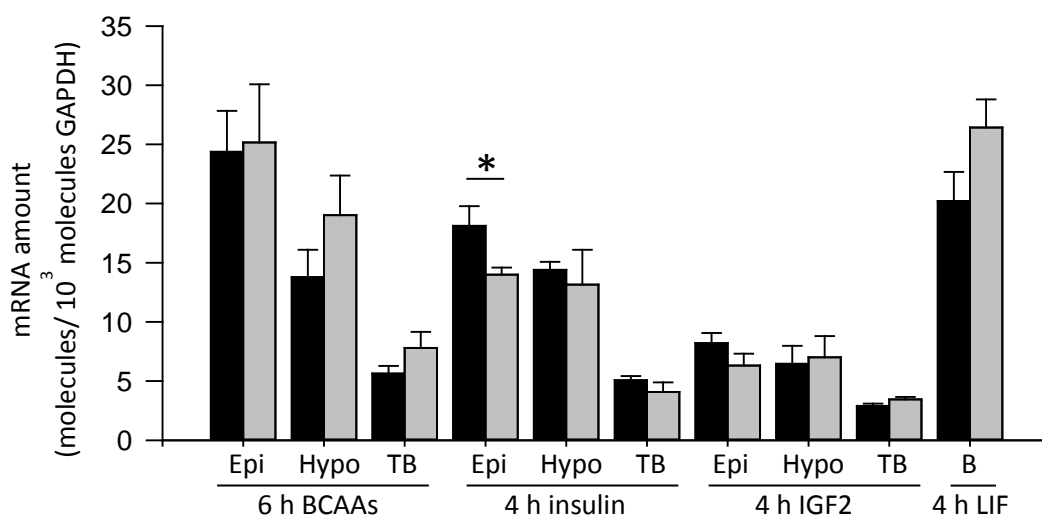


Figure 26. DNMT1 mRNA transcript levels in embryonic tissues from blastocyst at day 6 *p.c.* stage 1 after *in vitro* culture with BCAAs, insulin, IGF2 or LIF, respectively, quantified by RT-qPCR. Black bar – *in vitro* culture in media, gray bar – *in vitro* culture with hormone or nutrition factor; mean \pm SEM (N=3, n=6 (n=pool of 3 embryonic tissues from different embryos); * $p \leq 0.05$); Epi – epiblast, Hypo – hypoblast, TB – trophoblast, E – whole blastocyst.

3.7.2 Influence of *in vitro* culture with insulin, BCAAs, IGF2 or LIF on DNMT3A expression in embryonic tissues of rabbit blastocysts day 6 stage 1

Expression of DNMT3A was not influenced by *in vitro* culture with BCAAs, insulin, IGF2 or LIF (see details at Figure 27).

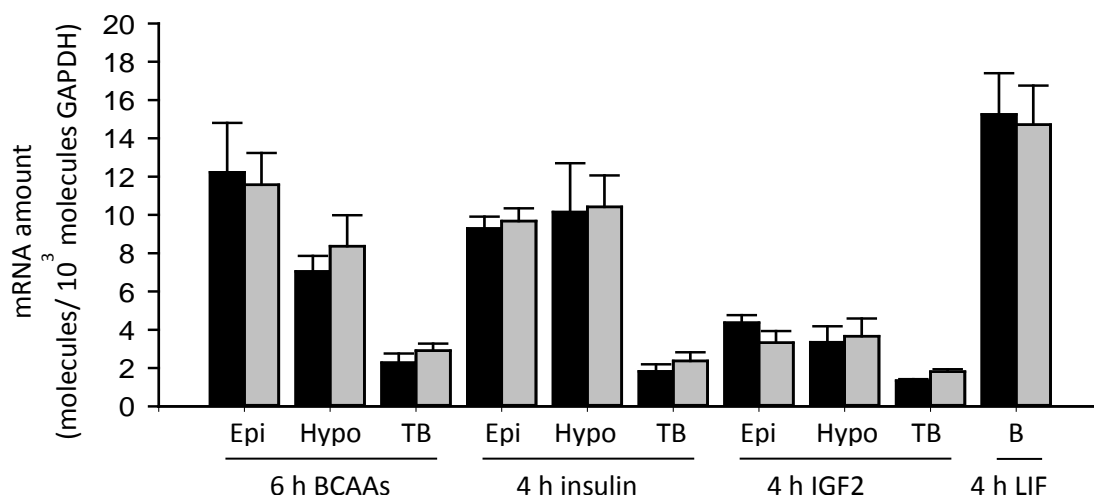


Figure 27. **DNMT3A mRNA transcript levels in embryonic tissues from blastocyst at day 6 p.c. stage 1 after *in vitro* culture with BCAAs, insulin, IGF2 or LIF, respectively, quantified by RT-qPCR.** Black bar – *in vitro* culture in media, gray bar – *in vitro* culture with hormone or nutrition factor; mean \pm SEM (N=3, n=6 (n=pool of 3 embryonic tissues from different embryos); * $p \leq 0.05$); Epi – epiblast, Hypo – hypoblast, TB – trophoblast, B – entire embryo.

3.7.3 Influence of *in vitro* culture with insulin, BCAAs, IGF2 or LIF on DNMT3B expression in embryonic tissues of rabbit blastocysts day 6 stage 1

DNMT3B mRNA amounts were not affected by culture with BCAAs, insulin or LIF. In epiblasts after *in vitro* culture with IGF2 the level of DNMT1 was higher than in the normal control without IGF2 stimulation (Figure 28).

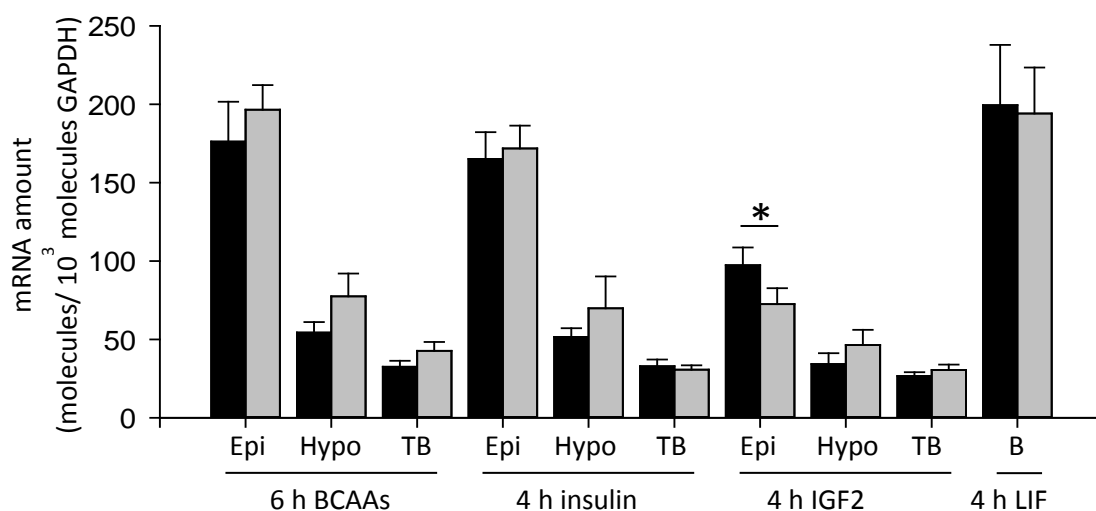


Figure 28. **DNMT3B mRNA transcript levels in embryonic tissues from blastocyst at day 6 p.c. stage 1 after *in vitro* culture with BCAAs, insulin, IGF2 or LIF, respectively, quantified by RT-qPCR.** Black bar – *in vitro* culture in media, gray bar – *in vitro* culture with hormone or nutrition factor; mean \pm SEM (N=3, n=6 (n=pool of 3 embryonic tissues from different embryos); * $p \leq 0.05$); Epi – epiblast, Hypo – hypoblast, TB – trophoblast, B – whole blastocyst.

3.8 Measurements of metabolites: S-adenosylmethionin and S-adenosylhomocystein in rabbit maternal blood plasma at day 6 of pregnancy

Concentrations of SAM and SAH were measured by stable-isotope dilution ultra-performance liquid chromatography tandem mass spectrometry (LC-MS/MS) in blood plasma of rabbits at day of 6 pregnancies (Figure 29A and B). The ratio between SAM and SAH stayed similar in maternal plasma at day 6 *p.c.* in healthy and diabetic pregnancies (Figure 29C).

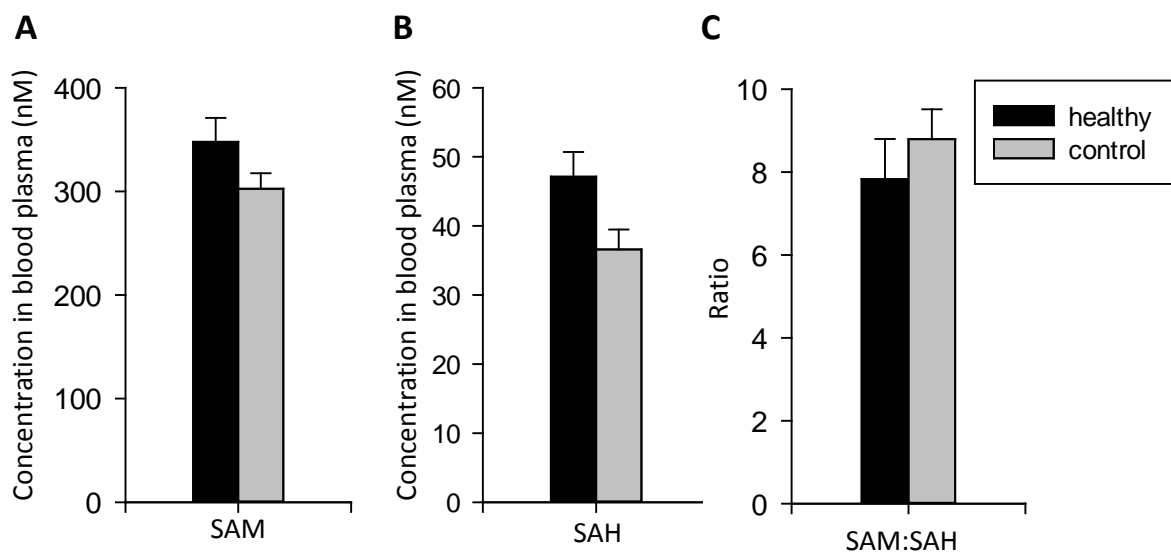


Figure 29. Concentrations of SAM and SAH in blood plasma of rabbits at day 6 from healthy and diabetic pregnancies by Liquid chromatography with tandem mass spectrometry (LC-MS/MS). Mean \pm SEM (N=3, n>9); A – concentration of SAM, B – concentration of SAH, C – ration SAM:SAH.

4. Discussion

4.1 Oct4 is a lineage specifier in early rabbit blastocyst

Oct4 pluripotency factor is known as an epiblast lineage specifier and plays a crucial role in human embryogenesis (Fogarty et al., 2017; Loh and Lim, 2011). Oct4 is expressed in a tissue-dependent manner in 6 day old rabbit blastocyst. The highest expression of Oct4 was found in epiblasts, then hypoblasts, and the lowest in trophoblast tissue in rabbit blastocysts. At the beginning of gastrulation a high level of Oct4 RNA is detectable in embryoblast cells, while trophoblast cells express Oct4 at a basal level. Rabbit blastocysts at the late stage of gastrulation (stage 2) express less Oct4 in epiblasts than in embryoblasts (stage 0), similar in the trophoblasts. It is likely that this change may be associated with the loss of pluripotency and the start of differentiation. A high Oct4 transcript level in epiblasts was already reported as a marker of mesodermal differentiation. The high Oct4 expression in embryoblasts confirmed these findings (Niwa et al., 2001). In the embryoblasts of blastocyst stage 2, Oct4 RNA level is lower than at blastocyst stage 0 and can be measured in two compartments: epiblasts and hypoblasts, with the epiblast showing higher Oct4 level than the hypoblast. In contrary to Canon et al., Oct4 expression was not addressed only to epiblasts of rabbit blastocysts, as we have observed Oct4 transcripts also in the hypoblast and trophoblast (Canon et al., 2014). Oct4 mRNA is also present in hypoblasts of chick embryos at epiblast differentiation, supporting our results (Lavial et al., 2007). In bovine preimplantation development Oct4 protein is found to be expressed in trophoblast cells, but its localization is outside of the nuclei (Madeja et al., 2013), indicating that Oct4 expression is not due to its function as nuclear transcriptional factor, but to its cytoplasmic protein regulator properties. Trophoblasts of rabbit stage 2 blastocysts have less Oct4 RNA than at stage 0. In blastocysts repression of Oct4 expression is associated with proper trophoblast differentiation (Niwa et al., 2000).

4.1.1 Pluripotency markers are upregulated in blastocysts of diabetic rabbits

In 6 day old rabbit blastocysts, maternal diabetes influences key genes of the pluripotency network. At stage 2 of gastrulation, the expression of Oct4 is twice higher in epiblasts of diabetic blastocysts than in healthy controls. Additionally, the expression of Sox2 is higher in epiblasts of diabetic blastocysts, and Nanog shows a similar tendency.

The upregulation of Oct4 and Nanog was also described in human visceral-derived adipose stem cells exposed to a diabetic milieu (Denteli et al., 2013). Moreover, Oct4 and Nanog positive cells can be found in peripheral blood of diabetic patients. Contrary to findings in these patients, Sox2 is downregulated (Potdar and D'suza, 2011). A diabetic pregnancy influenced Oct4 expression in hypoblasts of 6 day old rabbit blastocyst. In trophoblast cells an upregulation of Oct4 is observed already at the beginning of gastrulation in stage 0 blastocysts of diabetic rabbits, while at stage 2

Oct4 expression remains unchanged. While the loss of Oct4 expression indicates a proper trophoblast differentiation, a higher Oct4 expression in trophoblast of diabetic rabbits at stage 0 is a marker of a delay in development (Zeineddine et al., 2006). Trophoblasts of diabetic rabbits at stage 2 are already at the same Oct4 RNA level as healthy ones, but there is not clear evidence whether Oct4 is necessary for the correct development of trophoblast tissue.

4.1.2 Development in diabetic conditions impairs trophoblast lineages decisions

Cdx2 is a well-known marker of trophoblast differentiation in mouse blastocysts (Schiffmacher and Keefer, 2013; Strumpf et al., 2005). In 6 day old rabbit, blastocysts Cdx2 RNA amount decreases in trophoblast cells as gastrulation proceeds. In trophoblasts of healthy rabbits Cdx2 RNA amounts decrease from stage 0 to 2, what is correlating with the decline of Oct4 expression. This observation has already been reported in mouse and porcine blastocysts. A mechanism of Oct4 repression mediated by Cdx2 was proposed (Wang et al., 2013; Bou et al., 2016). Contrary to a developmentally programmed downregulation during gastrulation trophoblasts of diabetic rabbits show a tendency to upregulate Cdx2 RNA at stage 2. Additionally, no decline of Cdx2 RNA amounts could be measured between stage 0 and 2 trophoblasts of diabetic blastocysts, what might indicate retardation in trophoblast differentiation. Expression of Hex, an important marker of proper hypoblast differentiation (Blomberg et al., 2008), was not changed in the diabetic pregnancy.

4.2 Effect of maternal diabetes on specific (Oct4) promoter methylation

Specific gene promoter methylation in early development is an extensively investigated subject (Canovas and Ross 2016; White et al., 2016). The rate of methylation of a gene promoter is associated with its mRNA amounts. This phenomenon was first observed in adult organisms, where gene expression switch-off was paralleled by an increase in promoter methylation (Jones and Takai, 2001).

The decrease of Oct4 expression during embryonic development and its expressional switch-off is accompanied by an increased Oct4 promoter methylation (Lee et al., 2010). As Oct4 expression of rabbit blastocysts is impaired by maternal diabetes, we hypothesized that the Oct4 promoter is a potential target for diabetic effects.

Therefore conserved regions of the Oct4 promoter region (GenBank: AC235550.2) were chosen for methylation analysis to address the question to conserved sequence fragments of the Oct4 promoter region in mammalian species. Oct4 (POU5F1) promoter methylation was analyzed by bisulfite sequencing in adult rabbit heart tissue, to understand which pattern of the promoter methylation is present in mature and differentiated somatic cells. Kobolak et al., described rabbit Oct4 promoter organization (2600 bp) indicating 4 conserved regions (CR1-4) (Kobolak et al., 2009). CR1 was chosen for further analysis because it is placed in the minimal promoter, and CR1

covers transcriptional binding sites and the transcription start site, where methylation is known to be divergent from downstream elements in the gene cassette (Brenet et al., 2011). CR4 at 5`-UTR was previously described as the most likely to be responsible for Oct4 expression in mouse epiblasts and mouse ESCs, what makes it an interesting subject for DNA methylation studies (Yeom et al., 1996, Kobolak et al., 2009).

4.2.1 Methylation rate of the Oct4 promoter is higher in differentiated cells

Methylation of the Oct4 promoter region is high in adult tissues, but seems to be inconsistent in sequence. In CR4 at the 5`-UTR, it is higher than in CR1 at the transcription start site, the CpG methylation rates vary from 66 % down to 52 %. An average CpG methylation of Oct4 promoter is 58 %, what is close to the range of standard CpG methylation reported for differentiated cells in higher animals, 60 - 90 % (Ehrlich et al., 1982; Tucker, 2001). Lower methylation at transcription start site was already described (Gardiner-Garden, Frommer 1987; Antequera, Bird 1993). The CR1-overlapping fragment is located down to -220 bp from transcription start site, what might be a reason for a methylation rate below 60 %.

Additionally, Pamnani et al. suggested that the methylation of CpGs in Sp1/Sp3 binding site might be a reason for the absence of Oct4 expression in adult somatic tissues. It could be the same in the case of rabbit heart tissue (Pamnani et al., 2016). Additionally, Sp1 and Sp3 can stop epigenetic inactivations of several genes by binding to clustered GC-boxes and hence blocking CpG sites from methylation (Macleod et al., 1994). The most methylated CpGs are outside the CR1 region, while the lowest methylation level is noted close to the HRE and Sp1/Sp3 binding site (44 %), but both CR1- and CR4-overlapping fragments are in general highly methylated in rabbit heart tissue. The CR1-overlapping fragment is methylated to 52 %.

The CR4-overlapping fragment is even more methylated than the CR1-overlapping fragment. Interestingly CpGs in distal enhancer sequence were methylated only at 24 %. Average me-CpG at CR4 region is 66%, what is in range of methylation at 5`-UTR of Oct4 promoter already presented for adult liver tissue (Hattori et al., 2004).

4.2.2 Limitations of bisulfite conversion in DNA methylation studies

The bisulfite sequencing method is a useful tool for DNA methylation studies, but not free from limitations (Wojdacz et al., 2010). The bisulfite reaction is not distinguishing between DNA methylation and hydroxymethylation, what may impact the interpretation of the results. Furthermore, a concern in usage of this method is the ratio of the bisulfite reaction to convert cytosine into uracil. Incomplete conversion of cytosine is a common problem, which handling can be improved, but not eliminated. Therefore, the conversion ratio of sequences used in Oct4 methylation study is set to 90 %, what left a 10 % mistake in the interpretation of CpG

methylation. All results, expressed average percentage are interpreted as a change in DNA methylation, if the difference between two groups is greater than 10 %.

4.3 General scheme of DNA methylation dynamics and Oct4 promoter regulation in early development

Diabetic woman are subfertile, and the embryos challenged with maternal diabetes are often failing implantation. A higher methylation of the CR1-overlapping fragment in epiblasts of diabetic blastocysts shows that in some cases diabetes may be a factor influencing the epigenetic remodeling processes in early stage embryo. DNA methylation is a dynamic process in early development (Hackett and Surani 2013). Demethylation and *de novo* methylation are shown in Figure 30. The *de novo* methylation process in embryos is accomplished around the time of implantation. Therefore, DNA methylation of the Oct4 promoter was a subject of investigation in 6 day old rabbit blastocyst. To see how different methylations between blastocysts, at first blastocysts used for DNA methylation study were staged according to morphology, then sampled to epiblast, hypoblast and trophoblast and collected as a pool of epiblasts, hypoblasts and trophoblasts of 3 blastocysts. The material was collected during two experiments to evaluate the difference between pools of embryonic tissues from experimental replicates.

Total methylation of the epiblast, hypoblast and trophoblast pools from experiment 1 and 2 were related to the CR1- and CR4-overlapping fragments. The results of experiment 1 and 2 are comparable in most of the embryonic tissues investigated. Despite the fact that no equal number of sequences is obtained from experiment 1 and 2, in further analyse data can be combined in one plot to present all alleles found for a given embryonic tissue.

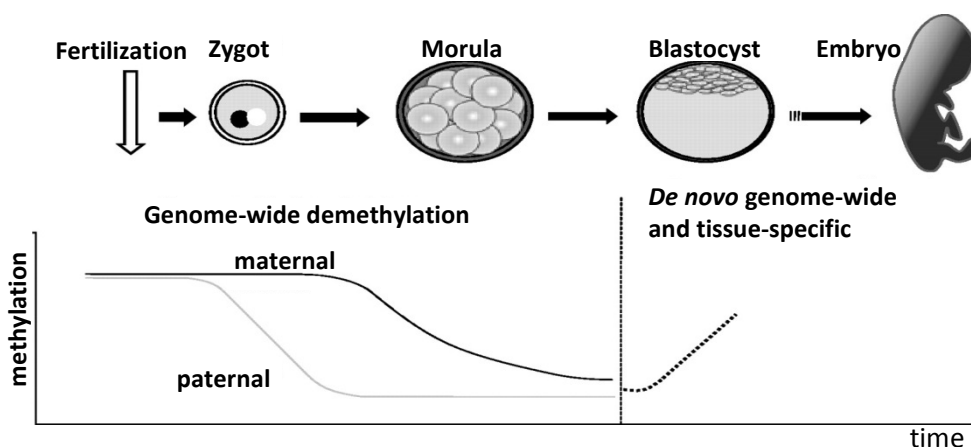


Figure 30. **Dynamic of DNA methylation changes during early development (modified after Atala and Lanza 2012).**

The most prominent difference between results of experimental group 1 and 2 was observed in epiblasts of diabetic embryos at the CR1-overlapping fragment, while no difference in methylation was observed at CR4-overlapping fragment.

The results of epiblasts of diabetic blastocysts obtained from the experimental group 1 show a higher methylation than the epiblasts of healthy blastocysts. The increase in CR1 methylation does not inhibit transcription of Oct4, which is also higher in epiblasts of diabetic rabbits. Changes in CR1 methylation may be a consequence of an ineffective demethylation process, such as in cloned mouse embryos, where impaired demethylation led only to gradual demethylation of the Oct4 promoter (Yamazaki et al., 2006). Results of Yamazaki et al., show failure in the development of cloned embryos as well as developmental retardation. The blastocysts of diabetic rabbits are also more likely to fail to carry out implantation and be delayed in development (Thieme et al., 2012; Ramin et al., 2010). It might be possible that differences between the methylation of the epiblast CR1-overlapping fragment from experimental group 1 and 2 can indicate a moderate demethylation process in diabetic blastocysts collected for experiment 1. Another explanation might be highlighted by a study of Oct4 methylation profile in human oocytes and ICSI embryos (Al-Khtib et al., 2012). It has been demonstrated that the methylation pattern of Oct4 is disturbed in oocytes of women with known infertility. Additionally, ICMs Oct4 promoter methylation of ICSI embryos arrested in development from infertile women was associated with high methylation of this region, while the ICSI embryos which were developing further showed hypomethylation. Al-Khtib et al., (2012) hypothesized that hypermethylation of Oct4 in embryos with poor implantation prognosis might be a result of incorrect remodeling at the epigenetic level.

4.3.1 Diverse methylation patterns of Oct4 promoter in embryonic tissues

In global methylation studies of early preimplantation of mouse embryo, the inner cell mass is hypomethylated until epiblast differentiation. The formation of the hypoblast correlates with the increase in CpG methylation (Li et al., 2016). Trophoblast cells remain globally hypermethylated. This is reflected in our observations of the Oct4 methylation state of rabbit embryonic tissues from gastrulating blastocyst (stage 2) (see details in Table 3). Epiblasts are the lowest methylated tissue: 11 % of CpG are methylated at the CR1-overlapping fragment and 10 % at the CR4-overlapping fragment. Hypoblast methylation is higher than in epiblasts, while the CR-overlapping fragment is lower methylated than the CR4-overlapping fragment, 42 % and 57 %, respectively. The methylation of trophoblasts at CR1- and CR4-overlapping fragments is similar to the hypoblast methylation level. Interestingly trophoblasts are highly methylated at CpGs outside the conserved regions. These data were gathered in consent with the investigation of Canon et al., of Oct4 promoter methylation in rabbit 6 day old blastocysts (Canon et al., 2014). They described very low methylation of epiblasts in all Oct4 conserved regions. In comparison to adult rabbit hearts, Oct4 promoter of all embryonic tissues is lower methylated (see summary in Table 3).

Pamnani et al., have shown the highest methylation of Oct4 methylation among the investigated somatic tissues in kidneys (50 % of methylated CpG),

Table 3. Summary of methylation at Oct4 promoter in CR4- (A) and CR1-overlapping fragment (B) and their functional elements.

me-CpG (%)	CR4-overlapping fragment methylation in:									me-CpG (%)	CR1-overlapping fragment methylation in:										
	Heart	Epiblast		Hypoblast		Trophoblast		Heart	Epiblast		Hypoblast		Trophoblast								
		healthy	diabetic	healthy	diabetic	healthy	diabetic		healthy		diabetic	healthy	diabetic	healthy	diabetic						
total	66	10	=	4	57	>	28	59	>	45	total	52	11	<	25	42	>	15	39	=	40
CR4	66	4	=	3	47	>	14	38	>	21	CR1	46	9	<	20	38	>	14	34	=	36
outside CR4	66	13	=	5	65	>	38	73	>	62	minimal promoter	53	11	<	29	44	>	16	48	=	45
DE-1A	24	9.5	=	9.5	56	>	12.5	50	>	4.5	outside CR1	67	14	<	46	56	>	21	78	>	61
Oct4/Sox2 binding site	71	5	=	0	46	>	4	37	>	0	exon	50	11	=	19	38	>	13	24	=	33
unmethylated CpG in position:	-	11, 15		13	-		13, 18	13		-	HRE and Sp1/Sp3	44	5	<	18	47	>	11	21	=	31
											unmethylated CpG in position :	-	1, 3		3, 4, 5-7, 9-11, 13	-		3, 5, 6	-		4

Unmethylated CpG position corresponds to CpGs, which were not methylated in all obtained sequences. Equal sign means that the difference in DNA methylation is not greater than 10 %; signs of inequality indicate lower or higher average methylation between epiblasts, hypoblasts and trophoblasts of healthy and diabetic rabbits.

while a low percentage was observed in germinal tissues for both testis and ovaries (~5 % of methylated CpG) (Pamnani et al., 2016). In rats, the Oct4 promoter region is reported as hypomethylated at day 4.5 *p.c.*, while at day 10.5 *p.c.* an increase of methylation is described (He et al., 2009). These publications support the view that Oct4 promoter gains methylation gradually during rabbit embryonic development and somatic cell differentiation.

4.3.2 Diabetic pregnancy influences methylation of Oct4 promoter in epiblasts, hypoblasts and trophoblasts of rabbit blastocysts

Development in a diabetic uterine milieu affects methylation of Oct4 promoter in rabbit blastocysts. Epiblasts of diabetic embryos are higher methylated at the CR1-overlapping fragment than the healthy ones (11 % and 25 %, respectively), especially at CpG outside the conserved region (46 %, observed just in experiment 1). As mentioned before, this can be explained by an aberrant demethylation process in early morula or by impaired chromatin remodeling (Yamazaki et al., 2006). In any case, development in a diabetic female influences epiblast Oct4 methylation at the CR1-overlapping fragment, but not at the CR4-overlapping fragment, of its promoter region.

The most prominent change in Oct4 promoter methylation among the embryonic tissues was observed in hypoblasts. Hypoblasts of diabetic blastocysts show a hypomethylation at both analyzed fragments of Oct4 promoter region: the CR1- and CR4-overlapping fragments, with about 25 % lower methylation detected in both cases. Loss of methylation was seen at CpG inside of conserved region 1 and 4, as well as outside the conserved regions and at exon in the CR1-overlapping fragment. Unmethylated CpG at functional elements of gene promoter are often a sign of occupation of them by transcriptional factors and chromatin remodelers (Jones, 2012). Since a decrease in methylation is observed at functional elements like in HRE and Sp1/Sp3 binding site and distal enhancer 1A (DH-1A) it might be that those parts of sequence are occupied by transcriptional factors. In this way Oct4 transcription activating factors can still recognize their consensus sequences and create a 'protection' for unmethylated CpG from the DNA methylation machinery.

Total methylation of trophoblasts of diabetic blastocysts at the CR1-overlapping fragment is similar to the percentage observed in healthy ones. Methylation of functional elements inside of CR1-overlapping fragment has not change in trophoblast cells upon development in diabetic pregnancy. It is contrary to a study of Hattori et al., of trophoblast stem cells (Hattori et al., 2004). Hypermethylation of CpG at the minimal promoter, proximal enhancer and 5'-UTR in POU5F1 (Oct4) promoter was observed and linked with DNA methylation studies of Sp1/Sp3 binding site inside the Oct4 promoter. Hattori et al., demonstrated that CpG in the Sp1/Sp3 binding site are completely unmethylated in trophoblast stem cells. The CR4-overlapping fragment is less

methyated in trophoblasts of diabetic blastocysts, as well as DE-1A and the Oct4/Sox2 binding sites in CR4 (Hattori et al., 2004). It suggests that the elements responsible for Oct4 activation can be bound to the distal enhancer or to the Oct4/Sox2 binding site. In this case, the distal enhancer and Oct4/Sox2 binding site inside of CR4 might be involved in the epigenetic regulation of Oct4 transcription in differentiating trophoblast cell population.

4.3.3 Oct4 expression correlates with level of Oct4 promoter methylation in rabbit embryonic tissues at the blastocyst stage

There is a correlation between the expression of Oct4 and its promoter methylation in rabbit embryonic tissues. In differentiated tissues, such as rabbit heart tissues high levels of the Oct4 promoter methylation (52-66 %) were found in comparison to the embryonic tissues of 6 day old blastocyst (Hopf, 2016). This indicates that the downregulation of Oct4 expression is governed by DNA methylation in early development. A decline of Oct4 RNA amounts during differentiation and development was reported in mouse early neuronal stem cells at 8.5 day of embryonic development with a decline to undetectable level by day 15.5. These events coincidence with an increase of DNA methylation at the Oct4 promoter region (Lee et al., 2010). Oct4 transcript levels decline during murine testicular growth from embryo to adult, while its promoter methylation pattern is described as inconsistent and heterogeneous (Pamnani et al., 2016). This study is focusing on the tissue compartments, instead of the cell types, so that the observed heterogeneity might be a result of mixed cell populations rather than developmental processes. In summary, the Oct4 expression depends on the DNA methylation of the Oct4 promoter and the Oct promoter CpG methylation is increasing during embryonic development, remaining methylated in adult somatic cells.

Oct4 mRNA levels correlate with its promoter methylation in rabbit blastocyst. The Oct4 transcript level is the highest among embryonic tissues in epiblasts and correlates with low methylation at the CR1- and CR4-overlapping fragment. High levels of Oct4 due to its promoter hypomethylation are reported in embryonic stem cells (Streck and Kumpf 2006). This also supports our observation that Oct4 expression is regulated by its promoter methylation.

The percentage of Oct4 promoter methylation is similar in hypoblasts and trophoblasts at the investigated conserved regions, but the Oct4 RNA level is higher in hypoblasts than in trophoblasts. Transcription of Oct4 in trophoblasts is close to basal levels in 6 day old rabbit blastocysts. The restriction of Oct4 expression in trophoblast stem cells was previously described by Hattori et al., together with hypermethylation of CpG at the POU5F1 (Oct4) promoter (Hattori et al., 2004). Therefore, a possible explanation why trophoblast tissue expresses less Oct4 than hypoblast tissue being equally methylated at the same time is that in gastrulating blastocysts the trophoblast is the first tissue which starts to lose pluripotency, while hypoblast development

starts together with gastrulation (at day 6 *p.c.*). Although the methylation of the Oct4 promoter is already accomplished in hypoblasts, the Oct4 mRNA transcripts can still be at a high level.

4.3.4 Diabetes affects embryonic lineages by influence on Oct4 expression through changes in its promoter methylation

Upregulation of Oct4 promoted by promoter hypomethylation is described in diseases, for example in recurrent gliomas (WU et al., 2015, Shi et al., 2013), and a decrease of the Oct4 promoter methylation combined with an expression increase is observed in mouse blastocysts after vitrification (Zhao et al., 2012). It suggests that Oct4 regulation through its promoter methylation is a sensitive target and might be easily modified in pathological states.

Oct4 acts in early development as a lineage specifier, its expression is restricted more to the embryoblast, and simultaneously with gastrulation proceeding onwards it becomes restricted to epiblast tissue. Upregulation of Oct4 in epiblasts of diabetic embryos indicates a delay in development of epiblast tissue, but there are only small differences in the Oct4 promoter methylation and surprisingly the Oct4 promoter of diabetic epiblasts is higher methylated. At this stage the Oct4 promoter region methylation is probably not a factor influencing its expression in embryos of diabetic rabbits. Other possibilities of the Oct4 transcription regulation need to be taken into account.

While the Oct4 expression is unchanged upon development in diabetic conditions in hypoblasts of 6 day old blastocysts, its promoter region methylation is affected by hypomethylation, so there is no direct correlation between changes in the Oct4 promoter methylation and Oct4 mRNA levels. The expression of the hypoblast differentiation marker Hex remained unchanged upon development in a diabetic pregnancy. An aberrant DNA methylation pattern can be associated with a delay in development (Li et al., 2012). It is known that proper hypoblast development is important in early fetal growth. A link between insulin secretion by the hypoblast during development to insulin-related diseases in adult life has been described (Moore et al., 2001). Beside that pregnancies challenged by type-1 DM have a predisposition to maternofetal transport dysfunction (Ivanisević et al., 2006, Aires et al 2015, Dong et al., 2016). There is also much evidence that diabetes impairs yolk sac formation and, therefore, sets a negative impact on the embryo and fetus. In rat postimplantation yolk sac development, diabetes induces changes through disruption of extracellular signal-regulated kinases (Reece et al., 2002). Furthermore, a correlation between the rate of embryonic malformations and endodermal-cell damage in the visceral yolk sac was observed (Zusman et al., 1987). Finally high glucose reduces the density of the vasculature in the yolk sac membrane model in chick embryos (Jin et al., 2013). In this light, hypomethylation of hypoblast needs more attention.

Trophoblasts of stage 2 blastocysts of diabetic rabbits express basal Oct4 RNA amounts and are equally methylated at the CR1-overlapping fragment, but interestingly the CR4-overlapping fragment is less methylated in trophoblasts of diabetic rabbits. This corresponds with previous observations where the minimal promoter and 5'-UTR regulatory elements are differentially activated by the promoter methylation, depending on the developmental stage of the mouse embryo (Yeom et al., 1996; Niwa, 2001; Oda et al., 2013). Stage 0 blastocysts of diabetic rabbits have higher Oct4 expression in trophoblasts, which is a sign of underdevelopment of trophoblast tissue. Although the expression of trophoblasts of diabetic rabbits remains unchanged, the Oct4 methylation is affected. This supports the view that the suppression of Oct4 expression in rabbit blastocyst might be governed synergistically with other cellular process.

4.3.5 Delay in epiblast differentiation is associated with hypoblast underdevelopment in diabetic blastocysts

The preimplantation period of rabbit embryo development is the timeframe for epiblast and hypoblast tissue differentiation. At this time, the embryo is modelling its anteroposterior polarity and setting on the neural specification and head patterning (Chapman et al., 2003). In rabbit embryos the trophoblast creates a morphological polarity in the blastocyst and co-ordinates the construction of germ layers (Idkowiak et al., 2005). Furthermore, in mammalian embryos the epiblast differentiation depends on signals from hypoblast tissue. The anterior-posterior axis is formed first in the hypoblast and, in the process of epithelio-mesenchymal transition, the molecular prepattern is transferred to the epiblast (Viebahn et al., 1995; Idkowiak et al., 2004). Therefore, a delay in hypoblast formation is directly affecting the epiblast progress. One hypothesis is that a delay in the development of hypoblast cells presented by hypomethylation of the Oct4 pluripotency gene in hypoblasts of diabetic rabbits can go together with a lack of patterning signals, what forces the epiblast to keep the pluripotency network on (upregulation of Oct4, Nanog and Sox2). In this context a trophoblast tissue underdevelopment in embryos of diabetic rabbits is likely to occur, because of the impaired Cdx2 and Oct4 expression at the beginning of gastrulation in 6 day old blastocyst stage 0, and due to hypomethylation at the CR4-overlapping fragment in trophoblasts of blastocysts stage 2.

4.3.6 Changes in Oct4 promoter methylation are not depending on global DNA methylation processes

The global DNA methylation level of gastrulating rabbit blastocysts at day 6 is not affected by a development in a diabetic pregnancy milieu (Grybel et al., unpublished). The process of global DNA methylation depends on the accessibility of DNA methyltransferases to a substrate for the methylation reaction – SAM and an indicator of methylation reaction efficiency - SAH. SAM and SAH are present in lower concentrations in blood plasma of diabetic rabbits at day 6 of pregnancy.

The ratio SAM:SAH, being an actual signature of methylation process dynamics, was similar to the plasma of healthy rabbits. The SAM:SAH ratio has previously been described as affected in embryopathies (De Castro et al., 2010) and to cause hypomethylation in neural tube defects (Wang et al., 2015). Moreover, measured SAM and SAH concentrations (Fig. 37) differ from levels in human plasma (Klepacki et al., 2013). Considering that global DNA methylation and SAM:SAH methylation reaction ratio are unchanged, they cannot be the reason for the observed alterations in Oct4 promoter region methylation in diabetic rabbit blastocyst. It is likely that the Oct4 promoter is regulated differently.

4.4 Delay in development due to maternal diabetes is manifested during organogenesis.

Oct4 is a well-known marker of mesodermal formation (Zeineddine et al., 2006). Observed signs of developmental delay related to Oct4 at the blastocyst stage might influence organogenesis. The heart is developing from mesoderm, so fetal hearts are an interesting object to follow up the diabetes effects in pregnancy.

Offspring of diabetic pregnancies are prone to develop heart malformations (Narchi and Kulaylat, 2000; Wren et al., 2003; Tabib et al., 2013). To understand if the delay in development is due to maternal diabetes during blastocyst development and continued through organogenesis, heart developmental markers were measured. Rabbit fetal hearts go through an extensive transformation from day 12 to 14 of embryonic development (Ghazi, 2014). For this reason a tight regulation of expression of transcriptional factors such as GATA4, GATA6, Mef2C and Nkx2-5 are crucial for proper heart development (Charron et al., 1999; Xin et al., 2006; McCulley et al., 2012). Among these genes, Gata6 and Nkx2-5 were lower expressed in hearts of embryos developed in a diabetic pregnancy. Moreover, a difference is seen only between hearts at day 14. Gata6 RNA amounts are increasing from day 12 to 14 in hearts of healthy embryos, what is not observed in the diabetic group. In case of Nkx2-5, the transcript levels are stable in healthy hearts at day 12 and 14, but decrease in hearts at day 14 developed in a diabetic pregnancy. Impaired GATA transcription factors are implicated in heart developmental malformations (Molkentin et al., 2000; Crawford et al., 2002). Interestingly, Nkx2-5 is known to enhance GATA6 expression through binding to its promoter enhancer region (Davis et al., 2000). This data indicate that transcription of Gata6 and Nkx2-5 may be involved in the formation of congenital heart defects due to a diabetic pregnancy, and support the hypothesis that a delay in development at the blastocyst stage is transferred to organogenesis.

4.5 DNA methyltransferases are highly expressed in embryonic tissues of 6 day old blastocysts and fetal rabbit heart

A proper DNA methylation pattern depends on *de novo* DNA methyltransferases (DNMT3A and B) and is preserved by DNMT1. Therefore, the transcriptional level of DNA methyltransferases

DNMT1, 3A and 3B was assessed at an early stage of embryo development in preimplantation embryos at the beginning of gastrulation (stage 0) and in late gastrulation (stage 2), as well as in rabbit fetal hearts day 12 and 14. All DNMTs shared the same expression pattern, with the highest RNA amounts in embryoblasts at stage 0. At stage 2 DNMTs transcripts are at the highest level in epiblasts, while hypoblasts expressed more DNMTs than trophoblasts. DNMT3B is transcribed almost 10 times more than DNMT1 and DNMT3A in 6 day old rabbit blastocyst. Contrary, in mouse embryos a decline of *de novo* DNA methyltransferases DNMT3A and DNMT3B expression was described during specification of trophoblast lineage (Oda et al., 2013). In 6 day old mouse blastocysts, *de novo* DNMTs are at a low level and remain with unchanged expression during gastrulation, what contradicts the obtained results obtained from rabbit blastocysts.

4.5.1 Maternal diabetes influences DNMTs expression in rabbit blastocysts

Since the DNA methylation of the Oct4 promoter region is not depending on global DNA methylation and on the SAM:SAH ratio in blastocysts of diabetic pregnancies, the expression enzymes responsible for DNA *de novo* methylation (DNMT3A and B) and DNA methylation maintenance (DNMT1) are of great interest. We hypothesized that the expression of DNA methyltransferases is a potential reason for the observed changes at the Oct4 promoter methylation.

DNMTs are downregulated in embryoblasts of diabetic rabbits, but at stage 2 they are already upregulated and their expression is more restricted to epiblast tissues. Organogenetic downregulation of *de novo* DNMTs is reported as a marker of preimplantation embryo development (Duymich et al., 2016). In this context, epiblasts of diabetic blastocysts might display another marker of delay in development. Data correlating the regulation of DNMTs expression and the development of embryopathies are poor. It is known that DNMT3B expression is sensitive to environmental signals at early development stages. An increase of DNA methylation levels was reported in neural tube and neural crest tissue from diabetic pregnancies (Wei et al., 2014). Moreover, Kamei et al., (2010) indicate that upregulation of DNMT3A might be due to obesity in adult mice (Kamei et al., 2010). Additionally, the DNMT1 inhibition study resulted in a decrease of glucose in patients with type 2 diabetes (Chen et al., 2016). Taken together, an impaired regulation of DNMTs in rabbit blastocysts needs to be elucidated by identification of factors influencing its expression.

4.5.2 DNA methyltransferases expression in fetal rabbit heart differs from the embryonic levels and is not influenced by maternal diabetes

Rabbit fetal hearts expressed DNMTs at day 12 and 14 of the embryonic development. The highest expression is observed for DNMT1, then DNMT3A and a basal transcript level is expressed for DNMT3B. The RNA amount of DNMT1 is at the same level in epiblast, DNMT3A is transcribed 3

times less than in epiblasts. The lowest level was detected for DNMT3B, where expression is about 200 times lower compared to its levels in epiblasts of 6 day old blastocysts. Only the *de novo* DNMTs expression declined during rabbit embryonic development, what is in consent with Duymich et al., (2016). The authors suggest that DNMT3 expression can be a marker of developmental progress. No difference was observed between the hearts developed in a diabetic and healthy pregnancy. In case of DNMT3A a tendency might be pointed out. An increase in DNMT1 and DNMT3B is described in the development of cardiac tissue fibrosis by hypoxia (Watson et al., 2014), but the direct DNMTs regulation in fetal hearts developing in diabetic pregnancy has not been clarified so far.

4.5.3 DNMT1 and DNMT3B showed a downregulation in diabetic epiblasts upon insulin and IGF2 *in vitro* culture

DNMTs expression was assessed after *in vitro* culture with BCAAs, insulin, IGF2 or LIF in embryonic tissues of 6 day old blastocysts, to see if any of these factors might be responsible for DNMTs upregulation in epiblasts of diabetic blastocysts. DNMT1 expression is negatively stimulated only by insulin, DNMT3B by IGF2, while DNMT3A expression remained unaffected. These findings suggest that in a diabetic intrauterine environment the lack of insulin and IGF can influence epiblast DNMTs levels. The observed phenomenon might be explained by a high capacity of insulin and IGFs to promote gastrulation in rabbit blastocysts (see Figure 31; Herrler et al., 1998; Thieme et al., 2012). Moreover, a tissue specific stimulation to epiblasts can be due to a restriction of insulin and IGFs receptors to embryoblasts of rabbit blastocysts (Navarrete Santos et al., 2008). Loss of *de novo* DNMTs expression might be a marker of development of preimplantation embryos (Duymich et al., 2016). Altogether, blastocysts after *in vitro* culture with IGF2 are proceeding in gastrulation, so as a consequence, they downregulate DNMT3B expression (see Figure 31). Contrary to *de novo* DNMTs, DNMT1 is constantly expressed from preimplantation, because it is responsible for DNA methylation pattern maintenance. Therefore, the downregulation of DNMT1 cannot be explained in epiblasts of 6 day old blastocyst after *in vitro* culture with and without insulin.

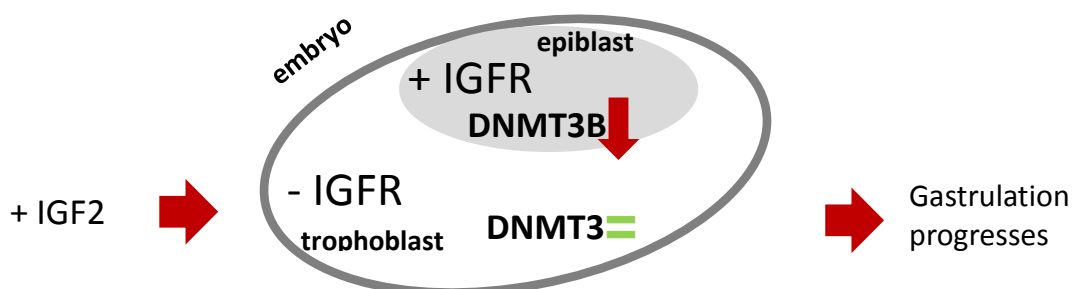


Figure 31. **Influence of IGF2 is tissue-specific in rabbit blastocysts and drives the gastrulation process marked by DNMT3B downregulation** (IGF -Insulin-like growth factor; IGFR – IGF2 receptor; (+) - expression; (-) - no expression).

5. Summary

Derivation of first embryonic tissues is a sensitive moment in embryogenesis. Formation of epiblast, hypoblast and trophoblast tissue occurs at day 6 *p.c.* of blastocyst development in the rabbit. In mammals, nutrients and hormonal signals from maternal intrauterine environment play an important role at the preimplantation stage of pregnancy. Adverse signals such as metabolic stress can promote long-lasting effects by 'adjustments' in epigenetic patterns. For this reason an influence of maternal diabetes on embryonic tissue formation and epigenetic modifications is of high interest worth clinically and in basic science.

The results can be summarized and concluded as follows:

The formation of embryonic tissues is disrupted by a diabetic pregnancy.

Marker genes of the epiblast - Oct4, Sox2 and Nanog - are upregulated in epiblasts from blastocysts derived from diabetic rabbits. The trophoblast development marker Cdx2 presents an altered expression pattern in trophoblast cells of diabetic rabbits. The transcriptional marker of the hypoblast cell lineage was not affected. Fetal heart developmental markers, Gata6 and Nkx2-5, are downregulated in hearts harvested at day 14 of a diabetic pregnancy. The transcriptional level of Mef2C and Gata4 remains unchanged. Concluding, the underdevelopment of embryonic tissues occurs as early as at the preimplantation stage and continues during organogenesis.

The DNA methylation patterns of the Oct4 (POU5F1) gene in hypoblasts are changed upon development under diabetic conditions.

The Oct4 gene promoter region methylation is changed in hypoblasts of late gastrulation blastocysts from diabetic rabbits. The observed change is a hypomethylation at the conserved regions of the gene promoter. Minor changes in Oct4 promoter region methylation were observed for trophoblast and epiblast tissues.

Lower methylation of the Oct4 promoter in hypoblasts of diabetic rabbits does not correlate with changes in the Oct4 transcriptional level.

Hypomethylation of the Oct4 promoter region in hypoblast of diabetic rabbits has no influence on Oct4 transcription. Moreover, an upregulation of Oct4 in epiblast of diabetic rabbit is not reflected in Oct4 promoter methylation. Regulation of Oct4 expression at this stage of development is not only executed through its promoter region methylation.

‘Shifted’ patterns of DNA methyltransferases expression in epiblasts of diabetic rabbits are a sign of delay in development.

DNMTs are downregulated in early stages of gastrulation in epiblasts of blastocysts from diabetic rabbits, while at late stages of gastrulation DNMTs are upregulated. The *de novo* expression of DNMTs corresponds to the DNA remethylation process. The observed difference in expression patterns might be interpreted as a signal of suspension of development at the preimplantation stage. In rabbit fetal hearts DNMTs have a different expression pattern, with *de novo* DNMTs less expressed than DNMT1. No difference in the DNMTs transcript levels between fetal hearts of healthy and diabetic rabbits was observed. *In vitro* culture of healthy blastocysts with insulin downregulated DNMT1, while culture with IGF2 downregulates DNMT3B. Therefore, regulation of DNMTs during preimplantation period of pregnancy seems to be multifactorial.

DNA methylation reaction-relevant metabolites are not changed by diabetic pregnancy.

SAM and SAH ratio is an indicator of methylation reaction dynamics and is not affected by a diabetic pregnancy, indicated by maternal blood plasma measurements. SAM is not limiting the methylation reaction, so it is not influencing the DNA global methylation status of preimplantation embryos.

6. Literature

Abboud N, Moore-Morris T, Hiriart E, Yang H, Bezerra H, Gualazzi MG, Stefanovic S, Guénantin AC, Evans SM, Pucéat M (2015) A cohesin-OCT4 complex mediates Sox enhancers to prime an early embryonic lineage. *Nat Commun.* 2015 Apr 8;6:6749.

Abu-Remaileh M, Gerson A, Farago M, Nathan G, Alkalay I, Zins Rousso S, Gur M, Fainsod A, Bergman Y (2010) Oct-3/4 regulates stem cell identity and cell fate decisions by modulating Wnt/ β -catenin signalling. *EMBO J.* 2010 Oct 6;29(19):3236-48.

Aires MB, Santos JR, Souza KS, Farias PS, Santos AC, Fioretto ET, Maria DA (2015) Rat visceral yolk sac cells: viability and expression of cell markers during maternal diabetes. *Braz J Med Biol Res.* 2015 Aug;48(8):676-82.

Al-Khtib M, Blachère T, Guérin JF, Lefèvre A (2012) Methylation profile of the promoters of Nanog and Oct4 in ICSI human embryos. *Hum Reprod.* 2012 Oct;27(10):2948-54.

Antequera F, Bird A (1993) Number of CpG islands and genes in human and mouse. *Proc Natl Acad Sci U S A.* 1993;90:11995–11999

Atala A and Lanza R (2012) *Handbook of Stem Cells*, 2nd Edition. Imprint: Academic Press; eBook ISBN : 9780123859433; Print Book ISBN : 9780123859426

Biechele S, Lin CJ, Rinaudo PF, Ramalho-Santos M (2015) Unwind and transcribe: chromatin reprogramming in the early mammalian embryo. *Curr Opin Genet Dev.* 2015 Oct;34:17-23.

Blomberg L, Hashizume K, Viebahn C (2008) Blastocyst elongation, trophoblastic differentiation, and embryonic pattern formation. *Reproduction.* 2008 Feb;135(2):181-95.

Bohuslavova R, Skvorova L, Cerychova R, Pavlinkova G (2015) Gene expression profiling of changes induced by maternal diabetes in the embryonic heart. *Reprod Toxicol.* 2015 Nov;57:147-56.

Bou G, Liu S, Guo J, Zhao Y, Sun M, Xue B, Wang J, Wei Y, Kong Q, Liu Z (2016) Cdx2 represses Oct4 function via inducing its proteasome-dependent degradation in early porcine embryos. *Dev Biol.* 2016 Feb 1;410(1):36-44.

Brenet F, Moh M, Funk , Feierstein E, Viale AJ, Socci ND, Scandura JM (2011) DNA methylation of the first exon is tightly linked to transcriptional silencing. *PLoS One.* 2011 Jan 18;6(1):e14524.

Brewer AC, Alexandrovich A, Mjaatvedt CH, Shah AM, Patient RK, Pizzey JA (2005) GATA factors lie upstream of Nkx 2.5 in the transcriptional regulatory cascade that effects cardiogenesis. *Stem Cells Dev.* 2005 Aug;14(4):425-39.

Burton A, Torres-Padilla ME (2014) Chromatin dynamics in the regulation of cell fate allocation during early embryogenesis. *Nat Rev Mol Cell Biol.* 2014 Nov;15(11):723-34.

Canon E, Blachère T, Daniel N, Boulanger L, Godet M, Duranthon V (Présentateur) (2014). DNA methylation of the POU5F1 regulatory region in rabbit first embryonic lineages. In: *Epigenetics and Periconception Environment* (p. 29). Presented at Epiconcept Workshop 2014, Epigenomic Toolbox: from Methods to Models, Las Palmas, ESP (2014-05-07 - 2014-05-09). Bruxelles, BEL : Cost Office.

Cañon S, Fernandez-Tresguerres B, Manzanares M (2011) Pluripotency and lineages in the mammalian blastocyst: an evolutionary view. *Cell Cycle.* 2011 Jun 1;10(11):1731-8.

- Canovas S, Ross PJ (2016) Epigenetics in preimplantation mammalian development. *Theriogenology*. 2016 Jul 1;86(1):69-79.
- Cauffman G, Liebaers I, Van Steirteghem A, Van de Velde H (2006) POU5F1 isoforms show different expression patterns in human embryonic stem cells and preimplantation embryos. *Stem Cells*. 2006 Dec;24(12):2685-91.
- Cauffman G, Van de Velde H, Liebaers I, Van Steirteghem A (2005) Oct-4 mRNA and protein expression during human preimplantation development. *Mol Hum Reprod*. 2005 Mar;11(3):173-81.
- Chandrasekhar K, Raman R (1997) *De novo* methylation of the proto-oncogene, c-fos, during development occurs step-wise and directionally in the laboratory mouse. *Mol Reprod Dev*. 1997 Dec;48(4):421-32.
- Chao CS, McKnight KD, Cox KL, Chang AL, Kim SK, Feldman BJ (2015) Novel GATA6 mutations in patients with pancreatic agenesis and congenital heart malformations. *PLoS One*. 2015 Feb 23;10(2):e0118449.
- Chapman SC, Schubert FR, Schoenwolf GC, Lumsden A (2003) Anterior identity is established in chick epiblast by hypoblast and anterior definitive endoderm. *Development*. 2003 Nov;130(21):5091-101.
- Charron F and Nemer M (1999) GATA transcription factors and cardiac development. *Semin Cell Dev Biol*. 1999 Feb;10(1):85-91.
- Charron F, Paradis P, Bronchain O, Nemer G, Nemer M (1999) Cooperative interaction between GATA-4 and GATA-6 regulates myocardial gene expression. *Mol Cell Biol*. 1999 Jun;19(6):4355-65.
- Chazaud C, Yamanaka Y (2016) Lineage specification in the mouse preimplantation embryo. *Development*. 2016 Apr 1;143(7):1063-74.
- Crawford SE, Qi C, Misra P, Stellmach V, Rao MS, Engel JD, Zhu Y, Reddy JK (2002) Defects of the heart, eye, and megakaryocytes in peroxisome proliferator activator receptor-binding protein (PBP) null embryos implicate GATA family of transcription factors. *J Biol Chem*. 2002 Feb 1;277(5):3585-92.
- Daughtry BL, Chavez SL (2016) Chromosomal instability in mammalian pre-implantation embryos: potential causes, detection methods, and clinical consequences. *Cell Tissue Res*. 2016 Jan;363(1):201-25.
- Davis DL, Wessels A, Burch JB (2000) An Nkx-dependent enhancer regulates cGATA-6 gene expression during early stages of heart development. *Dev Biol*. 2000 Jan 15;217(2):310-22.
- De Castro SC, Leung KY, Savery D, Burren K, Rozen R, Copp AJ, Greene ND (2010) Neural tube defects induced by folate deficiency in mutant curly tail (Grhl3) embryos are associated with alteration in folate one-carbon metabolism but are unlikely to result from diminished methylation. *Birth Defects Res A Clin Mol Teratol*. 2010 Aug;88(8):612-8.
- Dentelli P, Barale C, Togliatto G, Trombetta A, Olgasi C, Gili M, Riganti C, Toppino M, Brizzi MF (2013) A diabetic milieu promotes OCT4 and NANOG production in human visceral-derived adipose stem cells. *Diabetologia*. 2013 Jan;56(1):173-84.

- Do DV, Ueda J, Messerschmidt DM, Lorthongpanich C, Zhou Y, Feng B, Guo G, Lin PJ, Hossain MZ, Zhang W, Moh A, Wu Q, Robson P, Ng HH, Poellinger L, Knowles BB, Solter D, Fu XY (2013) A genetic and developmental pathway from STAT3 to the OCT4-NANOG circuit is essential for maintenance of ICM lineages *in vivo*. *Genes Dev.* 2013 Jun 15;27(12):1378-90.
- Dong D, Reece EA, Lin X, Wu Y, AriasVilella N, Yang P (2016) New development of the yolk sac theory in diabetic embryopathy: molecular mechanism and link to structural birth defects. *Am J Obstet Gynecol.* 2016 Feb;214(2):192-202.
- Duymich CE, Charlet J, Yang X, Jones PA, Liang G (2016) DNMT3B isoforms without catalytic activity stimulate gene body methylation as accessory proteins in somatic cells. *Nat Commun.* 2016 Apr 28;7:11453.
- Ehrlich M, Gama-Sosa MA, Huang LH, Midgett RM, Kuo KC, McCune RA, Gehrke C (1982) Amount and distribution of 5-methylcytosine in human DNA from different types of tissues of cells. *Nucleic Acids Res.* 1982, 10: 2709-2721.
- El Hajj N, Schneider E, Lehnen H, Haaf T (2014) Epigenetics and life-long consequences of an adverse nutritional and diabetic intrauterine environment. *Reproduction.* 2014 Dec;148(6):R111-20.
- Fischer B, Chavatte-Palmer P, Viebahn C, Navarrete Santos A, Duranthon V (2012) Rabbit as a reproductive model for human health. *Reproduction.* 2012 Jul;144(1):1-10.
- Fleming TP, Velazquez MA, Eckert JJ (2015) Embryos, DOHaD and David Barker. *J Dev Orig Health Dis.* 2015 Oct;6(5):377-83.
- Fogarty NME, McCarthy A, Snijders KE, Powell BE, Kubikova N, Blakeley P, Lea R, Elder K, Wamaitha SE, Kim D, Maciulyte V, Kleinjung J, Kim JS, Wells D, Vallier L, Bertero A, Turner JMA, Niakan KK (2017) Genome editing reveals a role for OCT4 in human embryogenesis. *Nature.* 2017 Oct 5;550(7674):67-73. doi: 10.1038/nature24033. Epub 2017 Sep 20.
- Frankenberg SR, de Barros FR, Rossant J, Renfree MB (2016) The mammalian blastocyst. *Wiley Interdiscip Rev Dev Biol.* 2016 Mar-Apr;5(2):210-32.
- Frum T, Halbisen MA, Wang C, Amiri H, Robson P, Ralston A (2013) Oct4 cell-autonomously promotes primitive endoderm development in the mouse blastocyst. *Dev Cell.* 2013 Jun 24;25(6):610-22.
- Gardiner-Garden M, Frommer M (1987) CpG islands in vertebrate genomes. *J Mol Biol.* 1987;196:261-282.
- Ghazi J (2014) Histological observation on cardiogenesis during second trimester of domestic rabbit's fetuses (*Oryctolagus Cuniculus*). *Wasit Journal for Science & Medicine* 2014 7(2): (159-171) 159.
- Godfrey KM, Costello PM, Lillycrop KA (2016) Development, Epigenetics and Metabolic Programming. *Nestle Nutr Inst Workshop Ser.* 2016;85:71-80.
- Goissis MD, Cibelli JB (2014) Functional characterization of SOX2 in bovine preimplantation embryos. *Biol Reprod.* 2014 Feb 13;90(2):30.
- Gu P, Goodwin B, Chung AC, Xu X, Wheeler DA, Price RR, Galardi C, Peng L, Latour AM, Koller BH, Gossen J, Kliewer SA, Cooney AJ (2005) Orphan nuclear receptor LRH-1 is required to maintain Oct4 expression at the epiblast stage of embryonic development. *Mol Cell Biol.* 2005 May;25(9):3492-505.

- Guibert S, Forné T, Weber M (2009) Dynamic regulation of DNA methylation during mammalian development. *Epigenomics*. 2009 Oct;1(1):81-98.
- Gürke J, Schindler M, Pendzialek SM, Thieme R, Grybel KJ, Heller R, Spengler K, Fleming TP, Fischer B, Navarrete Santos A (2016) Maternal diabetes promotes mTORC1 downstream signalling in rabbit preimplantation embryos. *Reproduction*. 2016 May;151(5):465-76.
- Hackett JA and Surani MA (2013) DNA methylation dynamics during the mammalian life cycle. *Philos Trans R Soc Lond B Biol Sci*. 2013 Jan 5; 368(1609): 20110328.
- Han DW, Tapia N, Joo JY, Greber B, Araúzo-Bravo MJ, Bernemann C, Ko K, Wu G, Stehling M, Do JT, Schöler HR (2010) Epiblast stem cell subpopulations represent mouse embryos of distinct pregastrulation stages. *Cell*. 2010 Nov 12;143(4):617-27.
- Hattori N, Nishino K, Ko Y, Hattori N, Ohgane J, Tanaka S, Shiota K (2004) Epigenetic Control of Mouse Oct-4 Gene Expression in Embryonic Stem Cells and Trophectoderm Stem Cells. *The Journal of Biological Chemistry* 279, 17063-17069.
- Herrler A, Krusche CA, Beier HM (1998) Insulin and insulin-like growth factor-I promote rabbit blastocyst development and prevent apoptosis. *Biol Reprod*. 1998 Dec;59(6):1302-10.
- Hopf L. (2016) Characterisation of the DNA methylation in rabbit tissues and preimplantation embryos, Bachelor thesis, Halle (Saale): Matrin Luther Universität
- Idkowiak J, Weisheit G, Plitzner J, Viebahn C (2005) Hypoblast controls mesoderm generation and axial patterning in the gastrulating rabbit embryo. *Dev Genes Evol*. 2004 Dec;214(12):591-605.
- Idkowiak J, Weisheit G, Viebahn C (2004) Erratum to: "Polarity in the rabbit embryo". *Sem. Cell Dev. Biol.* 15 (5) (2004) 607–617]
- Ivanisević M, Djelmis J, Jalsovec D, Bljajic D (2006) Ultrasonic morphological characteristics of yolk sac in pregnancy complicated with type-1 diabetes mellitus. *Gynecol Obstet Invest*. 2006;61(2):80-6.
- Jawerbaum A and White V (2010) Animal Models in Diabetes and Pregnancy. *Endocr Rev* (2010) 31 (5): 680-701.
- Jeltsch A, Jurkowska RZ (2014) New concepts in DNA methylation. *Trends Biochem Sci*. 2014 Jul;39(7):310-8.
- Jeltsch A, Jurkowska RZ (2016) Allosteric control of mammalian DNA methyltransferases - a new regulatory paradigm. *Nucleic Acids Res*. 2016 Oct 14;44(18):8556-8575.
- Jin B, Li Y, Robertson KD (2011) DNA methylation: superior or subordinate in the epigenetic hierarchy? *Genes Cancer*. 2011 Jun;2(6):607-17.
- Jin YM, Zhao SZ, Zhang ZL, Chen Y, Cheng X, Chuai M, Liu GS, Lee KK, Yang X (2013) High glucose level induces cardiovascular dysplasia during early embryo development. *Exp Clin Endocrinol Diabetes*. 2013 Aug;121(8):448-54.
- Jones PA (2012) Functions of DNA methylation: islands, start sites, gene bodies and beyond. *Nature Reviews Genetics* 13, 484-492 (July 2012)
- Jones PA, Takai D (2001) The role of DNA methylation in mammalian epigenetics. *Science*. 2001 Aug 10;293(5532):1068-70.

Kamei Y, Suganami T, Ehara T, Kanai S, Hayashi K, Yamamoto Y, Miura S, Ezaki O, Okano M, Ogawa Y (2010) Increased expression of DNA methyltransferase 3a in obese adipose tissue: studies with transgenic mice. *Obesity (Silver Spring)*. 2010 Feb;18(2):314-21

Kaneko KJ (2016) Metabolism of Preimplantation Embryo Development: A Bystander or an Active Participant? *Curr Top Dev Biol*. 2016;120:259-310.

Keating ST, El-Osta A (2015) Epigenetics and metabolism. *Circ Res*. 2015 Feb 13;116(4):715-36.

Kim KC, Friso S, Choi SW (2009) DNA methylation, an epigenetic mechanism connecting folate to healthy embryonic development and aging. *J Nutr Biochem*. 2009 Dec;20(12):917-26.

Kirsch SH, Knapp JP, Geisel J, Herrmann W, Obeid R (2009) Simultaneous quantification of S-adenosyl methionine and S-adenosyl homocysteine in human plasma by stable-isotope dilution ultra performance liquid chromatography tandem mass spectrometry. *J Chromatogr B Analyt Technol Biomed Life Sci*. 2009 Nov 15;877(30):3865-70.

Kiss AC, Lima PH, Sinzato YK, Takaku M, Takeno MA, Rudge MV, Damasceno DC (2009) Animal models for clinical and gestational diabetes: maternal and fetal outcomes. *Diabetol Metab Syndr*. 2009 Oct 19;1(1):21.

Klepacki J, Brunner N, Schmitz V, Klawitter J, Christians U, Klawitter J (2013) Development and validation of an LC-MS/MS assay for the quantification of the trans-methylation pathway intermediates S-adenosylmethionine and S-adenosylhomocysteine in human plasma. *Clin Chim Acta*. 2013 Jun 5;421:91-7.

Ko YG, Nishino K, Hattori N, Arai Y, Tanaka S, Shiota K (2005) Stage-by-stage change in DNA methylation status of Dnmt1 locus during mouse early development. *J Biol Chem*. 2005 Mar 11;280(10):9627-34.

Kobolak J, Kiss K, Polgar Z, Mamo S, Rogel-Gaillard C, Tancos Z, Bock I, Baji AG, Tar K, Purity MK, Dinnyes A (2009) Promoter analysis of the rabbit POU5F1 gene and its expression in preimplantation stage embryos. *BMC Mol Biol*. 2009 Sep 4;10:88.

Kodo K, Nishizawa T, Furutani M, Arai S, Ishihara K, Oda M, Makino S, Fukuda K, Takahashi T, Matsuoka R, Nakanishi T, Yamagishi H (2012) Genetic analysis of essential cardiac transcription factors in 256 patients with non-syndromic congenital heart defects. *Circ J*. 2012;76(7):1703-11.

Kuijk EW, Du Puy L, Van Tol HT, Oei CH, Haagsman HP, Colenbrander B, Roelen BA (2008) Differences in early lineage segregation between mammals. *Dev Dyn*. 2008 Apr;237(4):918-27.

Kumaki Y, Oda M, Okano M (2008) QUMA: quantification tool for methylation analysis. *Nucleic Acids Res*. 36, W170-W175 (2008)

Kurosaka S, Eckardt S, McLaughlin KJ (2004) Pluripotent lineage definition in bovine embryos by Oct4 transcript localization. *Biol Reprod*. 2004 Nov;71(5):1578-82.

Kvaratskhelia E, Tkemaladze T, Abzianidze E (2014) Expression pattern of DNA-methyltransferases and its health implication (short review). *Georgian Med News*. 2014 Mar;(228):76-81.

Lavial F, Acloque H, Bertocchini F, Macleod DJ, Boast S, Bachelard E, Montillet G, Thenot S, Sang HM, Stern CD, Samarut J, Pain B (2007) The Oct4 homologue PouV and Nanog regulate pluripotency in chicken embryonic stem cells. *Development*. 2007 Oct;134(19):3549-63.

Le Bin GC, Muñoz-Descalzo S, Kurowski A, Leitch H, Lou X, Mansfield W, Etienne-Dumeau C, Grabole N, Mulas C, Niwa H, Hadjantonakis AK, Nichols J (2014) Oct4 is required for lineage

priming in the developing inner cell mass of the mouse blastocyst. *Development*. 2014 Mar;141(5):1001-10.

Lee K, Hamm J, Whitworth K, Spate L, Park KW, Murphy CN, Prather RS (2014) Dynamics of TET family expression in porcine preimplantation embryos is related to zygotic genome activation and required for the maintenance of NANOG. *Dev Biol*. 2014 Feb 1;386(1):86-95.

Lee SH, Jeyapalan JN, Appleby V, Mohamed Noor DA, Sottile V, Scotting PJ (2010) Dynamic methylation and expression of Oct4 in early neural stem cells. *J Anat*. 2010 Sep;217(3):203-13.

Leseva M, Knowles BB, Messerschmidt DM, Solter D (2015) Erase-Maintain-Establish: Natural Reprogramming of the Mammalian Epigenome. *Cold Spring Harb Symp Quant Biol*. 2015;80:155-63.

Li J, Harris RA, Cheung SW, Coarfa C, Jeong M, Goodell MA, White LD, Patel A, Kang SH, Shaw C, Chinault AC, Gambin T, Gambin A, Lupski JR, Milosavljevic A (2012) Genomic hypomethylation in the human germline associates with selective structural mutability in the human genome. *PLoS Genet*. 2012;8(5):e1002692.

Li J, Li J, Chen B (2012) Oct4 was a novel target of Wnt signaling pathway. *Mol Cell Biochem*. 2012 Mar;362(1-2):233-40.

Li Y, Seah M, O'Neill C (2016) Mapping global changes in nuclear cytosine base modifications in the early mouse embryo. *Reproduction*(2016)151 83–95.

Liu S, Rouleau J, León JA, Sauve R, Joseph KS, Ray JG (2015) Impact of pre-pregnancy diabetes mellitus on congenital anomalies, Canada, 2002-2012. *Health Promot Chronic Dis Prev Can*. 2015 Jul;35(5):79-84.

Loh KM, Lim B (2011) A precarious balance: pluripotency factors as lineage specifiers. *Cell Stem Cell*, 2011 Apr 8;8(4):363-9.

Macleod D, Charlton J, Mullins J, Bird AP (1994) Sp1 sites in the mouse *aprt* gene promoter are required to prevent methylation of the CpG island. *Genes & Dev*. 1994. 8: 2282-2292.

Madeja ZE, Sosnowski J, Hryniewicz K, Warzych E, Pawlak P, Rozwadowska N, Plusa B, Lechniak D (2013) Changes in sub-cellular localisation of trophoblast and inner cell mass specific transcription factors during bovine preimplantation development. *BMC Dev Biol*. 2013 Aug 13;13:32.

Marcho C, Cui W, Mager J (2015) Epigenetic dynamics during preimplantation development. *Reproduction*. 2015 Sep;150(3):R109-20.

McCulley JD, Black BL (2012) Transcription Factor Pathways and Congenital Heart Disease. *Curr Top Dev Biol*. 2012; 100: 253–277.

Moazzen H, Lu X, Liu M, Feng Q (2015) Pregestational diabetes induces fetal coronary artery malformation via reactive oxygen species signaling. *Diabetes*. 2015 Apr;64(4):1431-43.

Molkentin JD, Antos C, Mercer B, Taigen T, Miano JM, Olson EN (2000) Direct activation of a GATA6 cardiac enhancer by Nkx2.5: evidence for a reinforcing regulatory network of Nkx2.5 and GATA transcription factors in the developing heart. *Dev Biol*. 2000 Jan 15;217(2):301-9.

Moore GE, Abu-Amero SN, Bell G, Wakeling EL, Kingsnorth A, Stanier P, Jauniaux E, Bennett ST (2001) Evidence that insulin is imprinted in the human yolk sac. *Diabetes*. 2001 Jan;50(1):199-203.

Narchi H and Kulaylat N (2000) Heart disease in infants of diabetic mothers. *Images Paediatr Cardiol*. 2000 Apr-Jun; 2(2): 17–23.

Navarrete Santos A, Ramin N, Tonack S, Fischer B (2008) Cell lineage-specific signaling of insulin and insulin-like growth factor I in rabbit blastocysts. *Endocrinology*. 2008 Feb;149(2):515-24.

Nichols J, Zevnik B, Anastasiadis K, Niwa H, Klewe-Nebenius D, Chambers I, Schöler H, Smith A (1998) Formation of pluripotent stem cells in the mammalian embryo depends on the POU transcription factor Oct4 *Cell*, 95 (1998), pp. 379–391

Niwa H, Miyazaki J, Smith AG (2000) Quantitative expression of Oct-3/4 defines differentiation, dedifferentiation or self-renewal of ES cells. *Nat Genet*. 2000 Apr;24(4):372-6.

Niwa H (2001) Molecular mechanism to maintain stem cell renewal of ES cells. *Cell Struct Funct*. 2001 Jun;26(3):137-48.

Oda M, Oxley D, Dean W, Reik W (2013) Regulation of lineage specific DNA hypomethylation in mouse trophectoderm. *PLoS One*. 2013 Jun 25;8(6):e68846.

Øyen N, Diaz LJ, Leirgul E, Boyd HA, Priest J, Mathiesen ER, Quertermous T, Wohlfahrt J, Melbye M (2016) Prepregnancy Diabetes and Offspring Risk of Congenital Heart Disease: A Nationwide Cohort Study (2016) *Circulation*. 2016 Jun 7;133(23):2243-53.

Pamnani M, Sinha P, Singh A, Nara S, Sachan M (2016) Methylation of the Sox9 and Oct4 promoters and its correlation with gene expression during testicular development in the laboratory mouse. *Genetics and Molecular Biology*. 2016;39(3):452-458.

Paparo L, di Costanzo M, di Scala C, Cosenza L, Leone L, Nocerino R, Canani RB (2014) The influence of early life nutrition on epigenetic regulatory mechanisms of the immune system. *Nutrients*. 2014 Oct 28;6(11):4706-19.

Pardo M, Lang B, Yu L, Prosser H, Bradley A, Babu MM, Choudhary J (2010) An expanded Oct4 interaction network: implications for stem cell biology, development, and disease. *Cell Stem Cell*.

Pauliks LB (2015) The effect of pregestational diabetes on fetal heart function. *Expert Rev Cardiovasc Ther*. 2015 Jan;13(1):67-74.

Potdar PD, D'souza SB (2011) Isolation of Oct4+, Nanog+ and SOX2- mesenchymal cells from peripheral blood of a diabetes mellitus patient. *Hum Cell*. 2011 Mar;24(1):51-5.

Ramin N, Thieme R, Fischer S, Schindler M, Schmidt T, Fischer B, Navarrete Santos A (2010) Maternal diabetes impairs gastrulation and insulin and IGF-I receptor expression in rabbit blastocysts. *Endocrinology*. 2010 Sep;151(9):4158-67.

Reece EA, Ma XD, Wu YK, Dhanasekaran D (2002) Aberrant patterns of cellular communication in diabetes-induced embryopathy. I. Membrane signalling. *J Matern Fetal Neonatal Med*. 2002 Apr;11(4):249-53.

Rizzino A, Wuebben EL (2016) Sox2/Oct4: A delicately balanced partnership in pluripotent stem cells and embryogenesis. *Biochim Biophys Acta*. 2016 Jun;1859(6):780-91.

Rohde Ch, Zhang Y, Reinhardt R, Jeltsch A (2010) BISMA - Fast and accurate bisulfite sequencing data analysis of individual clones from unique and repetitive sequences. *BMC Bioinformatics*201011:230

Rountree MR, Bachman KE, Herman JG, Baylin SB (2001) DNA methylation, chromatin inheritance, and cancer. *Oncogene*. 2001 May 28;20(24):3156-65. Review.

- Sawai K, Takahashi M, Moriyasu S, Hirayama H, Minamihashi A, Hashizume T, Onoe S (2010) Changes in the DNA methylation status of bovine embryos from the blastocyst to elongated stage derived from somatic cell nuclear transfer. *Cell Reprogram*. 2010 Feb;12(1):15-22.
- Schiffmacher AT, Keefer CL (2013) CDX2 regulates multiple trophoblast genes in bovine trophoctoderm CT-1 cells. *Mol Reprod Dev*. 2013 Oct;80(10):826-39.
- Sheng G (2015) Epiblast morphogenesis before gastrulation. *Dev Biol*. 2015 May 1;401(1):17-24.
- Shi J, Shi W, Ni L, Xu X, Su X, Xia L, Xu F, Chen J, Zhu J (2013) OCT4 is epigenetically regulated by DNA hypomethylation of promoter and exon in primary gliomas. *Oncol Rep*. 2013 Jul;30(1):201-6.
- Shi JJ, Cai DH, Chen XJ, Sheng HZ (2008) Cloning and characterization of the rabbit POU5F1 gene. *DNA Seq*. 2008 Feb;19(1):56-61.
- Shimozaki K, Nakashima K, Niwa H, Taga T (2003) Involvement of Oct3/4 in the enhancement of neuronal differentiation of ES cells in neurogenesis-inducing cultures. *Development*. 2003 Jun;130(11):2505-12.
- Silva AL, Amaral AR, Oliveira DS, Martins L, Silva MR, Silva JC (2017) Neonatal outcomes according to different therapies for gestational diabetes mellitus. *J Pediatr (Rio J)*. 2017 Jan - Feb;93(1):87-93.
- Simandi Z, Horvath A, Wright LC, Cuaranta-Monroy I, De Luca I, Karolyi K, Sauer S, Deleuze JF, Gudas LJ, Cowley SM, Nagy L (2016) OCT4 Acts as an Integrator of Pluripotency and Signal-Induced Differentiation. *Mol Cell*. 2016 Aug 18;63(4):647-61.
- Smith CJ, Ryckman KK (2015) Epigenetic and developmental influences on the risk of obesity, diabetes, and metabolic syndrome. *Diabetes Metab Syndr Obes*. 2015 Jun 29;8:295-302.
- Stefanovic S, Pucéat M (2010) [The dual role of OCT4]. *Med Sci (Paris)*. 2010 Apr;26(4):411-6.
- Streck R, Kumpf S (2006) QAMA RT-PCR analysis of the correlation of OCT4 expression with CpG methylation status at specific sites in the OCT4 promoter. *The FASEB Journal*. 2006;20:A884
- Strumpf D, Mao CA, Yamanaka Y, Ralston A, Chawengsaksophak K, Beck F, Rossant J (2005) Cdx2 is required for correct cell fate specification and differentiation of trophoctoderm in the mouse blastocyst. *Development*. 2005 May;132(9):2093-102.
- Tabib A, Shirzad N, Sheikhabaei S, Mohammadi S, Qorbani M, Haghpanah V, Abbasi F, Hasani-Ranjbar S, Baghaei-Tehrani R (2013) Cardiac Malformations in Fetuses of Gestational and Pre Gestational Diabetic Mothers. *Iran J Pediatr*. 2013 Dec; 23(6): 664–668.
- Táncos Z, Bock I, Nemes C, Kobolák J, Dinnyés A (2015) Cloning and characterization of rabbit POU5F1, SOX2, KLF4, C-MYC and NANOG pluripotency-associated genes. *Gene*. 2015 Jul 25;566(2):148-57.
- Thieme R, Ramin N, Fischer S, Püschel B, Fischer B, Santos AN (2012) Gastrulation in rabbit blastocysts depends on insulin and insulin-like-growth-factor 1. *Mol Cell Endocrinol*. 2012 Jan 2;348(1):112-9.
- Thieme R, Schindler M, Ramin N, Fischer S, Mühleck B, Fischer B, Navarrete Santos A (2012) Insulin growth factor adjustment in preimplantation rabbit blastocysts and uterine tissues in response to maternal type 1 diabetes. *Mol Cell Endocrinol*. 2012 Jul 6;358(1):96-103.

- Tucker KL (2001) Methylated cytosine and the brain: a new base for neuroscience. *Neuron*. 2001, 30: 649-652.
- Turek-Plewa J, Jagodziński PP (2005) The role of mammalian DNA methyltransferases in the regulation of gene expression. *Cell Mol Biol Lett*. 2005;10(4):631-47.
- Uysal F, Akkoyunlu G, Ozturk S (2015) Dynamic expression of DNA methyltransferases (DNMTs) in oocytes and early embryos. *Biochimie*. 2015 Sep;116:103-13.
- Vassena R, Dee Schramm R, Latham KE (2005) Species-dependent expression patterns of DNA methyltransferase genes in mammalian oocytes and preimplantation embryos. *Mol Reprod Dev*. 2005 Dec;72(4):430-6.
- Velazquez MA (2015) Impact of maternal malnutrition during the periconceptual period on mammalian preimplantation embryo development. *Domest Anim Endocrinol*. 2015 Apr;51:27-45.
- Viebahn C (1995) Epithelio-mesenchymal transformation during formation of the mesoderm in the mammalian embryo. *Acta Anat (Basel)*. 1995;154(1):79-97.
- Viebahn C, Mayer B, Hrabé de Angelis M (1995) Signs of the principal body axes prior to primitive streak formation in the rabbit embryo. *Anat Embryol* 192: 159-169
- Vijaya M, Manikandan J, Parakalan R, Dheen ST, Kumar SD, Tay SS (2013) Differential gene expression profiles during embryonic heart development in diabetic mice pregnancy. *Gene*. 2013 Mar 10;516(2):218-27.
- Wang F, Wu Y, Quon MJ, Li X, Yang P (2015) ASK1 mediates the teratogenicity of diabetes in the developing heart by inducing ER stress and inhibiting critical factors essential for cardiac development. *Am J Physiol Endocrinol Metab*. 2015 Sep 1;309(5):E487-99.
- Wang G, Huang WQ, Cui SD, Li S, Wang XY, Li Y, Chuai M, Cao L, Li JC, Lu DX, Yang X (2015) Autophagy is involved in high glucose-induced heart tube malformation. *Cell Cycle*. 2015;14(5):772-83.
- Wang K, Sengupta S, Magnani L, Wilson CA, Henry RW, Knott JG (2013) Brg1 is required for Cdx2-mediated repression of Oct4 expression in mouse blastocysts. *PLoS One*. 2010 May 12;5(5):e10622.
- Watson CJ, Collier P, Tea I, Neary R, Watson JA, Robinson C, Phelan D, Ledwidge MT, McDonald KM, McCann A, Sharaf O, Baugh JA (2014) Hypoxia-induced epigenetic modifications are associated with cardiac tissue fibrosis and the development of a myofibroblast-like phenotype. *Hum Mol Genet*. 2014 Apr 15;23(8):2176-88.
- Weaver JR, Susiarjo M, Bartolomei MS (2009) Imprinting and epigenetic changes in the early embryo. *Mamm Genome*. 2009 Sep-Oct;20(9-10):532-43.
- Wei D, Loeken MR (2014) Increased DNA methyltransferase 3b (Dnmt3b)-mediated CpG island methylation stimulated by oxidative stress inhibits expression of a gene required for neural tube and neural crest development in diabetic pregnancy. *Diabetes*. 2014 Oct;63(10):3512-22.
- White CR, MacDonald WA, Mann MR (2016) Conservation of DNA Methylation Programming Between Mouse and Human Gametes and Preimplantation Embryos. *Biol Reprod*. 2016 Sep;95(3):61.
- Wojdacz TK, Møller TH, Thestrup BB, Kristensen LS, Hansen LL (2010) Limitations and advantages of MS-HRM and bisulfite sequencing for single locus methylation studies. *Expert Rev Mol Diagn*. 2010 Jul;10(5):575-80.

- Wren C, Birrell G, Hawthorne G (2003) Cardiovascular malformations in infants of diabetic mothers. *Heart*. 2003 Oct; 89(10): 1217–1220.
- Wu G and Schöler H (2014) Role of Oct4 in the early embryo development. *Cell Regeneration* 2014;3:7
- Wu H, Tao J, Sun YE (2012) Regulation and function of mammalian DNA methylation patterns: a genomic perspective. *Brief Funct Genomics*. 2012 May;11(3):240-50.
- Wu Y, Reece EA, Zhong J, Dong D, Shen WB, Harman CR, Yang P (2016) Type 2 diabetes mellitus induces congenital heart defects in murine embryos by increasing oxidative stress, endoplasmic reticulum stress, and apoptosis. *Am J Obstet Gynecol*. 2016 Sep;215(3):366.e1-366.e10.
- Wu Y, Sun B, Shi W, Ni L, Chen J, Cai G, Shi J (2015) OCT4 is up-regulated by DNA hypomethylation of promoter in recurrent gliomas. *Neoplasma* Vol.63, No.3, p.378-384,2016
- Xin M, Davis CA, Molkentin JD, Lien C, Duncan SA, Richardson JA, Olson EN (2006) A threshold of GATA4 and GATA6 expression is required for cardiovascular development. *Proc Natl Acad Sci U S A*. 2006 Jul 25; 103(30): 11189–11194.
- Yamazaki Y, Fujita TC, Low EW, Alarcón VB, Yanagimachi R, Marikawa Y (2006) Gradual DNA demethylation of the Oct4 promoter in cloned mouse embryos. *Mol Reprod Dev*. 2006 Feb;73(2):180-8.
- Yeap LS, Hayashi K, Surani MA (2009) ERG-associated protein with SET domain (ESET)-Oct4 interaction regulates pluripotency and represses the trophectoderm lineage. *Epigenetics Chromatin*. 2009 Oct 7;2(1):12.
- Yeom YI, Fuhrmann G, Ovitt CE, Brehm A, Ohbo K, Gross M, Hübner K, Schöler HR (1996) Germline regulatory element of Oct-4 specific for the totipotent cycle of embryonal cells. *Development*. 1996 Mar;122(3):881-94.
- Zakhari S (2013) Alcohol metabolism and epigenetics changes. *Alcohol Res*. 2013;35(1):6-16.
- Zeineddine D, Papadimou E, Chebli K, Gineste M, Liu J, Grey C, Thurig S, Behfar A, Wallace VA, Skerjanc IS, Pucéat M (2006) Oct-3/4 dose dependently regulates specification of embryonic stem cells toward a cardiac lineage and early heart development. *Dev Cell*. 2006 Oct;11(4):535-46.
- Zhao XM, Du WH, Hao HS, Wang D, Qin T, Liu Y, Zhu HB (2012) Effect of vitrification on promoter methylation and the expression of pluripotency and differentiation genes in mouse blastocysts. *Mol Reprod Dev*. 2012 Jul;79(7):445-50.
- Zhao Z (2010) Cardiac malformations and alteration of TGFbeta signaling system in diabetic embryopathy. *Birth Defects Res B Dev Reprod Toxicol*. 2010 Apr;89(2):97-105.
- Zhao Z (2014) TGFβ and Wnt in cardiac outflow tract defects in offspring of diabetic pregnancies. *Birth Defects Res B Dev Reprod Toxicol*. 2014 Oct;101(5):364-70.
- Zusman I, Yaffe P, Ornoy A (1987) The effects of high-sucrose diets and of maternal diabetes on the ultrastructure of the visceral yolk sac endoderm in rat embryos developing *in vivo* and *in vitro*. *Acta Anat (Basel)*. 1987;128(1):11-8.

Theses

1. The epiblast lineage specifier – Oct4 – is upregulated in epiblasts from diabetic rabbits, while other genes of the pluripotency network (Sox2 and Nanog) are upregulated or show tendency to be upregulated, what is a sign of retardation in the loss of pluripotency and slower differentiation.
2. A delay in development is further observed throughout the diabetic pregnancy in the fetal heart maturation (day 14), as the downregulation of the heart developmental markers (Gata6 and Nkx2-5) occurs.
3. The expression of DNA methyltransferases (DNMTs) is unchanged by diabetes at the beginning of gastrulation, but it is upregulated in late gastrulation rabbit embryos from diabetic rabbits. The alteration in the DNMTs expression patterns may indicate an aberrant *de novo* DNA methylation or a repression of the process. In this context, DNMTs may be considered as developmental markers in early embryogenesis. In vitro culture with BCAAs, insulin and IGF2 has not identified a factor responsible for the upregulation of all of the DNMTs.
4. The methylation of Oct4 (POU5F1) promoter region is the lowest in epiblast and high in hypoblast and trophoblast tissue. The level of Oct4 promoter methylation correlates with the Oct4 expression in first embryonic lineages of rabbit preimplantation embryos.
5. Maternal diabetes affects the methylation pattern of Oct4 (POU5F1) promoter region. The most prominent difference is the hypomethylation of the hypoblasts from diabetic rabbits. The hypomethylation of hypoblasts is a mark of delay in development. Diabetic environment causes minor changes in the methylation in conserved regions of the Oct4 (POU5F1) promoter in epiblasts and trophoblasts.
6. The hypomethylation of Oct4 (POU5F1) promoter region does not influence the Oct4 expression in hypoblasts from diabetic rabbits. The regulation of transcription of Oct4 is more likely to be multifactorial at this stage of development.
7. The concentrations of metabolites involved in the DNA methylation reaction are not affected by diabetes in rabbit maternal blood plasma. The dynamic of DNA methylation is not disturbed by metabolite supply in rabbit diabetic pregnancy.
8. Diabetic pregnancy causes a delay in embryonic tissue formation with signatures of a change in expression of embryonic tissue-specific and developmental markers, as well as methylation patterns at the specific gene promoter (Oct4) without possible consequences on the global DNA methylation status.
9. A possible explanation of the delay in development is the improper interaction between hypoblast and epiblast due to diabetic environment. A diabetic pregnancy causes underdevelopment of hypoblast tissue, what induces inadequate signaling or absence of signalling from hypoblast cells and retardation in epiblast cell development.

7. Supplement

7.1 List of figures

Number	Title	Page
Figure 1.	Scheme of morphogenetic diversity in epiblast formation (modified after Sheng, 2015).	3
Figure 2.	Schematic representation of cytosine methylation reaction by DNA methyltransferases. DNMT converts cytosine to 5′methyl-cytosine (modified after Zakhari, 2013).	4
Figure 3.	Epigenetic reprogramming during the mammalian reproductive cycle (modified after Leseva M. et al., 2015).	4
Figure 4.	POU5F1 gene structure with indication of transcriptional factors and transcriptional factors binding sites relevant for Oct4 regulation (adapted after Wu et al., 2014).	8
Figure 5.	Model of Oct4 functions during first lineages development in mammalian embryogenesis (modified after Le Bin et al., 2014).	10
Figure 6.	Relation between the metabolism and epigenetic processes (modified after Keating and El-Osta, 2015).	11
Figure 7.	Rabbit blastocyst day 6 p.c. and its gastrulation stages (modified after Viebahn et al., 1995).	13
Figure 8.	Flow chart of the bisulfite sequencing method.	24
Figure 9.	CpG methylation assessment out experimental sequencing data (modified after Rohde et al., 2010).	31
Figure 10.	Oct4 mRNA amount in epiblasts, hypoblasts and trophoblasts from blastocyst at stage 0 and 2 from diabetic and healthy rabbits.	32
Figure 11.	Nanog and Sox2 mRNA amounts in epiblast tissue of blastocyst (stage 2) from diabetic and healthy rabbits.	33
Figure 12.	Cdx2 and Hex mRNA amount in trophoblasts and hypoblasts of blastocyst (stages 0 and 2) from healthy and diabetic rabbits.	33
Figure 13.	Transcript amounts of genes involved in heart development investigated in rabbit fetal hearts at day (d) 12 and 14 from healthy and diabetic pregnancies.	34
Figure 14.	Bisulfite sequencing DNA methylation data for Oct4 (POU5F1) promoter region in rabbit adult heart tissue.	36
Figure 15.	Total CpGs methylation at CR1- and CR4-overlapping fragment. Group 1 and 2 of epiblasts, hypoblasts and trophoblasts was sampled from blastocysts healthy and diabetic rabbits.	37
Figure 16.	Bisulfite sequencing DNA methylation data for CR1-overlapping fragment of Oct4 (POU5F1) promoter region in epiblasts of rabbit blastocysts from healthy (A) and diabetic (B) pregnancies.	40
Figure 17.	Bisulfite sequencing DNA methylation data for CR1-overlapping fragment of Oct4 (POU5F1) promoter region in hypoblasts of rabbit blastocysts from healthy (A) and diabetic (B) pregnancies.	41
Figure 18.	Bisulfite sequencing DNA methylation data for CR1-overlapping fragment of Oct4 (POU5F1) promoter region in trophoblasts of rabbit blastocysts from healthy (A) and diabetic (B) pregnancies.	42

Figure 19.	Bisulfite sequencing DNA methylation data for CR4-overlapping fragment of Oct4 (POU5F1) promoter region in rabbit adult heart tissues and embryonic tissues of blastocysts from healthy and diabetic pregnancies.	43
Figure 20.	Bisulfite sequencing DNA methylation data for CR4-overlapping fragment of Oct4 (POU5F1) promoter region in epiblasts of rabbit blastocysts from healthy (A) and diabetic (B) pregnancies.	46
Figure 21.	Bisulfite sequencing DNA methylation data for CR4-overlapping fragment of Oct4 (POU5F1) promoter region in hypoblasts of rabbit blastocysts from healthy (A) and diabetic (B) pregnancies.	47
Figure 22.	Bisulfite sequencing DNA methylation data for CR4-overlapping fragment of Oct4 (POU5F1) promoter region in trophoblasts of rabbit blastocysts from healthy (A) and diabetic (B) pregnancies.	48
Figure 23.	Bisulfite sequencing DNA methylation data for CR1-overlapping fragment of Oct4 (POU5F1) promoter region in rabbit adult heart tissues and embryonic tissues of blastocysts from healthy and diabetic pregnancies.	49
Figure 24.	DNMTs mRNA amounts in embryonic tissues of 6 day old blastocyst (at stage 0 and 2) from healthy and diabetic pregnancies (quantified by RT-qPCR).	50
Figure 25.	DNMT1, -3A and 3B RNA amount in fetal rabbit hearts day 12 and 14 from healthy and diabetic pregnancies quantified by RT-qPCR.	51
Figure 26.	DNMT1 mRNA transcript levels in embryonic tissues from blastocyst at day 6 p.c. stage 1 after in vitro culture with BCAAs, insulin, IGF2 and LIF quantified by RT-qPCR	52
Figure 27.	DNMT3A mRNA transcript levels in embryonic tissues from blastocyst at day 6 p.c. stage 1 after in vitro culture with BCAAs, insulin, IGF2 and LIF quantified by RT-qPCR	53
Figure 28.	DNMT3B mRNA transcript levels in embryonic tissues from blastocyst at day 6 p.c. stage 1 after in vitro culture with BCAAs, insulin, IGF2 and LIF quantified by RT-qPCR.	53
Figure 29.	Concentrations of SAM and SAH in blood plasma of rabbits at day 6 from healthy and diabetic pregnancies quantified by LC-MS/MS.	54
Figure 30.	Dynamic of DNA methylation changes during early development (modified after Atala and Lanza 2012).	58
Figure 31.	Influence of IGF2 is tissue-specific in rabbit blastocyst and drives gastrulation process marked by DNMT3B downregulation (IGFR – IGF2 receptor).	67

7.2 List of tables

Table 1.	Pairwise comparison method was used to compare the <i>POU5F1</i> regulatory regions of the rabbit and of the four mammalian species (adapted after Kobolak et al., 2009).	7
Table 2.	Primer list of oligonucleotides used in PCR reactions with the length of PCR reaction product.	24
Table 3.	Summary of methylation at Oct4 promoter in CR4- (A) and CR1-overlapping fragment (B) and their functional elements.	60

Statutory Declaration

I declare that I have developed and written the enclosed Doctoral Thesis completely by myself, and have not used sources or means without declaration in the text. Any thoughts from others or literal quotations are clearly marked. The Doctoral Thesis was not used in the same or in a similar version to achieve an academic grading or is being published elsewhere.

Location, Date, Signature

Curriculum vitae

08.2017 – 11.2017	Research associate at the MLU in Halle (Germany) Faculty of Medicine, Department of Anatomy and Cell Biology, Supervisors: Prof. Anne Navarrete Santos
Main project:	Histone modifications study in rabbit blastocysts
10.2016 – 03.2017	Graduate Scholarship for foreign young female scientists from Martin Luther University Halle-Wittenberg
09.2013 – 08.2016	PhD student as an Early Stage Researcher in the frame of the EU-funded Marie Curie ITN EpiHealthNet (FP7-PEOPLE-2012-ITN) at the Martin Luther University Halle-Wittenberg, Faculty of Medicine, Department of Anatomy and Cell Biology, Supervisors: Prof. Bernd Fischer, Prof. Anne Navarrete Santos
Main project:	Analysis of the DNA methylation processes and the histone post-translational modifications in rabbit embryos from healthy and diabetic pregnancies
05/06.2016	Secondment in frame of the EpiHealthNet ITN at the Avantea srl, Cremona (Italy), Supervisor: Dr. Giovanna Lazzari
Main project:	Production of embryos by assisted reproduction techniques
03.2016	Secondment in frame of the EpiHealthNet ITN at the MWM Biomodels GmbH, Moorversuchsgut (LMU München) Oberschleißheim, (Germany), Supervisor: Prof. Dr. Eckhard Wolf, Dr. Simone Renner
Main project:	Transgenic pigs as models for translational biomedical research
11.2014 – 12.2014	Short Term Scientific Mission funded by RGB-Net (COST Action TD1101), Department of Developmental and Reproduction Biology INRA, Jouy en Josas, France, Supervisor: Dr. Véronique Duranthon
Main project:	DNA methylation in POU5F1 regulatory regions in diabetic rabbit embryos
02.2014 – 04.2014	Secondment in frame of the EpiHealthNet ITN at the Szent Istvan University, Molecular Animal Biotechnology Laboratory, Gödöllo (Hungary), Supervisor: Prof. Andras Dinnyes
Main project:	Basic methods in stem cell culture - rabbit Embryonic Stem Cells (rES) and Induced Pluripotent Stem Cells (rIPS)

07.2012 - 09.2012	Internship at the University of Florence, Department of Pathology and Experimental Oncology, Florence (Italy), Supervisors: Prof. Annarosa Arcangeli, Dr. Olivia Crociani
Main project:	Study of expression K ⁺ channels belonging to the hERG1 family in various types of cancer
10.2010 – 12.2012	Master degree (mgr) at the University of Wrocław, Biotechnology Faculty, Department of Cell Pathology, specialization: Medical Biotechnology, Supervisor: Prof. Maria Malicka-Błaszkiwicz
Master thesis:	Potential apoptotic properties of N-pyridine oxides
04.2012 – 06.2012; 09.2011 – 10.2011	Internship at FSP Galena, Drug Production Department, Drug Quality Control Laboratory, Wrocław (Poland), Supervisor: Dr. Jolanta Kowalska
10.2007 – 10.2010	First degree at the University of Wrocław, Biotechnology Faculty, Department of Cell Pathology, field of study: Biotechnology, Supervisor: Prof. Maria Malicka-Błaszkiwicz
Bachelor thesis:	What do we know about the cytotoxicity of drugs commonly used?

PUBLICATIONS

J Gürke, M Schindler, M Pendzialek, R Thieme, [KJ Grybel](#), R Heller, K. Spengler, TP Fleming, B Fischer, A Navarrete Santos (2016), Maternal diabetes promotes mTORC1 downstream signalling in rabbit preimplantation embryos, *Reproduction*. 2016 May;151(5):465-76.

Seeling T, Čikoš Š, [Grybel KJ](#), Janštová Ž, Pendzialek SM, Schindler M, Špírková A, Santos AN (2017) A Diabetic Pregnancy Alters the Expression of Stress-Related Receptors in Gastrulating Rabbit Blastocyst and in the Reproductive Tract. *Reprod Sci*. 2017 Jan 1:1933719117707055.

Schindler M, Pendzialek M, [Grybel KJ](#), Seeling T, Gürke J, Fischer B, Navarrete Santos A. (2017) Adiponectin stimulates lipid metabolism via AMPK in rabbit blastocysts. *Hum Reprod*. 2017 May 4:1-11.

Fischer B, Schindler M, Mareike Pendzialek S, Gürke J, Haucke E, [Grybel KJ](#), Thieme R, Santos AN (2017) The Long-Term Effect of the Periconception Period on the Embryo's Epigenetic Profile and Phenotype: The Role of Maternal Disease Such as Diabetes and How the Effect Is Mediated (Example from a Rabbit Model) *Adv Exp Med Biol*. 2017;1014:107-115.

ORAL PRESENTATIONS

Grybel KJ, Canon E, Pendzialek SM, Schindler M, Guerke J, Seeling T, Blachère T, Godet M, Fischer B, Duranthon V and Navarrete Santos A (2015) Gestational diabetes changes the DNA methylation patterns at Oct4 promoter region in rabbit preimplantation embryos, 3rd Congress of Doctoral Students, 20.11.2015, Halle (Saale) (Germany)

Grybel KJ, Canon E, Pendzialek SM, Schindler M, Guerke J, Seeling T, Blachère T, Godet M, Fischer B, Duranthon V and Navarrete Santos A (2016) Gestational diabetes changes the DNA methylation patterns at Oct4 promoter region in rabbit preimplantation embryos, 49th Annual Conference on Physiology & Pathology of Reproduction and 41st Joint Conference of Veterinary and Human Reproductive Medicine, 11.02.2016, Leipzig (Germany)

Grybel KJ, Canon E, Pendzialek SM, Schindler M, Guerke J, Seeling T, Blachère T, Godet M, Fischer B, Duranthon V and Navarrete Santos A (2016) Impact of maternal diabetes on DNA methylation in rabbit blastocyst, Final Dissemination Workshop of the 'Epihealthnet' FP7 project, 20.04.2016, Budapest (Hungary)

Grybel KJ, Canon E, Knelangen J, Kradolfer D, Pendzialek SM, Schindler M, Guerke J, Blachère T, Godet M, Obeid R, Ulbrich S, Fischer B, Duranthon V and Navarrete Santos A (2017) Impact of maternal diabetes on DNA methylation in rabbit blastocyst, 50th Annual Conference on Physiology & Pathology of Reproduction and 42st Joint Conference of Veterinary and Human Reproductive Medicine, 17.02.2017, Munich (Germany)

Grybel KJ, Canon E, Knelangen J, Kradolfer D, Pendzialek SM, Schindler M, Guerke J, Blachère T, Godet M, Obeid R, Ulbrich S, Fischer B, Duranthon V and Navarrete Santos A (2017) Influence of maternal diabetes on the DNA methylation and first embryonic lineages in the rabbit preimplantation embryos, 10th World Congress on Developmental Origins of Health and Disease (DOHaD 2017), 15-18.10.2017, Rotterdam (the Netherlands)

AWARDS

2nd DGRM-Abstract-Prize 2017 at the 50th Annual Conference on Physiology & Pathology of Reproduction and also 42st Joint Conference of Veterinary and Human Reproductive Medicine, Munich (Germany), 15-17.02.2016

3rd poster prize at the Bilateral Symposium Poznan-Halle, Halle (Saale) (Germany), 23-25.10.2015

Note of thanks

Firstly, I would like to express my sincere gratitude to my advisor apl Prof. Anne Navarrete Santos for the continuous support of my PhD study and related research, for her patience, motivation, and immense knowledge. Her guidance helped me in all the time of research and writing of this thesis.

Besides my advisor, I would like to thank Prof. Bernd Fischer for his insightful comments and encouragement, but also for the hard question which incited me to widen my research from various perspectives.

My sincere thanks also goes to dr. Véronique Duranthon, who provided me an opportunity to join their team and who gave access to the laboratory and research facilities. Without their precious support it would not be possible to conduct this research.

A very special gratitude goes out to the EpiHealthNet project (Marie Curie Initial Training Network funded by European commission under FP7) for providing the funding for the work and organizing scientific workshops.

I thank my fellow labmates, with a special mention to Mareike S. Pendzialek and Tom Seeling for the cooperation at the methodological field, for the stimulating discussions and for all the fun we have had in the last four years. It is necessary to acknowledge Sabine Schrötter and Michaela Kirstein for an excellent technical support.

Last but not the least, I would like to thank my family: my parents and to my sisters for supporting me during last four years.